

The University of Southern Mississippi
The Aquila Digital Community

Dissertations

Fall 12-2008

Yellow Head Virus: Transmission and Genome Analyses

Hongwei Ma
University of Southern Mississippi

Follow this and additional works at: <https://aquila.usm.edu/dissertations>



Part of the [Aquaculture and Fisheries Commons](#), [Biology Commons](#), and the [Marine Biology Commons](#)

Recommended Citation

Ma, Hongwei, "Yellow Head Virus: Transmission and Genome Analyses" (2008). *Dissertations*. 1149.
<https://aquila.usm.edu/dissertations/1149>

This Dissertation is brought to you for free and open access by The Aquila Digital Community. It has been accepted for inclusion in Dissertations by an authorized administrator of The Aquila Digital Community. For more information, please contact aquilastaff@usm.edu.

The University of Southern Mississippi

YELLOW HEAD VIRUS: TRANSMISSION AND GENOME ANALYSES

by

Hongwei Ma

Abstract of a Dissertation
Submitted to the Graduate Studies Office
of The University of Southern Mississippi
in Partial Fulfillment of the Requirements
for the Degree of Doctor of Philosophy

December 2008

COPYRIGHT BY

HONGWEI MA

2008

The University of Southern Mississippi

YELLOW HEAD VIRUS: TRANSMISSION AND GENOME ANALYSES

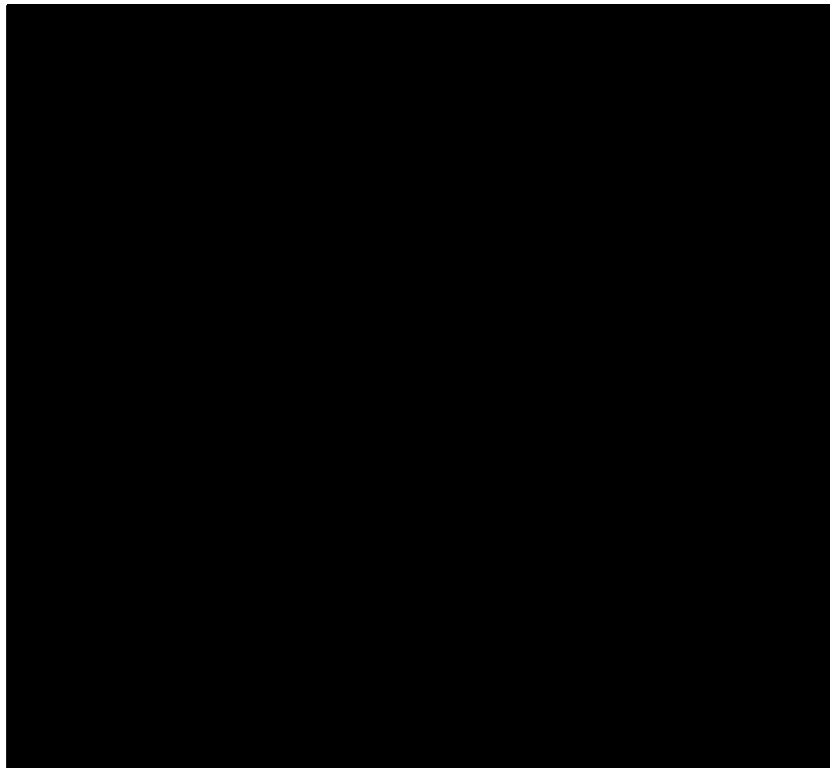
by

Hongwei Ma

A Dissertation

Submitted to the Graduate Studies Office
of The University of Southern Mississippi
in Partial Fulfillment of the Requirements
for the Degree of Doctor of Philosophy

Approved:



December 2008

ABSTRACT

YELLOW HEAD VIRUS: TRANSMISSION AND GENOME ANALYSES

by Hongwei Ma

December 2008

Yellow head virus (YHV) is an important pathogen to shrimp aquaculture. Among 13 species of naturally YHV-negative crustaceans in the Mississippi coastal area, the daggerblade grass shrimp, *Palaemonetes pugio*, and the blue crab, *Callinectes sapidus*, were tested for potential reservoir and carrier hosts of YHV using PCR and real time PCR. The YHV replicated in the daggerblade grass shrimp, and was still detectable on 36 d post-inoculation, causing 8% mortality after injection. However, YHV did not replicate in the blue crab. These data suggest that the daggerblade grass shrimp could act as a reservoir host for YHV.

Storage conditions of hemolymph samples containing YHV may result in a decline of virus or exhibit false-negative results in viral detection. The YHV-positive hemolymph was stored at either 4 or 25 °C for a 6-d period, the viral load number at 4 °C was not significantly different from that stored at 25 °C. The only difference was between the samples stored for 6-d at either 4 or 25 °C and those stored at -80 °C, suggesting that shrimp hemolymph can be stored at either 4 or 25 °C for 3–5 d without a significant reduction in measured YHV RNA levels.

The whole genome of 3 isolates in *Penaeus monodon* obtained from Thailand in 1992, 1995, and 1999 was sequenced. The only indel event in the coding region was located in the 5' end of ORF1a, containing a segment of 12 nt. Other indels occurred in the non-coding region. The 3' untranslated region (UTR) forms a putative pseudoknot,

with an octonucleotide motif being the counterpart in the 3' UTR of *Coronavirus*. The phylogeny of Nidovirales was reconstructed based on 48 nidovirus proteome sequences, demonstrating a consistency with the contemporary phylogeny.

Recombination in RNA viruses plays a major role in virus diversity and evolution. Seven recombination events were detected among the 4 YHV genomes with high statistical support. The divergence times for the most recent common ancestor of the YHV lineage were dated back to 1970-1980s based on 3 recombination-free data sets. These values were consistent with shrimp culture practice in Asia.

ACKNOWLEDGEMENTS

I would like to express my gratitude to the faculty, staff, and graduate students at the USM Gulf Coast Research Laboratory for their kindness and support. I especially owe much gratitude to my mentor, Dr. Robin M. Overstreet, for providing me with the opportunity and for providing his guidance and dedication to this research. I would also like to thank members of my committee, Drs. Marius Brouwer, Richard Heard, and Jeffrey Lotz, for their time and expert advice.

I want to thank Dr. Lotz's laboratory members, Mrs. Verlee Breland and Mr. John Ogle, for most willingly providing me with many of the SPF *Litopenaeus vannamei* that allowed this study to be a success, and Mrs. Marie Mullen for histology help.

Thanks are also extended to Dr. Brouwer's laboratory members, including Mrs. Thea Brouwer, Mrs. Rachel Ryan, and Dr. Alexander Pozhitkov, for their valuable technique support and permission to use their facilities.

Our Parasitology laboratory members contributed much of their wisdom, experience, time, and love to my dissertation. Mrs. Jean A. Jovonovich not only provided her molecular technique but also helped purchasing reagents as well as reviewing most of my manuscripts. Mr. Walter Grater taught me molecular technique. Mr. Joshua Cook, Mr. Jody Peterson, Ronnie Palmer, and Drs. S. Ashton Bullard and Stephen Curran helped me collect crustaceans. Mrs. Tershara Matthews and Kimberly Lamey contributed much assistance in the wet laboratory and with H&E staining.

I am grateful to Drs. D. V. Lightner and K. F. J. Tang of the University of Arizona for kindly providing 3 viral isolates and details of real time PCR method and to Dr. N. Sittidilokratna of BIOTEC, Bangkok, Thailand, and Dr. P. J. Walker of CSIRO

Livestock Industries, Australian Animal Health Laboratory, Geelong, Victoria, Australia, for sharing the sequence of the Chachoengsao 1998 YHV strain. I would like to thank Dr. Leigh Owens of the James Cook University for providing the gill-associated virus sample and Dr. Charles Laird of the University of Washington for reviewing the last chapter.

The research was supported by U.S. Department of Agriculture, CSREES Award No. 2006-38808-03589; U.S. Department of Commerce, NOAA, Award No. NA08NOS4730322 and Subaward No. NA17FU2841; and the National Science Foundation, Award No. 0529684.

I am especially grateful to my wife Lirong Liu, my son Zihao Ma, and my relatives and friends for their continuous support, patience, and encouragement.

TABLE OF CONTENTS

ABSTRACT.....	ii
ACKNOWLEDGEMENTS.....	iv
LIST OF ILLUSTRATIONS.....	viii
LIST OF TABLES.....	x
LIST OF ABBREVIATIONS.....	xi
CHAPTER	
I. INTRODUCTION.....	1
Yellow Head Disease and Yellow Head Virus	
Shrimp Viral Disease	
Shrimp Susceptibility to YHV and Antiviral Research	
Study Objectives	
II. DAGGERBLADE GRASS SHRIMP (<i>PALAEMONETES PUGIO</i>): A RESERVOIR HOST FOR YELLOW HEAD VIRUS (YHV).....	29
Abstract	
Introduction	
Materials and Methods	
Results	
Discussion	
III. STABLE YELLOW HEAD VIRUS (YHV) RNA DETECTION BY QRT- PCR DURING SIX-DAY STORAGE.....	48
Abstract	
Introduction	
Materials and Methods	
Results	
Discussion	
IV. GENOME ANALYSIS OF THREE ISOLATES OF YELLOW HEAD VIRUS (YHV) AND PHYLOGENY OF NIDOVIRALES.....	59
Abstract	
Introduction	
Materials and Methods	
Results	
Discussion	

V.	EVOLUTION OF YELLOW HEAD VIRUS THROUGH RECOMBINATION.....	82
	Abstract	
	Introduction	
	Materials and Methods	
	Results	
	Discussion	
	REFERENCES.....	104

LIST OF ILLUSTRATIONS

Figure	
1.	The genome organization of Nidovirales.....7
2.	Schematic organization of <i>Okavirus</i>12
3.	RNA secondary structure models for the ribosomal frameshift (RFS) sites in Nidovirales.....14
4.	qRT-PCR quantification of YHV RNA levels in the grass shrimp <i>Palaemonetes pugio</i> at different time periods after injection.....38
5.	Semi-nested RT-PCR amplification of RNA from grass shrimp.....39
6.	Semi-nested RT-PCR amplification of YHV in hemolymph of blue crab administered by feeding YHV-positive <i>Litopenaeus vannamei</i> tissue.....39
7.	The qRT-PCR quantification of YHV RNA levels in hemolymph of blue crab at different times.....40
8.	The qRT-PCR quantification of RNA levels in hemolymph of blue crab and white shrimp at different times.....41
9.	Conventional RT-PCR amplification of RNA from aliquoted hemolymph from <i>Litopenaeus vannamei</i> stored at different temperatures over 6 days.....52
10.	Standard curve generated from qRT-PCR and a 10-fold dilution series.....53
11.	Quantitative analysis of log scale in <i>Litopenaeus vannamei</i> hemolymph at 4 and 25 °C for 6 d storage.....54
12.	Schematic genomic organization of <i>Okavirus</i>67
13.	The indel event in the coding region of ORF1a and comparison in the intergenic regions.....68
14.	RNA secondary structure models for the ribosomal frameshift (RFS) sites and 3' untranslated region (UTR) of Roniviridae.....70
15.	Alignments and topology of the putative <i>Okavirus</i> hydrophobic transmembrane (TM) domains in pp1a.....73
16.	Predicted topology of <i>Okavirus</i> ORF3 and alignment of the transmembrane (TM) domains of okaviruses.....74
17.	Unrooted NJ tree by analysis of 48 amino acid sequences of Nidovirales using CVTree program.....79

18.	Cumulative substitution rates of 4 coding genes.....	89
19.	Recombinant regions detected within yellow head virus (YHV) sequences based on the RDP3 program.....	91
20.	Detection of recombination on ORF1a (A), ORF1b (B), and ORF3 (C) of <i>Okavirus</i>	93
21.	Phylogenetic analyses and divergence dates of <i>Okavirus</i> lineages based on alignments of 3 data sets.....	95
Supplement		
1.	RDP3 genome analysis of <i>Okavirus</i> (RDP3 project file).....	100
2A.	Tracer statistics of data set from 5' end of ORF1a for <i>Okavirus</i>	101
2B.	Tracer statistics of data set from 3' end of ORF1a for <i>Okavirus</i>	102
2C.	Tracer statistics of data set from 3' end of ORF3 for <i>Okavirus</i>	103

LIST OF TABLES

Table

1.	Comparison of the characteristics of the Roniviridae with those of other families in Nidovirales.....	9
2.	Penaeid viruses.....	21
3.	Experimental infection of yellow head virus in decapod and stomatopod crustaceans from coastal Mississippi determined by RT-PCR.....	37
4.	Comparison of YHV log viral copy/ μ g hemolymph RNA in <i>Callinectes sapidus</i> and <i>Litopenaeus vannamei</i> administered YHV.....	42
5.	Primers designed for RT-PCR and sequencing based on YHV and GAV sequences using Vector NTI Advance™ 10.....	63
6.	Sequence identity matrix for <i>Okavirus</i>	72
7.	Statistic data of nonsynonymous to synonymous substitutions for yellow head virus coding regions.....	88
8.	Statistic data detected by BEAST and Tracer program for <i>Okavirus</i>	90

LIST OF ABBREVIATIONS

\$	dollar
(+) ssRNA	positive-sense single-stranded ribonucleic acid
~	approximately
µg	microgram
µl	microlitre
µM	micromolar
3CLP	3C-like proteinase
aa	amino acid
ADRP	ADP-ribose 1 st -phosphatase
BEAST	Bayesian evolutionary analysis sampling trees
bp	base pairs
BSD	bamboo-shaped disease
c-AIC	Akaike information criterion
CBC	compensatory base changes
cDNA	complimentary deoxyribonucleic acid
CPD	cyclic phosphodiesterase
C _T	cycle threshold
C-terminal	carboxyl-terminal
CV	coefficient of variation
CVTrees	composition vector trees
DAD	defender against apoptotic death
d	day
d _N	average of Jukes-Cantor correction for non-synonymous substitution rate
d _S	average of Jukes-Cantor correction for synonymous substitution rate
d _S /d _N	average ratio of synonymous to nonsynonymous substitution
ESS	effective sample size
ExoN	5'-to-3' exonuclease
g	gram
g	surface gravity
GARD	genetic algorithms for recombination detection

GAV	gill-associated virus
gp116	glycoprotein 116
gp64	glycoprotein 64
h	hour
H&E	hematoxylin and eosin
HPD	highest posterior density
HPV	hepatopancreatic parvovirus
IBV	infectious bronchitis virus
IGR	intergenic region
IHHNV	infectious hypodermal and hematopoietic necrosis virus
im	intra-muscularly
IMNV	infectious myonecrosis virus
IMNV	infectious myonecrosis virus
kDa	kilodalton
LC50	median lethal concentration
LD50	median lethal dose
LDV	lactate dehydrogenase elevating virus
LO	lymphoid organ
LSNV	Laem-Singh virus
LSS	loose shell syndrome
M	marker
MBV	monodon baculovirus
MCMC	Markov chain Monte Carlo
ME	minimum evolution
MEGA	molecular evolutionary genetics analysis
MHV	mouse hepatitis virus
mM	millimolar
mRNA	messenger ribonucleic acid
MSGs	monodon slow growth syndrome
NJ	neighbor-joining
nd	not detectable

nt	nucleotide
N-terminal	amino-terminal
O-M	2'-O-methyltransferase
ORF	open reading frame
PI	post-inoculation
pS/pN	average ratio of proportion of synonymous to non-synonymous substitution
RdRp	RNA-dependent RNA polymerase
RNA	ribonucleic acid
RT-PCR	reverse transcription polymerase chain reaction
SARS-CoV	severe atypical respiratory syndrome-coronavirus
sg mRNA	subgenomic messenger ribonucleic acid
sg	subgenomic
SPF	specific pathogen free
ss	single-stranded
TEM	transmission electron microscopy
TGEV	transmissible gastroenteritis virus
TM	transmembrane
TMRCA	time for the most recent common ancestor
TRS	transcription-regulating sequence
TSV	Taura syndrome virus
UN	uridylyate-specific endoribonuclease
WSSD	white spot syndrome disease
WSSV	white spot syndrome virus
YHD	yellow head disease
YHV	yellow head virus

CHAPTER I

INTRODUCTION

The focus of this research is to detect whether some crustaceans in the coastal area of the Gulf of Mexico can serve as reservoir or carrier hosts for a highly pathogenic virus, yellow head virus (YHV), to analyze how long YHV can be stable for diagnosis in hemolymph samples, to analyze 4 isolates of YHV genome, and to analyze the phylogeny of Nidovirales and the evolution of YHV.

Yellow head disease (YHD) has caused serious economic damage to Asian shrimp aquaculture in the 1990s, and YHV has been detected by Nunan et al. (1998) and our laboratory in the US in frozen commodity shrimp imported from Asia. This product can cause mortality in bioassay shrimps (Durand et al. 2000, Overstreet et al. unpublished). If local Gulf of Mexico animals get infected with YHV and serve as reservoir hosts, hosts in which virus replicates, or as carrier hosts, hosts in which virus does not replicate but can be transmitted, the virus may both be endangering local penaeid shrimp stocks in the wild and in penaeid aquaculture facilities. Defining a representative carrier and reservoir host will provide a useful tool to investigate the threat of YHV to the natural biodiversity and to predict the future epidemics for YHD.

Genomic information is important in unveiling YHV replication and transcription strategies. By comparing the genomes of YHV and other nidoviruses, I analyzed the genomic profiles of YHV; by analyzing the natural recombination of YHV isolates collected on different years, I predicted the evolution of YHV and the interaction between YHV and global shrimp aquaculture.

Yellow Head Disease and Yellow Head Virus

History of YHD and YHV

YHD is a highly pathogenic disease. It was first recognized in Thailand in 1990 and was named for the gross signs of disease that included a yellowish cephalothorax and pale overall coloration of moribund, infected shrimp (Limsuwan 1991, Boonyaratpalin et al. 1993, Chantanachookin et al. 1993). Histologically, YHV infections can be easily recognized by densely basophilic inclusions, particularly in hematoxylin and eosin (H&E) stained gill sections (Flegel et al. 1997, Flegel 2006). Smears are useful in early stages of infection but not later when hemocyte populations have been depleted by the virus. YHV was first mistakenly considered to be a baculovirus (Chantanachookin et al. 1993, Wongteerasupaya et al. 1995a, Takahashi et al. 1996), but it was soon discovered during purification and characterization that some morphological features differed from that of baculoviruses (Wongteerasupaya et al. 1995a). By electron microscopy, thin tissue sections revealed the presence of unusual filamentous nucleocapsid precursors and much shorter, mature, rod-shaped, enveloped virions within the cytoplasm in necrotic lymphoid organ (LO) and gill cells, in masses underlying the cuticle of secondary gill lamellae, and in intercellular spaces. With negative staining, the virus particles were found to be enveloped with a halo of appendages characteristic of some RNA viruses. Then, it was found that the genome consisted of single-stranded (ss) RNA of positive sense (Wongteerasupaya et al. 1995a, Tang & Lightner 1999). Diagnostic probes were prepared by cDNA preparation and cloning (Tang & Lightner 1999) and reverse transcription polymerase chain reaction (RT-PCR) methods (Wongteerasupaya et al. 1997).

YHV-like viruses are found in wild and farmed penaeid shrimp. After the discovery of YHD, a virus morphologically indistinguishable from YHV, but characterized by spheroids within LO, was observed in healthy wild and farmed *P. monodon* in Australia in 1993-1994 and was named lymphoid organ virus (LOV) (Spann et al. 1995). Later, a disease with gross signs of a reddish host body and a brownish-pink discoloration of gills was subsequently observed in the summer seasons of 1995-1996, and the causative virus was named “gill-associated virus” (GAV) by its characteristic virions accumulating in abundance in the gills as well as in LO cells. The tissue distribution of GAV and histopathological alterations caused in LO and other tissues were very similar to those found in YHD, but the typical signs, including pale-yellowish coloration of the carapace and the rapid mortality, were not observed in shrimp infected with GAV. However, comparison of GAV from moribund shrimp and LOV from healthy shrimp indicated that they shared more than 97% sequence identity. Moreover, injection of filtered LO extract from LOV-infected *P. monodon* can induce acute GAV disease, and the diluted GAV inoculum prepared from moribund shrimp can result in an asymptomatic, chronic LOV-like infection that is primarily restricted to LO spheroid cells, indicating that GAV and LOV appear to represent the same virus recovered from chronic and acute infection states (Cowley et al. 2000).

Following the discovery of YHD, YHV-like virions were also detected commonly in healthy wild and farmed shrimp in Southeast Asia and the Indo-Pacific Region (see Munro & Owens 2007). Retrospective examination of earlier electron micrographs revealed the existence of virus in healthy broodstock prior to the emergence of YHD in Thailand (Flegel et al. 1995b). GAV infection was 98% in wild and farmed *P. monodon*

in Australia during 1997-1999 by the RT-PCR method (Cowley et al. 2000). Currently, there are at least 6 genotypes of YHV-like viruses detected, of which only YHV (genotype 1) and GAV (genotype 2) are pathogenic to penaeid shrimps. Genotype 1 was detected in Thailand, GAV/LOV (genotype 2) was detected in Australia, Thailand, and Vietnam, genotype 3 was detected in India, Malaysia, Mozambique, Taiwan, and Vietnam, genotype 4 was detected in India, genotype 5 was detected in Malaysia, Philippines, and Thailand, and genotype 6 was detected in Mozambique (Wijegoonawardane et al. 2008).

Screening the histologically diagnosed YHV-positive shrimp tissue from South Carolina, Texas, South and Central Americas using probe and RT-PCR, it was concluded that YHV was not present in America (Tang & Lightner 1999). But the frozen commodity shrimps imported from Asia were reported as YHV and white spot syndrome virus (WSSV) positive and the bioassay shrimp showed mortality after infected by either YHV or WSSV from the frozen commodity shrimps (Lightner et al. 1997, Durand et al. 2000). Recently, *Litopenaeus vannamei* cultured in salt and freshwater environments in Mexico along the Pacific coast were tested YHV-positive by RT-PCR and dot blot methods (de la Rosa-Vélez et al. 2006, Sánchez-Barajas et al. 2008). Moreover, WSSV and YHV have been detected by histological and PCR methods from penaeid shrimps in the Gulf of Mexico (Matthews & Overstreet, unpublished) before Hurricane Katrina in 2005, they apparently disappeared after hurricane for about 1.5 years, perhaps because of no shrimp processing plant was in operation during those period. Above data indicate that YHD may have emerged in Mexico or other American countries and the Gulf of Mexico.

The reason for the sudden emergence of a highly virulent YHV genotype in intensive *P. monodon* aquaculture in Thailand in the early 1990s remains unknown. Morphological, morphogenetic, pathological, and genetic evidences support that YHV may also have been involved in the crash of the shrimp farming industry in Taiwan in the mid-1980s (Chantanachookin et al. 1993, Walker et al. 2001). It is possible that YHD may have emerged from the asymptomatic chronic infections in *P. monodon* as a result of chance mutation or recombination event rather than host-switching of YHV because viruses in the YHV-complex display a strong natural host preference for *P. monodon* (see Cowley & Walker 2008). Pond densities and stock distribution networks in the intensive coastal aquaculture regions of Asia played an important role in accelerating outbreaks once YHD had emerged. Evidence showed that a low dose of GAV and YHV can develop a chronic persistent infection but escape disease (Flegel et al. 1995b, Anantasomboon et al. 2008). It is also known that changes in water pH or reduced dissolved oxygen can induce acute YHV infection in asymptomatic hosts (Flegel et al. 1995a). It is believed that YHV (genotype 1), like other genotypes, is a natural infection of *P. monodon* occurring at low prevalence as a chronic infection in wild populations before environmental stress factors can trigger acute replication of virus and produce acute morbidity and mortality (Cowley & Walker 2008).

Taxonomy

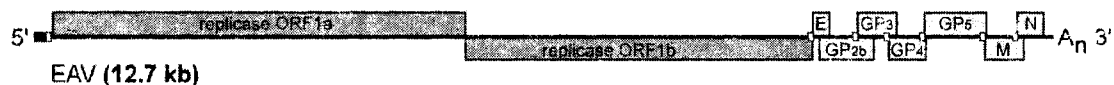
The order Nidovirales includes 3 families, Coronaviridae (consisting of the genera *Coronavirus* and *Torovirus*), Arteriviridae (consisting of *Arterivirus*), Roniviridae (consisting of *Okavirus*), and the unclassified genus *Bafinivirus*. The genus *Coronavirus* is further subdivided into 3 groups. Nidoviruses are enveloped, positive-sense, ss RNA

viruses that share similar genome organization (Figure 1) and replication strategy. However, they differ significantly from each other in terms of genome size (12.7 kb to more than 30 kb), virion morphology, host range, and various biological properties (Snijder & Meulenberg 1998, Gorbalenya et al. 2006, Siddell & Snijder 2008).

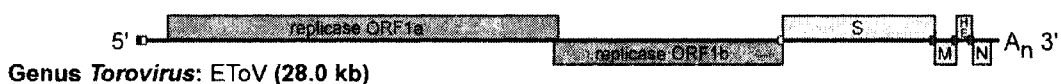
Nidoviruses have a linear ss RNA genome that contains a 5' cap structure and a 3' poly (A) tail (Figure 1). The nidovirus replicase gene comprises 2 large and overlapping open reading frames (ORFs) with each encoding a large replicase polyprotein, pp1a and pp1ab, respectively. These are proteolytically processed by 3 or 4 virus-encoded proteinases to produce the functional subunits, such as key viral enzymes like helicase and RNA-dependent RNA polymerase (RdRp) (Figure 2). Expression of the downstream ORF1b is mediated by a programmed -1 ribosomal frameshifting (RFS) just upstream of the ORF1a termination codon (Ziebuhr et al. 2000). A nested set of at least 2 (but usually 5 to 9) 3' co-terminal subgenomic (sg) mRNAs is produced in the infected cell to express the viral structural proteins and occasionally accessory proteins from genes located in the 3' -proximal third of the genome (the region downstream of ORF1b), which remains inaccessible for ribosomes translating the genome RNA (Figure 1). Generally, expressed are the ORFs contained within the 5' unique regions only of each mRNA, i.e. the regions not found in the next smallest mRNA. Arterivirus and coronavirus transcription is regulated by several transcription-regulating sequences (TRSs) that are located both at the 5' end of the genome and preceding each ORF in the 3'-terminal third of the genome (van Marle et al. 1999, Zúñiga et al. 2004, van den Born 2006). Transcription of the largest torovirus sg mRNA is presumably also regulated by such a TRS element. Transcription of all other torovirus sg mRNAs and each ronivirus sg

mRNA is regulated by TRS-like promoter element (Cowley & Walker 2002, van Vliet et al. 2002).

Arteriviridae



Coronaviridae



Roniviridae



Figure 1. The genome organization of Nidovirales. Images redrawn from van den Born (2006) and van den Born & Snijder (2008).

All nidoviruses are distinguished by a common backbone of conserved functional domains in their nonstructural proteins. This conservation can be identified as the linear arrangement of (a) 3C-like protease (3CLP) flanked by 2 hydrophobic transmembrane domains, (b) a large RdRp, (c) a zinc finger binding and helicase domains, and (d) a uridylate-specific endoribonuclease (UN) (Siddell & Snijder 2008). Depending upon the specific nidovirus family, this backbone may be adorned by additional functions, including 1 or more papain-like protease (PLPs), ADP-ribose 1' -phosphatase (ADRP), RNA primase, 5' -to-3' exonuclease (ExoN), 2' -O-methyltransferase (O-MT), and cyclic phosphodiesterase (CPD) (Table 1).

Based on virion morphology, YHV was originally named yellow-head baculovirus (YBV) (Boonyaratpalin et al. 1993, Chantanachookin et al. 1993). However, after the discovery of a >22 kb RNA genome, Wongteerasupaya et al. (1995a) suggested

that YHV was more likely a rhabdovirus or coronavirus. The YHV genome was confirmed to be ~ 22 kb in length and comprising ssRNA, possessing negative polarity and related to rhabdoviruses (Nadala et al. 1997). However, these data were refuted by evidence that viral RNA isolated from clarified shrimp hemolymph containing mature YHV particles only could be detected by in situ hybridization using an RNA probe of negative polarity with respect to a continuous ORF, or by RT-PCR using cDNA synthesized in this orientation, indicating that the YHV genome comprises positive sense ssRNA and that the virus could not be a rhabdovirus (Tang & Lightner 1999).

After finding that GAV has overlapped ORF1a and ORF1b coding the important replicase as other nidoviruses, and has 2 3' coterminal sg RNAs, Cowley & Walker (2002) regarded YHV and GAV as belonging to nidoviruses. Based on genomic organization and RNA transcriptional strategy, GAV was designated as the type species of a new genus *Okavirus* in the new family Roniviridae within the order Nidovirales (Mayo 2002, Sittidilokratna et al. 2002, Walker et al. 2005).

Evidences that support inclusion of GAV and YHV in the order Nidovirales include the following: (a) large genome (>26 kb) of ss (+) RNA with 3' polyA tail; (b) intracellular transcription of 2 3' coterminal sg RNAs and dsRNA equivalents; (c) the translation of polyprotein pp1ab through a -1 ribosomal frame shifting sequence characterized by a slippery sequence AAAUUUU and a large pseudoknot; and (d) the existence of a 3C-like proteinase (3CLP) domain in ORF1a and 'SDD' motif in RdRp, metal binding domain, helicase 1, and other domains in ORF1b as in Nidovirales.

Characteristics of Roniviridae

As a unique family in Nidovirales, Roniviridae has the following characteristics:

Table 1

Comparison of the characteristics of the Roniviridae with those of other families in Nidovirales.

	<i>Coronaviridae</i>	<i>Torovirus</i>	<i>Arterivirus</i>	<i>Bafinivirus</i>	<i>Okavirus</i>
Host	vertebrate	vertebrate	vertebrate	fish	crustacean
Virion					
architecture	spherical	discal or rod-shaped	spherical	rod-shaped	rod-shaped
envelope	+	+	+	+	+
envelope spikes	+	+	-		knob-like projection
nucleocapsids symmetry	helical symmetry	helical symmetry	icosahedral	helical symmetry	helical symmetry
virion size	120-160 nm	120-140 nm	45-60 nm		150 × 40 nm
spike glycoprotein (S)	180-220 kDa	200 kDa			
major surface glycoprotein (GP5)			30-45 kDa		
minor surface glycoprotein (GP2)			25 kDa		
minor surface glycoprotein (GP3)			36-42 kDa		
minor surface glycoprotein (GP4)			15-28 kDa		
large spike glycoprotein (gp116)					110-135 kDa
small spike glycoprotein (gp64)					60-65 kDa
membrane protein (M)	23-35 kDa	27 kDa	16 kDa		
small envelope protein (E)	9-12 kDa		9 kDa		25.4 kDa?
nucleocapsid protein (N)	50-60 kDa	19 kDa	12 kDa		20-22 kDa
hemagglutinin-esterase (HE)	65 kDa	65 kDa			

Table 1 (continued).

	<i>Coronavirus</i>	<i>Torovirus</i>	<i>Arterivirus</i>	<i>Bafivirus</i>	<i>Okavirus</i>
Genome					
(+) ssRNA	27.4-31.4 kb	28.5 kb	12.7-15.7 kb	26.6 kb	26.2-26.7 kb
sgRNA	7	4	6	3	2
ORFs	5-9	4-9	7		3-4
5'UTR	195-528 nt	858 nt	156-224 nt	905 nt	68-71 nt
5' leader	+	+/-*	+	+	-
slippery sequence	UUUAAAC	UUUAAAC	UUUAAAC	UUUAAAC	AAUUUUU
pseudoknot structure	2-3 helices	2 helices	2-4 helices	2 helices	4 helices
TM domain in pp1a	3	3	3	3	4
3CLP	+	+	+	+	+
PLP1	+	+	+	+	+
PLP2	+	+	+	?	?
UN	+	+	+	+	+
ExoN	+	+	-	+	+
O-MT	+	+	-	+	+
CPD	+/-	+	-	-	-
ADRP	+	+	-	+	-
RNA primase	+	?	?	?	?
3'UTR	231-645 nt	195 nt	59-151 nt	260 nt	129-316 nt

* Present in the longest of the 4 sgRNAs; 3C-like protease (3CLP), papain-like protease (PLPs), ADP-ribose 1"-phosphatase (ADRP), 5'-to-3' exonuclease (ExoN), uridylylate-specific endoribonuclease (UN), 2'-O-methyltransferase (O-MT), and cyclic phosphodiesterase (CPD).

- (a) members parasitizing invertebrates, especially penaeid shrimps (Cowley & Walker 2008);
- (b) rod-shaped rather than spheroidal or discal (Boonyaratpalin et al. 1993, Chantanachookin et al. 1993);
- (c) 5' untranslated region (UTR) short, 68-71 nt, without a typical 5' leader structure as seen in other nidoviruses (Dhar et al. 2004);
- (d) hydrophobic transmembrane (TM) domains 4 rather than 3 as in pp1a of Coronaviridae and Arteriviridae (Cowley et al. 2000, Cowley & Walker 2008);
- (e) genetic organization of structural proteins differ, e.g., nucleocapsid (N) protein is the first structural protein rather than the last as in members of Coronaviridae and Arteriviridae (van den Born & Snijder 2008); and
- (f) ORF4 truncated (Wijegoonawardane et al. 2008, Sittidilokratna et al. 2008).

Okavirus Genome Organization

The unique features of *Okavirus*, the type genus in the family Roniviridae (Mayo 2002), are listed in Table 1. The complete nucleotide sequences have been determined for the (+)sense ss RNA genomes of GAV (26,235 nt) and YHV (26,662 nt) (Cowley et al. 2000, Sittidilokratna et al. 2008). As shown in Figure 2, the GAV genome contains 5 long ORFs arranged in the order 5' -ORF1a/b-ORF2-ORF3-ORF4-3' and is polyadenylated at the 3' terminus (Cowley & Walker 2008). The ORF4 gene of *Okavirus* varies. In YHV, the ORF4 gene is truncated relative to GAV due to a nucleotide insertion near the 5' end of the gene (Sittidilokratna et al. 2008).

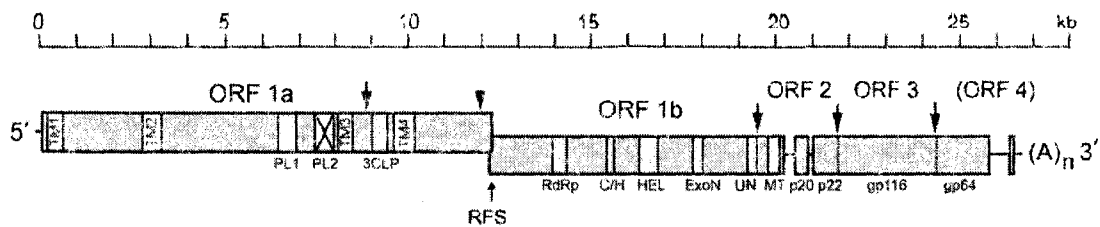


Figure 2. Schematic organization of *Okavirus*. Image redrawn from Sittidilokratna et al. (2008). Functional domains in ORF 1a: hydrophobic transmembrane regions (TM1-TM4), 3C-like protease (3CLP), papain-like protease (PL1), and a domain (PL2) homologous to PL1. Functional domains in ORF 1b: RNA dependent RNA polymerase (RdRp), cysteine- and histidine-rich domain (C/H), helicase (HEL), exoribonuclease (ExoN), uridylate-specific endoribonuclease (UN), and ribose-O-methyl transferase (MT). ORF2 encodes the nucleoprotein (p20, also N protein). ORF3 encodes a polyprotein post-translated to envelope proteins (gp116 and gp64) and N-terminal unknown protein (p22). The ribosomal frameshift sequence (RFS) allows read-through translation of pp1ab from ORF1a and ORF1b, with known (arrows) and possible (arrowhead) sites of proteolytic cleavage of polyproteins indicated.

Secondary Structure of Ribosomal Frameshifting Sequence

RNA pseudoknots are structural elements found in almost all classes of RNA. Pseudoknots form when a single-stranded region in the loop of a hairpin base-pairs with a stretch of complementary nucleotides elsewhere in the RNA chain. This simple folding strategy is capable of generating a large number of stable 3-dimensional folds that display a diverse range of highly specific functions in a variety of biological processes.

Nidoviruses produce 2 large replicase polyproteins, pp1a and pp1ab. Translation of ORF1a terminates at a translation stop codon in a region where ORF1a and ORF1b briefly overlap. Translation can either be terminated at the ORF1a stop codon or continued following a -1 RFS just upstream of this termination codon. RFS signals generally contain 2 elements: a heptanucleotide slippery sequence (XXXYYYN) and a

frameshift RNA pseudoknot, located 5-9 nt downstream the slippery sequence. In general, the slippery sequence consists of triplets of A, U or G residues, followed by the tetranucleotide UUUA, UUUU or AAAC (Jacks et al. 1988, ten Dam et al. 1990, 1994, Brierley 1995, Cowley et al. 2000, Giedroc et al. 2000, Sittidilokratna et al. 2002) (Figure 3). This type of -1 RFS signal has been identified in a number of virus groups, such as retroviruses (Jacks et al. 1988, Chamorro et al. 1992), double-stranded RNA viruses of yeast (Tzeng et al. 1992, Lopinski et al. 2000), astroviruses (Marczinke et al. 1994, Lewis & Matsui 1997), and luteoviruses (Prüfer et al. 1992). Among Nidovirales, the RNA elements responsible for RFS during nidovirus genome translation were first identified for infectious bronchitis virus (IBV), a member of group 3 coronavirus (Brierley et al. 1987, 1989, 1991). The frameshift signal of IBV consists of a heptanucleotide UUUAAAC stretch, which is highly conserved in coronaviruses, followed by an RNA pseudoknot (Figure 3L).

The primary structure of this pseudoknot apparently is not a determinant in the frameshifting mechanism. Frameshift-inducing pseudoknots similar to that of IBV were identified in coronavirus group 1 (Figure 3G & H) and group 2 (Figure 3I-K). A slippery sequence and downstream pseudoknot were also identified in the genome of the torovirus BEV (Figure 3F) and the recently sequenced *Bafinivirus* (Figure 3B), and both were similar to those in coronaviruses but with a relatively short connecting loop. RFS signals similar to those of coronaviruses were also predicted by some research groups studying arterivirus genomes (Figure 3C-E) (Snijder et al. 1990, Godeny et al. 1993, Snijder & Meulenberg 1998, Wootton et al. 2000).

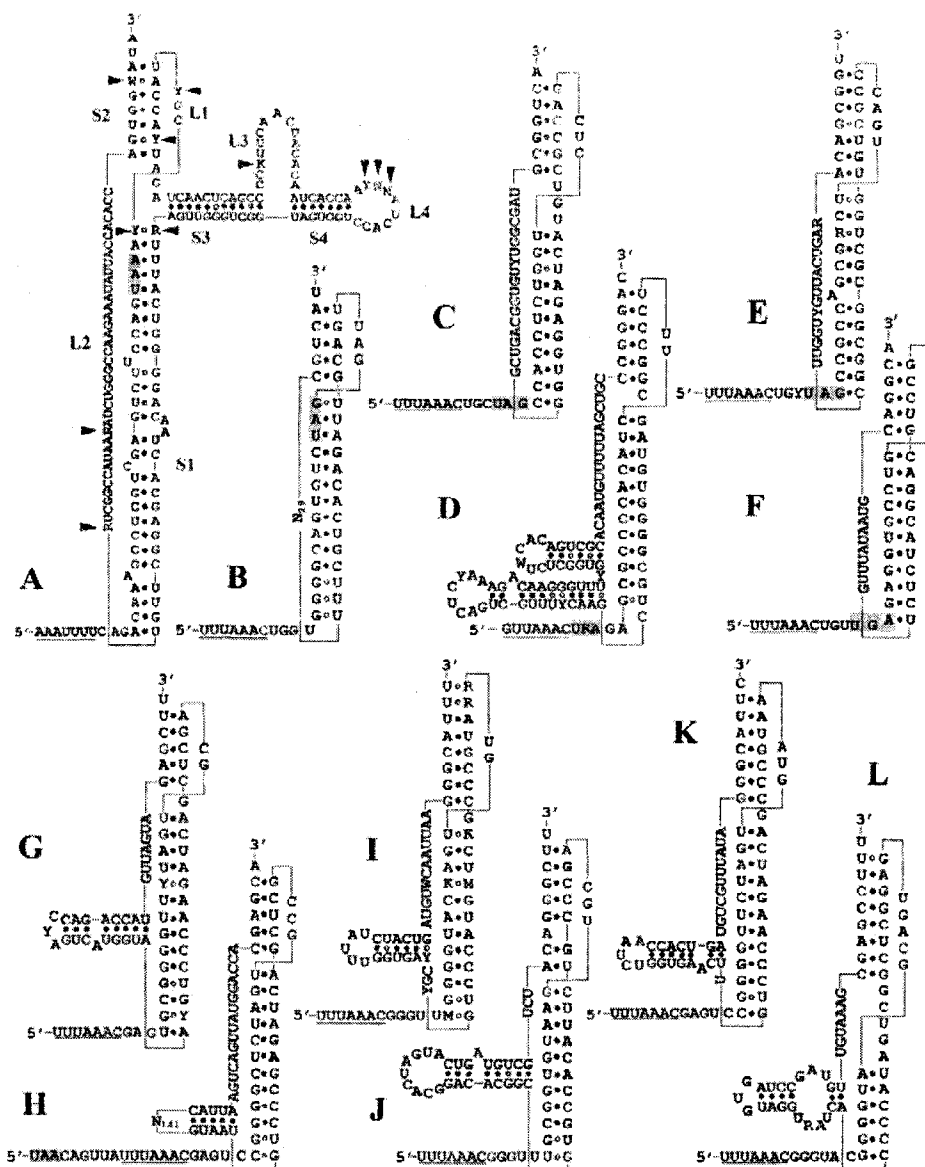


Figure 3. RNA secondary structure models for the ribosomal frameshift (RFS) sites in Nidovirales. (A) Roniviridae, arrowheads showing the compensatory base changes (CBC) and semi-CBC between yellow head virus (YHV) and gill-associated virus (GAV). (B) White bream virus (genus *Bafinivirus*) (from Schütze et al. 2006). (C) *Lactate dehydrogenase-elevating virus* (Godeny et al. 1993). (D) *Equine arteritis virus*. (E) *Porcine reproductive and respiratory syndrome virus*. (F) *Breda Torovirus*. (G) *Coronavirus* group 1. (H) Human coronavirus 229E. (I) *Coronavirus* group 2a. (J) SARS *Coronavirus*. (K) *Coronavirus* group 2c. (L) *Coronavirus* group 3.

Compared with other nidoviruses, the RFS of *Okavirus* has the following characteristics:

- (a) a unique “slippery” sequence AAAUUUU rather than UUUAAAC as in *Coronavirus*, *Torovirus*, *Bafinivirus*, and *Arterivirus* (only EAV has a GUUAAAC);
- (b) stop codon UAA of ORF1a occurs ~ 30-nt downstream of the slippery sequence; while the stop codon of coronaviruses locates upstream of the slippery sequence, in arteriviruses, the stop codon locates immediately 0-3 nt downstream slippery sequence, but in *Bafinivirus*, it is located 18 nt downstream from the slippery sequence;
- (c) more nucleotides involved in the formation of RFS than other nidoviruses (except human coronavirus 229E); and
- (d) 2 special stem and loop structures (S3, S4, L3, and L4) involving RFS formation (Figure 3).

In *Coronavirus*, there is a third stem-loop structure in addition to the pseudoknot (Figure 3G-L), whereas arteriviruses do not have this stem-loop (except for EAV); specifically, the stem-loop structure is different in position, nucleotide number and configuration.

Structural Protein Genes

Other distinguishing features of *Okavirus* genome organization are the number, order, and structure of genes encoding the structural proteins (Figure 2, Table 1). Okaviruses contain only 2 structural protein genes even though there are 3 putative genes. The ORF2 gene, encoding the N protein (p20), is located upstream of the glycoprotein gene rather than near the 3' end of the genome as in other nidoviruses; *Okavirus* ORF3 gene is unique in that it encodes a polyprotein from which the 2 structural glycoproteins

are released by posttranslational enzymatic cleavage (Cowley & Walker 2002, Jitrapakdee et al. 2003) (Figure 2). Proteolytic cleavage of ORF3 is also predicted to generate a small triple-membrane-spanning protein (p22 as in Figure 2) that is similar in size and structure to the integral membrane proteins M and 3a proteins of other nidoviruses. However, other nidovirus M and 3a proteins, encoded in discrete cistrons, are structural components of the virion, and have a membrane topology in which the N terminus is external. The *Okavirus* M-like protein is not a major component of virions and is predicted to have a membrane topology in which the C-terminus is external. Another unique characteristic of *Okavirus* is that the ORF4 is extremely truncated, with 20 amino acids in YHV, 36 amino acids in genotype 3 and 4, 37 amino acids in genotype 5, and 83 amino acids in GAV (genotype 2) (Wijeeonawardane 2007, Sittidilokratna et al. 2008).

Mechanism of Subgenomic RNA Synthesis

Transcription of a 3' -coterminial nested set of sg mRNAs is a prerequisite for classification within the order Nidovirales. In *Okavirus*, 3 mRNAs were detected, of which the first is a genome-length RNA (RNA1), the second is an ~ 6-kb sg mRNA, and the third is an ~ 5.5-kb sg mRNA.

An *Okavirus*-like transcription strategy of without 5' leader sequence appears to be employed to produce all but the largest of the *Torovirus* sg mRNAs (van den Born & Snijder 2008). However, the TRS present in the *Torovirus* intergenic region (IGR) is also highly conserved, and, like in okaviruses, directs the synthesis of sg mRNAs with 5' -AC dinucleotide termini (Cowley & Walker 2008).

The development of a reverse genetics system to rescue modified synthetic genomes, which in recent years has facilitated the analysis of the transcriptional mechanisms used by arteriviruses and coronaviruses (see Curtis et al. 2004, Yount et al. 2003, 2006, Masters & Rottier 2005, Deming & Baric 2008), may help explore the molecular mechanisms governing okavirus replication and transcription. However, such technology awaits establishment of a continuous cell line from shrimp or another crustacean that supports the replication of okaviruses.

Virion Morphology and Assembly

Okavirus virion is an enveloped rod-shaped structure with size of $150\text{-}200 \times 45$ nm (Boonyaratpalin et al. 1993, Chantanachookin et al. 1993, Lu et al. 1994, Spann et al. 1995, 1997, Wongteerasupaya et al. 1995a, Wang et al. 1996, Smith 2000). The lipid envelope is studded with regularly spaced projections, ~ 8 nm thick and up to 11 nm long. The internal nucleocapsid is a tightly coiled structure with a diameter of ~ 25 nm and a 5-7 nm helical periodicity. Unassembled nucleocapsids appear slightly smaller in diameter (14-18 nm), varying substantially in length from ~ 80 to over 800 nm (Chantanachookin et al. 1993, Spann et al. 1995). Nucleocapsids bud at endoplasmic reticulum/Golgi membranes or occasionally at the plasma membrane or nuclear envelope into cytoplasmic vesicles (Boonyaratpalin et al. 1993, Chantanachookin et al. 1993). Release of mature virions into intercellular space appears to occur primarily by the fusion of vesicles with the plasma membrane.

The *Okavirus* particle comprises 2 envelope glycoproteins, gp116 and gp64, and a p20 structural N protein that are associated with the genomic RNA to form the helical viral nucleocapsids (Jitrapakdee et al. 2003).

Transmission

Horizontal transmission of YHV in *P. monodon* occurs readily following cannibalism of infected carcasses and through exposure to infected shrimp tissue in sea water (Flegel et al. 1995b, Lightner et al. 1998). In high-density aquaculture systems, cannibalism of weak, infected shrimp is a common behavior and accounts for the rapid escalation of disease and mortalities after YHV and GAV introductions. YHV has also been transmitted to *P. monodon* by feeding the non-penaeid shrimps *Acetes* spp. and *Palaemon styliferus* collected from ponds affected by YHD (Flegel et al. 1997), implicating non-penaeid crustacean species as sources of infection. Feeding tissue of diseased shrimp to *P. monodon* postlarvae has also been shown to induce mortalities in 20-d postlarval (PL20) shrimp but not in PL15 shrimp, suggesting an age-related susceptibility of postlarvae to disease (Flegel et al. 1995b). Frozen commodity shrimps are 1 of the major routes by which YHV may be dispersed to other countries (Durand et al. 2000). Unlike TSV, however, feces of birds fed shrimp with YHD have not been shown to transmit disease, which might be expected since the virus particles possess a lipid envelope. The lipid envelope of YHV may be digested in the digestive tract of birds, suggesting that birds are unlikely to transmit YHV among ponds and farms by feces (Vanpatten et al. 2004). Recently, some marine microalgae have been shown to transmit WSSV (Liu et al. 2007), but whether such microalgae can transmit YHV to shrimp remains unknown.

Vertical transmission of GAV has been detected in *P. monodon* from wild and farmed individuals and may occur for YHV. Unlike YHV, GAV has been detected by RT-PCR in spermatophores and in mature ovarian tissue (Walker et al. 2001). In

spermatophores, in situ hybridization and TEM have identified the presence of virions in seminal fluid of adult males reared in captivity (Cowley et al. 2002). Furthermore, GAV levels detected in eggs, nauplii, protozoa, and PL5 suggested that transmitted virus was associated with the egg (Cowley et al. 2002). PCR detection showed that YHV and GAV at high prevalence in healthy postlarvae in hatcheries in Vietnam also suggested that virus transmitted in eggs from brooders is the likely source of infection (Phan 2001).

Host Range

YHV has been reported to infect a range of crustacean species. In addition to *P. monodon* (Flegel et al. 1995b, Flegel 1997, Walker et al. 2001, Dhar et al. 2004, Walker 2006, Cowley & Walker 2008), natural infections have been reported in *P. merguensis* and *Metapenaeus ensis* as well as the non-penaeids *Palaemon styliferus*, *Euphasia superba* (Flegel et al. 1995b, 1997). The Western Hemisphere species, *Litopenaeus stylirostris* and *L. vannamei*, are also susceptible to experimental infection, disease, and mortalities (Lu et al. 1994, Lightner et al. 1998). However, even though juvenile *Farfantepenaeus aztecus*, *F. duorarum*, and *L. setiferus* showed disease and mortalities when fed with YHV-infected shrimp carcasses, postlarvae are refractive to disease, indicating again that disease susceptibility is age- or stage-related (Lightner et al. 1998). *Metapenaeus ensis* and *Fenneropenaeus merguensis* can be infected by injection or exposure to membrane-filtered tissue extracts of YHV-infected *P. monodon* (Flegel et al. 1995b). The extracts of *Acetes* spp. from YHD-affected ponds can produce YHD in *P. monodon* by injection, indicating that non-penaeid species can serve as potential reservoirs of YHV. *Palaemon styliferus* was also shown to be a reservoir host to transmit YHV to *P. monodon* (Flegel et al. 1995b). Five palaemonid shrimp species,

Macrobrachium rosenbergii, *M. lanchesteri*, *M. sintangense*, *P. styliferus*, and *P. serrifer*, were experimentally exposed to YHV, and all but *M. rosenbergii* and *M. lanchesteri* were susceptible to YHV; however, natural infection has not been reported in those species (Longyant et al. 2005).

Shrimp Viral Diseases

Reservoir and Carrier Host Concepts

The term “reservoir host” refers to a host in which the agent replicates and the host serves as a reservoir of a virus able to infect another host of interest. A chronic infection in the reservoir host can provide long-term storage of virus between epidemics in penaeids. “Carrier hosts” are those vectors in which the virus does not replicate, but virus can remain active until departing the host or transmitted through food webs.

Pathogenicity and Virulence

“Pathogenicity” is the quality or state of being pathogenic, the potential ability to produce disease; whereas, “virulence” is the disease producing-power of an organism, or the degree of pathogenicity within a group. Pathogenicity is a qualitative term, an “all-or-none” concept; whereas, virulence is a term that quantifies pathogenicity (Shapiro-Ilan et al. 2005). These definitions readily apply to both lethal and non-lethal diseases.

Invertebrate pathologists commonly use dose-response bioassays to estimate virulence as LD50 or LC50 (dose or concentration needed to kill 50% of hosts exposed, Thomas & Elkinton [2004]).

Table 2

Penaeid viruses. (As of August 2008; modified from Lightner 1999).

Family	Virus	References
Nimaviridae (dsDNA)	white spot syndrome virus (WSSV)	Wongteerasupaya et al. 1995b
Baculoviridae (dsDNA)	Baculovirus penaei-type (BP)	Couch 1974, Broch et al. 1986
	Penaeus monodon-type (MBV)	Lightner 1983, Lester et al. 1987
	Baculoviral midgut gland necrosis virus (BMV)	Brock & Lightner 1990
	Type C baculovirus of <i>P. monodon</i> (TCBV)	Lightner 1996b
	Hemocyte-infecting nonoccluded baculo-like virus (PHRV)	Owens 1993F
Iridoviridae (dsDNA)	Shrimp iridovirus	Lightner & Redman 1993
Parvoviridae (ssDNA)	Infectious hypodermal and hematopoietic necrosis virus (IHHNV)	Lightner et al. 1983, Bonami et al. 1990
	Hepatopancreatic parvovirus (HPV)	Lightner & Redman 1985
	Spawner-isolated mortality virus (SMV)	Fraser and Owens 1996
	Lymphoidal parvo-like virus (LPV)	Owens et al. 1991
Dicistroviridae (ssRNA+)	Taura syndrome virus (TSV)	Brock et al. 1995, Hasson et al. 1995
Roniviridae (ssRNA+)	Yellow head virus (YHV)	Boonyaratpalin et al. 1993
	Gill-associated virus (GAV)	Spann et al. 1997
	Lymphoid organ virus (LOV)	Spann et al. 1995
Togaviridae (ssRNA+)	Lymphoid organ vacuolization virus (LOVV)	Bonami et al. 1992
Totiviridae (dsRNA)	Infectious myonecrosis virus (IMNV)	Lightner et al. 2004
Reoviridae (dsRNA)	Reo-like virus III	Tsing & Bonami 1997
	Reo-like virus IV	Hukuhara & Bonami 1991
Rhabdoviridae (ssRNA-)	Rhabdovirus of penaeid shrimp (RPSV)	Nadala et al. 1992
unknown	Laem-Singh virus (LSNV)	Sritunyalucksana et al. 2006

Important and Emerging Viral Diseases in Shrimps

The most economically important diseases of cultured penaeid shrimps are caused by infectious agents (Flegel 1997, Flegel & Alday-Sanz 1998, Lightner 1999). Since the first recognized shrimp virus, baculovirus penaeid type virus (BP), was reported (Couch 1974), over 20 shrimp viruses have been described (Lightner 1999; Table 2). Of those, infectious hypodermal and hematopoietic necrosis virus (IHHNV), Taura syndrome virus (TSV), WSSV, YHV, and baculoviruses have caused severe economic losses in the shrimp farming industry (Lightner 1999).

As a consequence of the rapid growth and development of the penaeid aquaculture industry, many of the most significant shrimp pathogens were moved from the regions where they initially appeared to new regions (Lightner 1996, Flegel & Alday-Sanz 1998). The viral diseases caused by IHHNV, TSV, and WSSV were all transferred before their etiology was understood and diagnostic methods were established. International trade accelerated the transmission of viral diseases between 2 hemispheres. Frozen commodity shrimp have been implicated as the route of spread of WSSV from Asia to Americas. TSV was transferred to Asia with infected live broodstock from Central America (Nunan et al. 1998, Durand et al. 2000, Yu & Song 2000, Nielsen et al. 2005, Do et al. 2006, Liu et al. 2007). Recently, after infectious myonecrosis virus (IMNV) was detected in Brazil in 2004 (Tang et al. 2005, Poulos & Lightner 2006, Poulos et al. 2006), this dsRNA virus was then detected in 2006 in Indonesia, where it caused serious disease (Senapin et al. 2007). The pandemic outbreaks due to the penaeid viruses have cost the shrimp industry billions of dollars, e.g., \$5-7 billion from WSSV,

\$1-2 billion from TSV, \$0.5 billion from YHV, and \$0.5-1 billion from IHHNV (Lightner 2003).

More recently, additional emerging diseases have been found in shrimp aquaculture, such as monodon slow growth syndrome (MSGs) that may be caused by Laem-Singh virus (LSNV) (Chayaburakul et al. 2004, Anantasomboon et al. 2006, Sakaew 2006, Sritunyalucksana et al. 2006, Prakasha et al. 2007), loose shell syndrome (LSS) (Mayavu et al. 2003, Gopalakrishnan & Parida 2005, Alavandi et al. 2007), and bamboo-shaped disease (BSD) (Sakaew 2006). Viruses may be the cause even though they are yet to be confirmed for these emerging diseases.

Shrimp Susceptibility to YHV and Antiviral Research

Penaeid cellular Receptors and Genes Related to Viral Infection

Shrimp defense mechanisms, including the signaling system, are poorly understood. Nonetheless, interest in understanding shrimp immunity has increased because of its importance in the control of diseases.

There are 2 putative cell receptors that have been cloned and analyzed. A Toll receptor gene has been cloned from *L. vannamei* (Yang et al. 2007). The Toll contains 926 residues, with a putative signal peptide of 19 residues expressed in many tissues, including hemocyte, gill, heart, brain, stomach, intestine, pyloric cecum, muscle, nerve, hypodermis, and sperm. A putative cell receptor for YHV of ~ 65 kilodalton (kDa) protein has been identified by using a virus overlay protein binding assay (Assavalapsakul et al. 2006). Double-stranded RNA corresponding to the coding sequence of this receptor has been shown to markedly reduce expression levels in LO cells and YHV RNA levels detected following virus challenge, indicating that this protein

plays a role in the intracellular transmission of YHV. However, whether it indeed functions directly as the YHV cell surface receptor or indirectly through co-association with heparin sulfate or glycosaminoglycans remains to be determined (Assavalapsakul et al. 2006).

Some penaeid shrimp pattern-recognition protein genes have been cloned. The β -1,3-glucan binding protein genes have been cloned from *P. monodon* (Sritunyaluksana et al. 2002) and *L. vannamei* (Romo-Figueroa et al. 2004, Cheng et al. 2005). Lipopolysaccharide gene has been cloned from *L. vannamei* by Cheng et al. (2005) and *L. stylirostris* by Roux et al. (2002). Lectin genes have been cloned from *P. monodon* by Luo et al. (2006) and *L. schmitti* by Cominetti et al. (2002). A defender against apoptotic death gene (DAD1), expressed in the hepatopancreas, hemocytes, and digestive tissue was recently cloned from *P. monodon* (Molthathong et al. 2008). Real-time RT-PCR with RNA extracts from hemocyte of *P. monodon* exposed to YHV revealed that the transcriptional level of DAD1 declined dramatically after YHV exposure. Moreover, an apoptosis-associated shrimp translational controlled tumor protein (TCTP) has a similar gene expression pattern to DAD1 in viral infected shrimp, suggesting that the DAD1 protein would be more likely to act in concert with other proteins in the control of apoptosis (Bangrak et al. 2004). Although this interaction suggests that DAD1 or TCTP may play a role in mortality caused by YHV, control of apoptosis is complex and involves the interaction of many proteins, few of which have been characterized for shrimp. Hence, the role of DAD1 awaits the description and characterization of other proteins.

Inhibition of YHV Replication by dsRNA and Morpholino

RNA interference (RNAi) is a dsRNA-induced gene silencing mechanism that is known to mediate antiviral responses in invertebrates, vertebrates, and plants (e.g., Cowley & Walker 2008). Recent studies demonstrated that introduction of dsRNA into shrimp prior to viral challenge can prevent viral propagation and shrimp mortality (Robalino et al. 2004, 2005, Tirasophon et al. 2005, Yodmuang et al. 2006, Tirasophon et al. 2007). Synthetic dsRNAs corresponding to regions in the 3CLP, RdRp, and helicase domains of the YHV replicase genes have shown to abrogate cytopathologic effects and substantially reduce viral RNA and gp116 levels in YHV-infected LO cells. Injection into juvenile shrimp with a 3CLP-specific dsRNA also inhibited YHV replication (Yodmuang et al. 2006). Both in LO cell culture and in shrimp treated *in vivo*, the sequence-specific inhibitory effects of dsRNA were dose dependent and sustained for up to 5 days (Tirasophon et al. 2005, Yodmuang et al. 2006). RNAi is considered a promising strategy for controlling viral diseases and has demonstrated in many organisms. However, many obstacles in development of the RNAi-based approach into a practical means of antiviral control need to be overcome. Delivery of dsRNA to target cells or tissues is one of the major bottlenecks in development of RNAi-based drugs and therapeutics (Tirasophon et al. 2007). Although injected dsRNA provides effective antiviral activity, it may not provide sustainable antiviral immunity in shrimps.

Antisense phosphorodiamidate morpholino oligomers (PMOs) are short chains of about 25 morpholino subunits with high binding affinity and exquisite specificity to mRNA. They can block translation initiation in the cytosol (by targeting the 5' UTR through the first 25 bases of coding sequence), can modify pre-mRNA splicing in the

nucleus, or can inhibit mRNA maturation and activity. Morpholinos are stable in cells and do not induce innate immune responses. The novel delivery systems like ‘endo-porter’ for cultured cells and vivo-morpholinos make it easy to deliver morpholinos into cells or animals (Summerton 1999, 2005, 2007, Bastide et al. 2006). The strong antiviral effect observed suggests that with further development, PMO may provide an effective therapeutic approach against a broad range of coronavirus and arterivirus infections (Neuman et al. 2005, 2006, van den Born et al. 2005, Burrer et al. 2007). However, as indicated above, morpholino delivery remains the major obstacle to overcome before this approach can be used to protect shrimp from viral infection.

Study Objectives

Can Some of the Crustaceans Commonly Found in the Gulf of Mexico Serve as Reservoir or Carrier Hosts for YHV?

Prior studies of local penaeids and locally processed imported commodity frozen shrimp products from Asia suggested that YHV may be introduced into local waters. If local Gulf of Mexico animals are getting infected with YHV, then the virus may be endangering local penaeid stocks and possibly other invertebrates. Moreover, if the virus infects local animals, it can also infect similar animals in Florida and Texas and endanger penaeid culture facilities located near shrimp processing plants in those states.

I will initiate experimental studies on some representative invertebrates to determine susceptibility to YHV (e.g., blue crab, fiddler crabs, stone crab, grass shrimps, penaeids, and other representative invertebrates). The animals will be fed and injected with YHV-positive tissue and homogenate, respectively. The samples (hemolymph and other tissues) will be collected and stored at -80 °C before RNA extraction. The YHV

infection will be detected by conventional PCR, semi-nested PCR or real-time PCR to determine whether these local crustaceans can serve as a representative reservoir host and carrier host being pathogenic or infective to the penaeids in the Gulf of Mexico.

How Long Can YHV in Shrimp Samples Be Stable For Diagnosis by RT-PCR?

It is of interest to know how long after collection YHV in shrimp samples can be detected by conventional RT-PCR. Shrimp farmers and managers usually care about how long the shrimp samples can be stored and still be useful for detection of viral pathogens.

Genome Analysis of YHV Isolated from Penaeus monodon

YHV is a disastrous agent to the shrimp aquaculture and causes serious economic losses compared with its congener GAV that had been completely sequenced in 2000. The whole genome of an early isolate collected in 1992 from Thailand is still not sequenced though it has been researched for bioassay, pathology, in situ hybridization, and molecular biology by most of the U.S. researchers in Arizona and Hawaii. Moreover, 2 YHV isolates from frozen commodity shrimp imported from Thailand in 1995 and 1999 proved to be able to infect and kill bioassay shrimp.

Sequencing and analyzing of these isolates collected from different years will enable us not only to understand the evolution and of this virus, but also provide us with information for the replication and transcription strategies for this virus.

Evolution of YHV through Natural Recombination

Recombination is a common phenomenon in viruses, especially RNA viruses. After sequencing different isolates of YHV collected from different years and different sources, I can predict how this virus evolves under natural environments using some

recently developed programs. I may analyze the putative divergence time when YHV emerged as a pathogenic agent to shrimp aquaculture.

CHAPTER II

DAGGERBLADE GRASS SHRIMP (*PALAEMONETES PUGIO*): A RESERVOIR
HOST FOR YELLOW HEAD VIRUS (YHV)

Abstract

Yellow head virus (YHV) is a major pathogen in penaeid shrimps. I surveyed small samples of 13 crustacean species in 8 families from 2 orders, commonly found in the Mississippi coastal area and freshwater environments for potential reservoir or carrier hosts of YHV using semi-nested PCR, without detecting any natural infection. The daggerblade grass shrimp, *Palaemonetes pugio*, and the blue crab, *Callinectes sapidus*, were exposed to YHV by injection and per os. The dynamics of YHV in the cephalothorax of daggerblade grass shrimp and in the hemolymph of blue crab were detected by semi-nested RT-PCR and qRT-PCR. The YHV replicated in daggerblade grass shrimp, causing 8% mortality (9/112) after injection. The viral titer in daggerblade grass shrimp reached a peak at 14 d post-inoculation (PI) and was still detectable on 36 d PI. The infection rate and viral load, however, in daggerblade grass shrimp were low when the virus was administered by feeding. Viral RNA in hemolymph of blue crab by injection was sustained at a low level for 3 d and expired after 7 d PI, and viral RNA by feeding reached a peak on 3 d PI, and was still detectable on 7 d PI, but became undetectable by 14 and 21 d PI. These data suggest that the daggerblade grass shrimp under some conditions could act as a reservoir host for YHV but that the blue crab cannot; the blue crab could serve as a poor carrier host.

Introduction

Yellow head virus (YHV) was first described from an epizootic infection in Thailand shrimp farms (Limsuwan 1991). Subsequent outbreaks of YHV have been reported from cultivated shrimp throughout Asia (Walker 2006). Infections have also been reported from frozen imported commodity shrimp in the United States (Durand et al. 2000, Ma & Overstreet, unpublished) and from 2 cultured penaeid shrimps, *Litopenaeus vannamei* and *Litopenaeus stylirostris*, along the west coast of Mexico (de la Rosa-Vélez et al. 2006, Sánchez-Barajas et al. 2008). As the cause of an important emerging shrimp disease, YHV has caused an estimated economic loss of \$500 million US from its discovery in 1991 until 2006 (Lightner, personal communication). The YHV and 2 other related viruses from Australia, gill-associated virus (GAV) and lymphoid organ virus (LOV), have been placed in the family Roniviridae of the order Nidovirales (see Cowley & Walker 2002, Gorbalenya et al. 2006).

Populations of grass shrimps (*Palaemonetes* spp., Palaemonidae, Decapoda) are important consumers and are the key prey for many crustacean and fish species. Among these grass shrimp species, the daggerblade grass shrimp, *Palaemonetes pugio*, living in habitats of shallow water in or around tidal marshes, submerged vegetation, and oyster reefs (Anderson 1985), is distributed in Atlantic and Gulf coasts from Massachusetts to Texas. They survive in salinity less than 1 to over 30-ppt (Heard 1982) and constitute more than 95% of all grass shrimps from estuarine tidal areas in many locations along the coast lines.

The blue crab, *Callinectes sapidus*, occurs commonly along the Gulf of Mexico; its natural distribution includes most coasts of the western Atlantic Ocean from Nova

Scotia to Argentina. It comprises 1 of the most valuable commercial fisheries in the U.S. (Kennedy et al. 2007). Recent research has shown that the blue crab can serve as a reservoir host for the white spot syndrome virus (WSSV) (Chapman et al. 2004, Matthews & Overstreet, unpublished).

Studies by Thai researchers on YHV carrier or reservoir hosts reported a limited number of hosts such as the sergestid *Acetes* sp. (Flegel et al. 1995a, b) and the palaemonids *Palaemon serrifer*, *P. styliferus*, *Macrobrachium sintangense*, and *M. lanchesteri* but not 16 species of crabs belonging to 6 families (Longyant et al. 2006). The purpose of this study was to probe the dynamics of YHV in the cephalothorax of daggerblade grass shrimp and the hemolymph of blue crabs by qRT-PCR after injection exposure and by semi-nested RT-PCR after per os exposure to evaluate their potential as reservoir and carrier hosts of YHV.

Materials and Methods

YHV Isolate

The YHV isolate (YHV92) used in this study was originally collected in 1992 from *Penaeus monodon* in Thailand; this viral isolate has been used by previous authors (e.g., Lu et al. 1994, 1997, Natividad et al. 1999, Tang & Lightner 1999). Partial sequences of this isolate were deposited in GenBank with acc. no. DQ978355-DQ978363 by de la Rosa-Vélez and colleagues. I sequenced the whole genome of this isolate and deposited the sequence in GenBank as acc. no. XXXXXX. YHV92 homogenate was prepared as follows: 10 g cephalothorax tissue was homogenized in 90 ml TN buffer, centrifuged at $1800 \times g$ and 4°C for 5 min. The supernatant was decanted and centrifuged again at $1800 \times g$ and 4°C for 5 min. The resultant supernatant was

centrifuged at $18000 \times g$ and $4\text{ }^{\circ}\text{C}$ for 20 min. This supernatant was then aliquoted into numerous 1.5 ml vials and stored at $-80\text{ }^{\circ}\text{C}$. In injection experiments, an aliquot was diluted with 2% saline and filtered through a $0.45\text{-}\mu\text{m}$ membrane. A $100\text{-}\mu\text{l}$ inoculum of 1:1000 diluted tissue homogenate of YHV92 was injected into the third abdominal segment of specific pathogen free (SPF) *Litopenaeus vannamei* (obtained from Shrimp Improvement System, Florida). When some shrimp became moribund 3 d post-inoculation (PI), the hemolymph was drawn using an EDTA-coated 1-ml syringe and samples were pooled as a reference stock of the virus. The pooled shrimp hemolymph and tissue samples were stored in aliquots at $-80\text{ }^{\circ}\text{C}$ until required.

Experimental Animals

During May-September 2007, I collected 13 species of crustaceans belonging to 8 families in 2 orders in the coastal areas and a freshwater bayou in Mississippi (Table 3). *Palaemonetes pugio*, 4 species of *Uca*, *Armases cinereum* and *Sesarma reticulatum* were collected from the coast near Ocean Springs, Mississippi ($30^{\circ}23'45.99''\text{N}$, $88^{\circ}48'36.53''\text{W}$); *Callinectes sapidus*, *Clibanarius vittatus*, *Menippe adina*, and *Squilla empusa* were captured near Deer Island, Biloxi, Mississippi ($30^{\circ}21'56.15''\text{N}$, $88^{\circ}50'14.03''\text{W}$); *Emerita talpoida* was collected from Horn Island, Mississippi ($30^{\circ}14'34.10''\text{N}$, $88^{\circ}39'44.29''\text{W}$); and *Palaemonetes kadiakensis* was collected from a bayou in Gulfport, Mississippi ($30^{\circ}28'16.68''\text{N}$, $89^{\circ}9'37.09''\text{W}$). After collection, the cephalothorax were tested for natural infection using semi-nested PCR, and then the uninfected animals were acclimatized in 19-l tanks containing artificial sea water (Marinemix, Houston) at the same salinity as the collection sites for 7 d before administration of YHV.

Virus Administration

Five Pacific white shrimp (*Litopenaeus vannamei*) (mean 12 g) were cultured individually in 19-l aerated tanks for 7 d. Blue crab hemolymph was drawn and the RNA extracted and tested for YHV, white spot syndrome virus (WSSV), and the dinoflagellate disease-agent *Hematodinium* sp. The blue crabs negative for YHV, WSSV, and *Hematodinium* were cultured individually in 19-l aerated tanks containing 20-ppt artificial sea water (Marinemix, Houston) for 7 d before being administered YHV. About 200 daggerblade grass shrimp were distributed equally among 10 19-l aerated tanks containing 20-ppt artificial sea water for 7 d before being administered YHV. Sixty Mississippi grass shrimp were cultured in 6 19-l aerated tanks containing freshwater for 7 d before being administered YHV. Crabs of genera *Uca* and *Sesarma* were cultured in tanks containing wet sand. For other crustaceans, 1-10 individuals, depending on animal size, were cultured in 19-l aerated tanks containing 20-ppt artificial sea water for 7 d before being administered YHV. These animals were fed once a day with commercial pelleted feed (size # 3, Rangen, Buhl, Idaho,); half of the sea water was changed every other day, and the temperature was controlled at 26 ± 0.5 °C by placing the tanks in a single water bath.

A 100- μ l inoculum of 1:1000 diluted homogenate of YHV92 with a total virus copy number of 2.36×10^4 (as determined by qRT-PCR) was injected into the third abdominal segment of 5 white shrimp, a 20- μ l inoculum of 1:100 diluted YHV92 homogenate with a 4.72×10^4 virus copy number was injected into 120 daggerblade grass shrimp and 60 Mississippi grass shrimp; a 200 μ l inoculum of 1:100 diluted homogenate of YHV92 with a total viral copy number of 4.72×10^5 was injected intra-muscularly (im)

into the propodus of the cheliped through the flexible arthrodistal membrane joining the dactyl in 5 blue crabs, and the same number of viral particles was also injected into the body cavity through the right rear coxa of 5 additional crabs. Other experimental animals were injected im with a total virus copy number of 4.72×10^4 .

In the feeding experiments, 5 blue crabs were fed 1 g of YHV-positive *L. vannamei* tissue for 3 consecutive d, and 50-70 μ l of hemolymph was drawn from each 6 h after the third feeding, which was recorded as 6 h PI. Thereafter, the blue crabs were fed pelleted food. Eighty grass shrimp were distributed among 4 tanks, and 1 g of minced YHV-positive tissue was introduced into each tank for 3 consecutive days of feeding after which the shrimp were switched to pelleted food. The same feeding protocol was applied to all other animals.

At 1, 3, 5, 7, 14, 21, and 36 d PI, 2 grass shrimp were randomly picked from each tank and stored in RNeasyTM (Ambion Inc.) at 4 °C overnight and then stored at -20 °C until RNA extraction. About 50-70 μ l of hemolymph from *L. vannamei* and *C. sapidus* was drawn into EDTA-coated 1 ml syringes at 6 h PI and at 1, 3, 7, and 14 d PI, and those samples were stored at -80 °C.

In all other species, 3 to 10 individuals were sampled on 3, 7, and 14 d PI and stored as indicated above.

Total RNA Extraction

Tissue RNA was extracted using the protocol from the High Pure Tissue RNA Kit (Roche). Briefly, the animals were rinsed with autoclaved distilled water, and 9-20 mg of cephalothorax tissue was sliced and homogenized in 400 μ l of lysis/binding buffer using a pestle in a 1.5 ml tube. After being digested in DNase I and washed, the RNA was

eluted into 100 µl of autoclaved RNase-free water and stored at -80 °C. Hemolymph RNA was extracted following the protocol from the High Pure Viral Nucleic Acid Kit (Roche). Briefly, 150 µl of autoclaved nuclease-free water was added to 50 µl of hemolymph and mixed with 250 µl of binding buffer containing poly A and proteinase K. The extracted RNA was eluted into 100 µl of autoclaved RNase-free water, measured using a Thermo Scientific NanoDrop™ ND1000 Spectrophotometer, and stored at -80 °C.

Semi-Nested RT-PCR

The non-stop, semi-nested RT-PCR was conducted using SuperScript™ III One-Step RT-PCR System with Platinum® Taq High Fidelity (Invitrogen) in 25 µl of reaction mixture containing 1.1 µM P64A1 (5'-CTA GGA TCG TTT GGC TTT GGT TC-3'), 0.1 µM P64S1 (5'-ATT ACA CCG CAG ACT TCA AGA CAA-3'), 0.2 µM P64S2 (5'-GTC TCC TCC TGA ATC CGC AT-3'), and 0.8 µM P64S3 (5'-TCA CTA TTA CTC CAG TTA TCA-3') (Kiatpathomchai et al. 2004). The reaction was initiated by reverse transcription at 50 °C for 30 min followed by transcriptase inactivation at 94 °C for 2 min. This procedure was followed by the sequential cycling protocols of (1) 5 cycles of 94 °C for 15 s, 60 °C for 45 s, and 72 °C for 1 min, followed by (2) 15 cycles of 94 °C for 15 s, 55 °C for 30 s, and 72 °C for 30s, followed by (3) 35 cycles of 94 °C for 15 s, 50 °C for 30 s, and 72 °C for 30 s, and finally by (4) 1 cycle of 72 °C for 5 min after which the reaction was placed on hold at 4 °C. Following amplification of the product, I examined 10 µl by electrophoresis in a 1.2% (w/v) agarose gel as stained with ethidium bromide and viewed on a FluorS MultiImage analyzer (Bio-Rad).

qRT-PCR

The iScript™ One-Step RT-PCR Kit for Probes (BioRad) was used to perform qRT-PCR with primers YHV141F: 5'-CGT CCC GGC AAT TGT GAT C-3', YHV206R: 5'-CCA GTG ACG TTC GAT GCA ATA-3' (Dhar et al. 2002), and YHV TaqMan probe: 5'-/FAM™/CCA TCA AAG CTC TCA ACG CCG TCA/TAMRA™-Sp-3' (Integrated DNA Technologies, Inc.). The standard was a 72 bp segment from a sequence (GenBank AF148846), which contained 66 bp amplicon with an extra 3 bp on both ends.

The qRT-PCR amplifications were undertaken in an iCycler Thermocycler (BioRad). The qRT-PCR was conducted in a 25 µl reaction volume containing 2 µl RNA, 12.5 µl 2 × RT-PCR reaction mix for probe, 300 nM of primers, 100 nM probe, and 0.5 µl iScript Reverse Transcriptase Mix for One-Step RT-PCR. The thermal profile of qRT-PCR was 10 min at 50 °C for cDNA synthesis, 5 min at 95 °C for iScript reverse transcriptase inactivation, 40 cycles of 15 s at 95 °C and 30 s at 56 °C (data collection step) for amplification then held at 4 °C (Ma et al. 2008).

Results

Natural and Administered Infection

Among the 13 species of crustaceans examined and tested for infection of YHV by semi-nested PCR (Table 3), I did not find any naturally occurring YHV in those tested. Using 1-step PCR, 2 species of palaemonids and the blue crab were positive and all other species of crustaceans tested negative. Although experimental infections from either feeding or injection of YHV had some species showing positive results using semi-nested PCR, they became negative by 14 d PI.

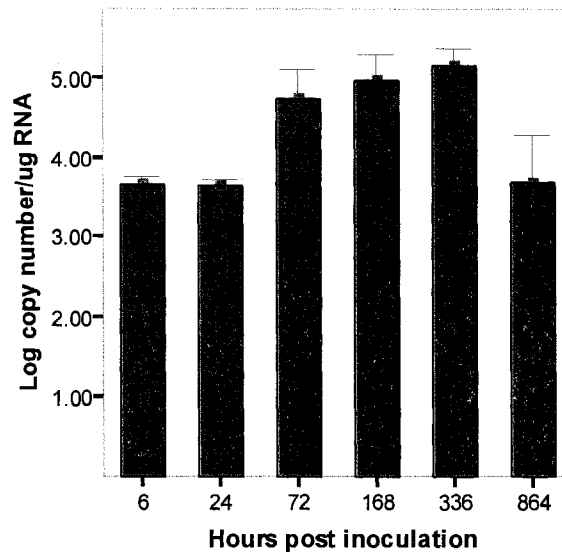


Figure 4. qRT-PCR quantification of YHV RNA levels in the grass shrimp *Palaemonetes pugio* at different time periods after injection. The log viral copy per μg RNA of combined data from 72-336 h PI is significantly higher than those of 6-24 h PI and 864 h PI, respectively ($P < 0.05$, one-way ANOVA).

Viral Dynamics in Palaemonetes pugio

A total of 20 *P. pugio* from the Davis Bayou, Ocean Springs, Mississippi, were examined for YHV using semi-nested RT-PCR, of which none was infected. In grass shrimp, PCR of YHV after im injection showed the viral copy number per μg RNA increased gradually during the 36 d period. The mean log viral copy number per μg RNA at 6, 24, 72, 168, 336, and 864 h PI was 3.659 ± 0.224 , 3.770 ± 0.428 , 4.770 ± 0.975 , 4.969 ± 0.817 , 5.142 ± 0.589 , and 3.681 ± 1.361 , respectively (Figure 4). The mean log viral copy number of per μg RNA in combined samples of 72-336 h PI was significantly higher than those of 6-24 h PI and 864 h PI, respectively ($p < 0.05$, one-way ANOVA).

Semi-nested RT-PCR also showed slightly brighter bands during the 3-14 d PI (Figure 5, lower panel). The mortality of im injected grass shrimp was 8% (9/112).

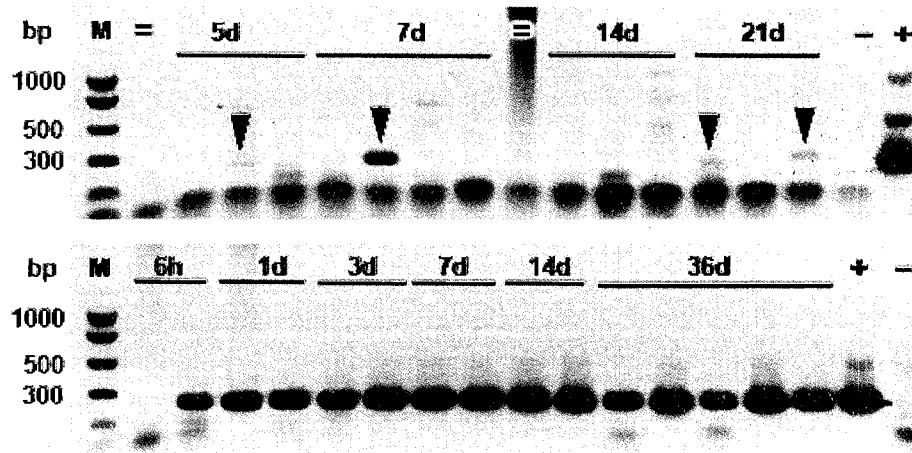


Figure 5. Semi-nested RT-PCR amplification of RNA from grass shrimp. Upper panel, fed; lower panel, injected. Lane M, 100 bp ladder DNA marker; +, positive control from *Litopenaeus vannamei* administered YHV; -, RNase-free water; =, shrimp injected with autoclaved saline for 5 and 14 d, respectively. Arrows show the faint infection of YHV.

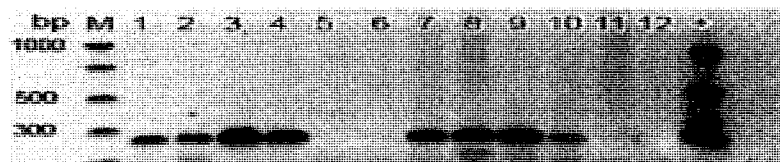


Figure 6. Semi-nested RT-PCR amplification of YHV in hemolymph of blue crab administered by feeding YHV-positive *Litopenaeus vannamei* tissue. M, 100 bp ladder DNA marker; 1-6, crab A; 7-12, crab B; +, positive control from *Litopenaeus vannamei* administered YHV showing 3 positive bands; -: negative control. 1, 7: 6 h PI; 2, 8: 1 d PI; 3, 9: 3 d PI; 4, 10: 7 d PI; 5, 11: 14 d PI; and 6, 12: 21 d PI.

Grass shrimp administered YHV orally did not demonstrate any mortality (0/80). The semi-nested RT-PCR showed that the viral load in fed individuals was lower than

that of injected ones (Figure 5). A few shrimp showed a faint positive result by semi-nested RT-PCR (Figure 5, arrowheads).

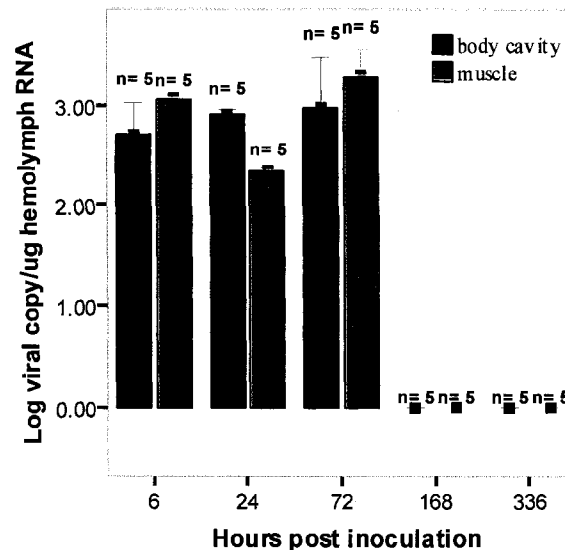


Figure 7. The qRT-PCR quantification of YHV RNA levels in hemolymph of blue crab at different times. 4.72×10^5 YHV copies was injected into the body cavity and muscle.

Viral Dynamics in Callinectes sapidus and Litopenaeus vannamei

A total of 30 *Callinectes sapidus* from Back Bay and Deer Island of Biloxi, Mississippi, were collected and examined for YHV using semi-nested RT-PCR, but none was infected. After these crabs were exposed to YHV-positive tissue per os, semi-nested RT-PCR was positive at 6 h PI, reaching the highest signal 3 d after the last feeding, with the signal becoming weaker at 7 d PI and undetectable at 14 d PI (Figure 6). The positive control (YHV-infected *Litopenaeus vannamei*) showed a strong signal of 3 bands; blue crab hemolymph showed 1 positive band, indicating that the viral load was low. The blue crab experienced different infection patterns after feeding and injection. The viral load in

blue crab hemolymph reached its peak on 3 d PI after the 3 d of feeding, but was still detectable 7 d PI. Thereafter, the viral number decreased to undetectable levels. When YHV was injected into the blue crab muscle or body cavity, viral load did not show a significant difference at 6, 24, and 72 h PI and the viral number did not increase to a peak as seen in crabs fed the virus. The viral load was undetectable in injected groups on 7 d PI.

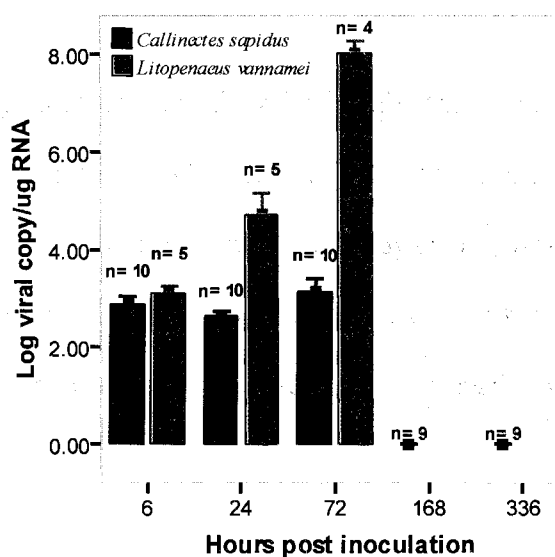


Figure 8. The qRT-PCR quantification of RNA levels in hemolymph of blue crab and white shrimp at different times. 4.72×10^5 and 2.36×10^4 copies of YHV were injected, respectively.

The mean log viral copy number per μg blue crab hemolymph RNA during the first 72 h is shown in Table 4 and Figure 7. There was no statistically significant difference between injection into the body cavity and muscle in regard to mean log viral copy number, so the 2 groups were combined; there also was no statistically significant difference among copy number at 6, 24, and 72 h PI. The results showed that YHV did

not replicate in the blue crab, but the number was sustained for 72 h after which the virus was rapidly eliminated. In contrast, YHV replicated quickly after being injected into *Litopenaeus vannamei*, and the initial mortality appeared before 72 h PI, with mortalities progressing to 100% before 120 h PI (Table 4, Figure 8).

Table 4

Comparison of YHV log viral copy/ μ g hemolymph RNA in *Callinectes sapidus* and *Litopenaeus vannamei* administered YHV.

Host	Time (h PI)	Injection site	N	Mean of log viral copy/ μ g RNA	SD
<i>Callinectes sapidus</i>	6	body cavity	5	2.70	0.710
	6	muscle	5	3.06	0.059
	6	total	10	2.88	0.511
	24	body cavity	5	2.92	0.104
	24	muscle	5	2.34	0.080
	24	total	10	2.63	0.318
	72	body cavity	5	2.97	1.106
	72	muscle	5	3.28	0.568
	72	total	10	3.12	0.844
<i>Litopenaeus vannamei</i>	6	muscle	5	3.08	0.364
	24	muscle	5	4.74	0.935
	72	muscle	4	8.04	0.432

Discussion

The term “reservoir host” as used here refers to a host in which the agent replicates and the host serves as a reservoir of virus able to infect a host of interest. In this case, the reservoir host daggerblade grass shrimp may serve as a source of YHV for commercial penaeid shrimps. The chronic infection in the grass shrimp can serve as a long-term reservoir of virus that can infect penaeids in areas without an abundance of free virus or during seasons when no other source would be available. “Carrier hosts” are

those vectors in which the virus does not replicate but it can remain active until departing the host.

Most tested penaeid shrimps are susceptible to YHV, such as *Farfantepenaeus aztecus*, *Farfantepenaeus duorarum*, *Fenneropenaeus indicus*, *Fenneropenaeus merguensis*, *Litopenaeus setiferus*, *Litopenaeus stylirostris*, *Litopenaeus vannamei*, *Metapenaeus affinis*, *Metapenaeus brevicornis*, *Metapenaeus ensis*, *Metapenaeus japonicus*, and *Penaeus monodon* (Flegel et al. 1995b, Flegel 2006, Wang et al. 1996, Lightner et al. 1997, Lu et al. 1997, Longyant et al. 2005). However, whether they are reservoir or carrier hosts is rarely reported. *Acetes* sp. and *Palaemon styliferus* may serve as reservoir hosts (Flegel et al. 1997). Longyant et al. (2005) screened 5 species of palaemonid shrimp, *Macrobrachium rosenbergii*, *Macrobrachium lancesteri*, *Macrobrachium sintangense*, *Palaemon styliferus*, and *Palaemon serrifer*, collected near farms containing *Penaeus monodon* in Thailand using RT-PCR and monoclonal antibodies specific to structural proteins of YHV, but they did not detect a natural YHV infection in any individual examined. After injection with YHV, a small proportion of *Macrobrachium lancesteri* showed mild YHV infections at 3 d but no infection at 10 and 30 d; *Macrobrachium sintangense*, *Palaemon styliferus*, and *Palaemon serrifer* were susceptible to YHV (Longyant et al. 2005).

To determine whether the daggerblade grass shrimp and blue crab serve as reservoir or carrier hosts, the 1-step primer usually did not work well because the YHV load was 1 to several log values lower than those in susceptible hosts (e.g., *Penaeus monodon* and *Litopenaeus vannamei*). This may be the reason why Longyant et al. (2006) did not detect YHV after 3 d in 16 species of crabs after injection. The more sensitive

semi-nested RT-PCR can grade infections into 3 levels depending on bands present on a gel (Kiatpathomchai et al. 2004) and serves as a more useful method than the 1-step primer method for detecting vector hosts. From our observations, the semi-nested RT-PCR is as sensitive as qRT-PCR; however, conventional 1-step RT-PCR can produce negative results when a 1-step primer is used to evaluate YHV in grass shrimp and blue crab fed the virus or even the early stages injected im. But the disadvantage to using the semi-nested RT-PCR method is that it may produce a false positive result because of high sensitivity. In an attempt to make the results comparable to those obtained by Kiatpathomchai et al. (2004) using their original semi-nested RT-PCR method for YHV, I decreased the number of amplification cycles in consideration of both sensitivity and specificity values.

In grass shrimp feeding experiments, the semi-nested RT-PCR amplification detected the virus in the cephalothorax on 5, 7, and 21 d PI, even though the viral concentration was low. There are several reasons that can cause this situation (1) some shrimp may consume more viral particles than others and (2) grass shrimp may have a different feeding habit from blue crab, consuming only a small amount of YHV-positive tissue. After im injection, the semi-nested RT-PCR still showed positive results at 36 d PI in 5 random samples with a viral load at about 10^4 copies μg^{-1} RNA. If the grass shrimp is preyed upon by susceptible hosts, there exist opportunities for penaeid shrimps as well as other hosts to acquire the infection.

Grass shrimp, penaeid shrimps, and the blue crab constitute the primary crustacean food source for fishes, crustaceans, and other animals in most estuarine habitats from Texas to Northeast Florida as well as along the Atlantic coast (e.g.,

Christmas & Langley 1973, Kneib & Wagner 1994, Rozas & Minello 2001, Granados-Dieseldorff 2006). As hypothesized by Odum et al. (1982), those crustaceans appear to represent a major link between detritus production in wetlands and coastal food webs.

Palaemonetes pugio is the primary dietary component for many fishes. For example, it dominates the diet of juvenile red drum (*Sciaenops ocellatus*). In Alabama, it occurs in 3 cm standard length (SL) fish and becomes the most important component in 4 to 7cm SL fish (Morales & Dardeau 1987), and it also contributes heavily to the diet of larger red drum in Mississippi (Overstreet & Heard 1978). Overstreet & Heard (1982) also report other inshore fishes in Mississippi as consumers of *Palaemonetes pugio* and *Palaemonetes vulgaris*. Predation of infected hosts by fishes results in infected feces, another source for infections in penaeids, grass shrimps, and other vectors.

Palaemonetes pugio is a permanent resident of the inshore estuaries. Commercial penaeids and the blue crab are not, but they use the estuaries as nurseries; the shrimps spawn offshore and the blue crab spawns near barrier islands. The grass shrimp feeds on postlarval blue crabs (Olmi & Lipcius 1991). Its behavior shows that it is not a “search and capture” predator but rather it depends on chance encounters and state of hunger (Morgan 1980); it also feeds on epiphytes, detritus, and algae (Quiñones-Rivera & Fleeger 2005). As trophic generalists with mixed diets, the grass shrimps as well as the shrimp and crab all feed on each other, depending on body size, habitat type, time of day and tide, and season. Penaeids have been shown to eat grass shrimps (e.g., Leber 1985, Kneib 1987), and the blue crab feeds on grass shrimps and other caridean shrimps as well as on penaeids, other blue crabs, and fishes (Laughlin 1979). Seasonal differences and overlapping of these different crustaceans in the northern Gulf of Mexico (e.g.,

Livingston 1984, 2004) allow continual feeding on each other and potential transmission of YHV and other agents.

The Mississippi grass shrimp, *Palaemonetes kadiakensis*, which is commonly found in freshwater environment in central and southern U.S. (Pennak 1978, Anderson 1985), also showed YHV-positive by 1-step and semi-nested RT-PCR after being either injected or fed. As a congener of the daggerblade grass shrimp, the Mississippi grass shrimp is also a potential reservoir host for YHV. Hence, both freshwater and brackish palaemonids from different continents seem to serve as reservoir hosts for YHV.

After administered YHV by injection, other animals, e.g., *Armases cinereum*, *Clibanarius vittatus*, *Emerita talpoida*, *Menippe adina*, *Sesarma reticulatum*, *Squilla empusa*, *Uca longisignalis*, *Uca panacea*, *Uca spinicarpa*, and *Uca virens*, were YHV-negative using 1-step PCR and by feeding using semi-nested PCR, demonstrating a low possibility for these animals to serve as reservoir or carrier hosts. Even though some crustacean species were tested positive after injection by semi-nested PCR, it appears that these crustaceans cannot harbor virus more than 7 d. For example, the commonly occurring 4 ocypodids and 2 grapsids in soft sand or mud near or around the edges of shallow salt marshes of Mississippi, the contaminated individuals, may not be important vectors for transmission of YHV.

Reasons for different infection patterns by feeding and injection in the blue crab are not clear. The individuals may have consumed YHV-positive tissue at different times. Even if they all consumed tissue at the same time, the viral number in the tissue may differ. Hence, the qRT-PCR may not be an exact method for evaluating virus in fed animals. One reason that YHV was lost more quickly from the hemolymph of blue crabs

injected rather than fed might be that the relatively large amount of virus injected all at once induced a rapid host response eliminating the virus. However, the fed virus may take longer to pass from the digestive tract to the hemolymph or it may have remained free in the hemolymph longer and not been sequestered as rapidly by host hemocytes.

CHAPTER III
STABLE YELLOW HEAD VIRUS (YHV) RNA DETECTION BY QRT-PCR
DURING SIX-DAY STORAGE

Abstract

Storage conditions of haemolymph samples which contain yellowhead virus (YHV) may result in a decline of YHV RNA concentration or false-negative results in the detection of YHV. I evaluated the stability of YHV RNA in haemolymph stored at different temperatures for 6 d with conventional RT-PCR and TaqMan qRT-PCR. Specific pathogen free individuals of *Litopenaeus vannamei* were challenged with YHV92TH isolate, and haemolymph samples of 3 groups of 10 pooled moribund shrimp were aliquoted and stored at 4 and 25 °C for 0, 2, 6, 12, 24, 48, 72, 96, 120, and 144 h. All samples were evaluated by conventional RT-PCR and qRT-PCR. After the optimization of experimental conditions, TaqMan qRT-PCR showed a very strong linear relationship between the log scale of the standard DNA copy number and the cycle threshold (C_T) values ($R^2 = 0.999$) over a 7-log range from 10^2 to 10^8 copy number per reaction. Even though the haemolymph was stored at either 4 or 25 °C for a 6-d period, the viral load number at 4 °C was not significantly different from that stored at 25 °C. The only difference was between the samples stored for 144 h at either 4 or 25 °C and those stored at -80 °C. I conclude that shrimp haemolymph can be drawn from shrimp at farms or in the wild and stored at either 4 or 25 °C for 3–5 d without a significant reduction in measured YHV RNA levels and without having to immediately freeze the samples.

Introduction

Yellow head virus (YHV), lethal to most commercially cultivated penaeid shrimp species (Walker 2006), was first described as an epizootic from Thai shrimp farms (Limsuwan 1991); subsequent outbreaks of YHV have been reported from cultivated shrimp in many locations in Asia (Walker 2006). The YHV agent has been reported from frozen imported commodity shrimp in the United States (Nunan et al. 1998, Durand et al. 2000) and from *Litopenaeus vannamei* (according to Pérez Farfante & Kensley [1997], also referred to as *Penaeus vannamei* by others [Flegel 2007]) and *L. stylirostris* cultured on the northwest coast of Mexico. (de la Rosa-Vélez et al. 2006). As an important shrimp emerging disease, YHV has caused an estimated economic loss of \$500 million since its discovery in 1991 until 2006 (Lightner, personal communication). The YHV and 2 other related disease-causing viruses from Australia, gill-associated virus (GAV) and lymphoid organ virus (LOV), have been placed in the family Roniviridae of the order Nidovirales (Cowley & Walker 2002, Gorbalenya et al. 2006).

Many molecular methods have been developed to diagnose YHV such as conventional RT-PCR (Wongteerasupaya et al. 1997, Cowley et al. 2004, Kiatpathomchai et al. 2004), gene probe (Tang & Lightner 1999, Tang et al. 2002, 2007), qRT-PCR (Dhar et al. 2002), and loop-mediated isothermal amplification (LAMP) (Mekata et al. 2006). Among these, qRT-PCR has become the “gold-standard” for various research and clinical studies because of its sensitivity and specificity.

Hemolymph has been widely used as the source of material to assess acute shrimp viral diseases, especially the viral dynamics and host gene expression after viral challenge. A common protocol was to draw the hemolymph quickly and to store it at -70

°C or liquid nitrogen as soon as possible. The question remained whether the hemolymph drawn at a shrimp farm or some other sites distant from the testing laboratory and stored at either 4 °C or room temperature for 3–5 d would still contain active YHV or a high enough copy number for diagnosis. The objective of this study was to determine whether hemolymph was still useful for diagnosis and quantification of YHV using conventional and qRT-PCR after being stored at different temperatures and time periods.

Materials and Methods

Experimental Challenge and Sample Storage

A 100 µl inoculum of 1:1000 diluted homogenate of YHV isolate TH92 was injected into the third abdominal segment of 30 specific pathogen free (SPF) shrimp (*Litopenaeus vannamei*, Kona TSV-sensitive stock, Oceanic Institute, average 15 g). These shrimps were fed once a day with commercial pelleted feed (Rangen, Buhl, Idaho) divided among 6 aerated 19-l aquariums containing 20 ppt artificial seawater, maintained in a water bath at 26.0 ± 0.5 °C. When some shrimp became moribund after 3 d post-inoculation, the hemolymph from 3 random groups of 10 shrimp each was drawn into an EDTA coated 1-mL syringe and then pooled, producing 3 sample groups. Then 21 aliquots of 50 µl hemolymph were collected from each sample group. They were divided by storing 9 aliquots at 4 °C, another 9 aliquots at room temperature (~25 °C), and the remaining 3 aliquots at -80 °C. At 2, 6, 12, 24, 48, 72, 96, 120, and 144 h of storage, 1 subsample from each aliquot of the 3 sample groups at 4 and 25 °C (for a total of 54 subsamples with an additional 9 subsamples at -80 °C) was randomly picked and stored at -80 °C until analysis.

Total RNA Extraction

Hemolymph RNA was extracted following the protocol of the High Pure Viral Nucleic Acid Kit (Roche). Each stored 50 µl hemolymph aliquot had 150 µl autoclaved RNase-free water added; this solution was mixed with 250 µl binding buffer working solution containing poly A and proteinase K. The RNA was then eluted into 100 µl of autoclaved RNase-free water and stored at -80 °C.

Conventional RT-PCR

Conventional RT-PCR was processed following the protocol of SuperScript™ III One-Step RT-PCR System with Platinum® Taq High Fidelity (Invitrogen) in which the following primers were added: primer 273F: 5'-CAA GAT CTC ACG GCA ACT CA-3' and 273R: 5'-CCG ACG AGA GTG TTA GGA GG-3' (Tang & Lightner 1999). The total RNA extracted was incubated at 50 °C for 30 min to synthesize the cDNA. Inactivation of the reverse transcriptase at 94 °C for 2 min was followed by 40 cycles of denaturation at 94 °C for 15 sec, annealing at 55 °C for 30 sec, and extension at 68 °C for 30 sec. A final extension step at 68 °C for 5 min completed the reaction after which it was held at 4 °C.

qRT-PCR

The iScript™ One-Step RT-PCR Kit for Probes (BioRad) was used to perform qRT-PCR with primer YHV141F: 5'-CGT CCC GGC AAT TGT GAT C-3', YHV206R: 5'-CCA GTG ACG TTC GAT GCA ATA-3' (Dhar et al. 2002) and YHV TaqMan: 5'-/FAM™/CCA TCA AAG CTC TCA ACG CCG TCA/TAMRA™-Sp-3' (Integrated DNA Technologies, Inc.). The positive control used for the standard curve was a 72-bp synthesized oligo (Invitrogen Co.) which contained the 66-bp amplicon and an extra 3 bp

on both ends based on GenBank accession no. AF148846. A gradient cycler (PTC200 DNA Engine) was used to adjust the annealing temperature to an optimal condition before performing qRT-PCR. The amplification products were separated using 2% agarose gel electrophoresis and analyzed with a Fluor-STM MultiImager (BioRad). The qRT-PCR was optimized by using salt-free YHV positive oligo and different concentrations of primers and probe.

The qRT-PCR amplifications were undertaken in an iCycler Thermocycler (BioRad). The qRT-PCR was conducted in duplicate, with each 25- μ l reaction volume containing 2 μ l RNA (= 1 μ l original hemolymph), 12.5 μ l 2 x RT-PCR reaction mix for probe, 300 nM of primers, 100 nM probe, and 0.5 μ l iScript Reverse Transcriptase Mix for One-Step RT-PCR. The thermal profile of qRT-PCR was 10 min at 50 °C for cDNA synthesis, and 5 min at 95 °C for iScript reverse transcriptase inactivation, with 40 cycles of 15 sec at 95 °C and 30 sec at 56 °C (data collection step) for amplification.

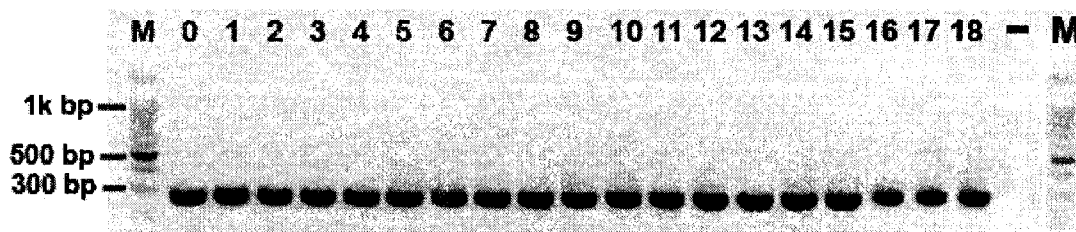


Figure 9. Conventional RT-PCR amplification of RNA from aliquoted hemolymph from *Litopenaeus vannamei* stored at different temperatures over 6 days. M, 1k bp DNA ladder (Promega, G829A); lane 0, stored at -80 °C; lanes 1, 3, 5, 7, 9, 11, 13, 15, and 17 are samples stored at 25 °C for 2, 6, 12, 24, 48, 72, 96, 120, and 144 h, respectively; lanes 2, 4, 6, 8, 10, 12, 14, 16, and 18 are samples stored at 4 °C for 2, 6, 12, 24, 48, 72, 96, 120, and 144 h, respectively.

Results

RT-PCR

When RNA samples were tested for YHV by the conventional RT-PCR method, subsamples of all 3 groups tested YHV-positive during the 6 d storage at 4 and 25 °C; Figure 9 shows the RT-PCR result for 1 group of subsamples during the 6 d storage at 4 and 25 °C.

qRT-PCR

The TaqMan qRT-PCR method showed a very strong linear relationship between the log scale of the standard DNA copy number and cycle threshold (C_T) values ($R^2 = 0.999$) over a 7-log range from 10^2 to 10^8 copy numbers per reaction (Figure 10). The PCR efficiency was as high as 95.4 %.

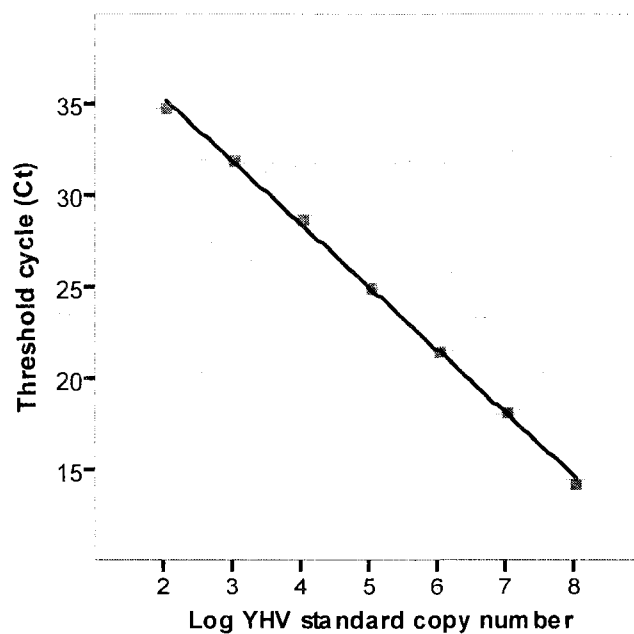


Figure 10. Standard curve generated from qRT-PCR and a 10-fold dilution series. $R^2 = 0.999$, $\hat{Y} = -3.436 X + 42.203$.

Even though the hemolymph subsamples were stored at 4 and 25 °C for a 6 d period, the viral load numbers at 4 °C were not significantly different from the corresponding value at 25 °C as analyzed by 2-way ANOVA (Figure 11). The only statistical difference was between the samples stored for 144 h at both 4 and 25 °C and those stored at -80 °C.

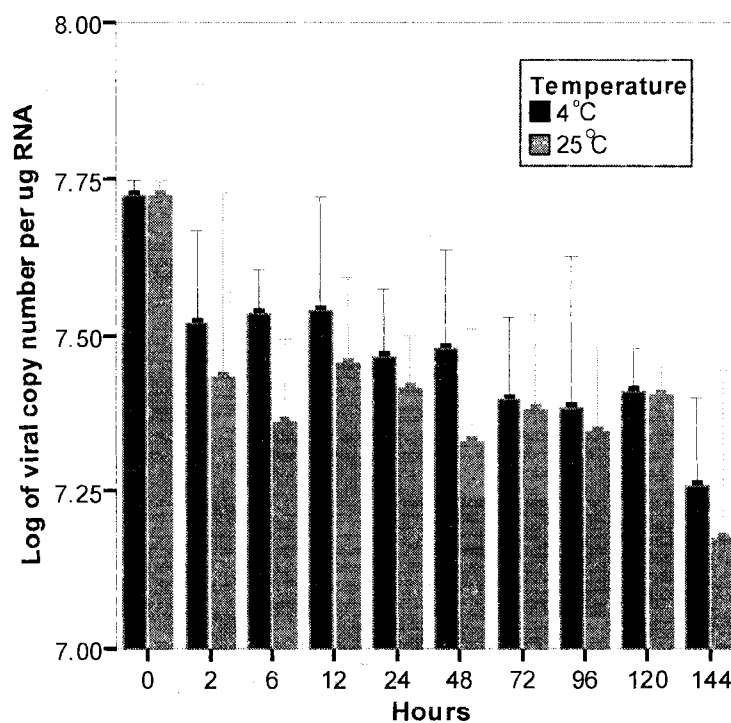


Figure 11. Quantitative analysis of log scale in *Litopenaeus vannamei* hemolymph at 4 and 25 °C for 6 d storage. Bars exhibit mean value, and error bars express mean \pm 1 SE.

Discussion

The real-time PCR method has been graded as the “gold-standard” for pathogen detection, gene expression, and various studies because of its simplicity, sensitivity, and reproducibility as well as its amenability to high-output screening and ability to

accurately quantify infection levels (Mackay et al. 2002, Espy et al. 2006, Rajendran et al. 2006, Watzinger et al. 2006, Belák 2007). Consequently, several qRT-PCR (or qPCR) protocols have been developed for viral RNA/DNA detection, including those by either TaqMan probe or SYBR Green chemistry for infectious hypodermal and hematopoietic necrosis virus (IHHNV) (Dhar et al. 2001, Tang & Lightner 2001), WSSV (Dhar et al. 2001, Durand & Lightner 2002), Taura syndrome virus (TSV) (Dhar et al. 2002, Mouilletteaux et al. 2003, Tang et al. 2004), YHV (Dhar et al. 2002), GAV (de la Vega et al. 2004), Mourilyan virus (Rajendran et al. 2006), and infectious myonecrosis virus (IMNV) (Andrade et al. 2007). However, the viral copy number in different tissues or different host individuals may vary significantly and can not provide reasonably comparable data. Many factors may affect results significantly such as the time point when the sample was collected, tissue type, viral dose administered, administration methods (per os or muscularly), RNA extraction method, and other aspects of qRT-PCR. Theoretically, TaqMan probe has more advantages over SYBR Green chemistry because its high specificity and stability can reduce the possibility of false-positive results produced by SYBR Green. More simplified qRT-PCR kits for probes obtained from different companies allows qRT-PCR to be used easily as a routine standard method for pathogen detection in shrimp. Even though most of the cited authors claimed that qPCR can detect as few as 10 copies of a viral molecule, one should be very cautious when interpreting data because the linear quantification may not be reliable at that level due to inevitable inconsistencies in the distribution of specific target molecules in the aliquot added to the reaction. At the same time, pipetting procedures and the experimental environment can also increase inconsistencies. When samples have about 10 copies of the

viral molecule, a more reliable detection can be achieved by running a gel together with the negative control sample and determining whether an inconsistency results from a non-specific amplification or a primer dimer.

Our conventional RT-PCR results agreed well with those of qRT-PCR because large amounts of virus occurred in hemolymph, e.g., 5.0×10^7 copies/ μg at 0 h and 1.5×10^7 copies/ μg at 144 h storage. When viral loading in the hemolymph is relatively low, conventional RT-PCR may not detect the viral copies that would be detectable by qRT-PCR (e.g., Chen et al. 2007).

Suboptimal storage temperatures may affect YHV RNA stability and influence viral load measurements. From our experiment, the YHV copy number of aliquoted samples was not statistically significantly different when samples were stored at 4 or 25 °C for a 5 d period, even though a statistically significant difference existed between the samples stored for 6 d (144 h) at both 4 and 25 °C and those immediately stored at -80 °C after being collected and aliquoted. This result for YHV may be consistent with that of hepatitis C virus (HCV) RNA, even though both viruses belong to different orders. Some reports have claimed that HCV RNA in serum is stable for at least 3–4 d at 4 °C or room temperature (Krajden et al. 1999a, b, de Gerbehaye et al. 2002). Also, the concentration of HCV RNA remained stable in serum specimens subjected to 3 to 8 freeze-thaw cycles (Krajden et al. 1999a). Grant et al. (2000) reported that infected whole blood anticoagulated with EDTA or CPDA-1/EDTA could be stored for 5 d at ≤ 25 °C without any significant loss in the plasma HCV RNA level. Moreover, Kiatpathomchai et al. (2004) used Isocode (R) filter paper to store dried hemolymph for YHV semi-nested PCR for up to 6 months at room temperature.

Different studies using different blood collection tubes and different processing times are not really comparable. The general profile of both HCV and YHV virions may be more stable than previously thought. The reason could be because the stable virion can protect viral RNA from being degraded by chemical factors in hemolymph, as the host hemocyte RNA can breakdown and degrade more easily than the RNA in an active virion. Unfortunately, no data are available about how long YHV particles retain infectivity in the environment. When in water, isolated TSV is infective for over a month in 25 ppt salinity, but the DNA virus WSSV becomes inactive in less than 1 h (unpublished). One experiment showed that the avian influenza virus (H6N2) having a 1×10^6 mean tissue-culture infective dose can persist at 17 °C in 0 ppt at pH 8.2 for 100 d and at 28 °C in 20 ppt at pH 8.2 for 9 d (Stallknecht et al. 1990). Consequently, environmental factors influence the persistence of viral infectivity.

The practical aspects of our experiment show that hemolymph 1) can serve as an important diagnostic medium; it can be drawn at a shrimp farm and kept at either 4 or 25 °C and then delivered to a reference laboratory for diagnosis or viral quantification and 2) does not have to be stored in RNA stabilization buffers (e.g. RNAlater™ or PrepProtect™ Stabilization Buffer) if it is used specifically for viral PCR or viral quantification as long as the viral RNA can be extracted from it within 5 d before being analyzed or stored at -80 °C until analysis can be performed.

Because *Penaeus monodon* is highly susceptible to WSSV, more and more Asian shrimp farms are switching from *P. monodon* to *L. vannamei* as their animal for culture (Wyban 2007). However, because the naïve *L. vannamei* is also susceptible to YHV (Lu et al. 1994, 1995, Lightner 1996a), shrimp farmers, managers, and researchers should be

very cautious to avoid reemergence of the pandemic YHV disease in Asian shrimp farms. As a valuable tool, qRT-PCR can be used as a routine protocol for surveillance and diagnosis of YHV in shrimp farms and hatcheries.

CHAPTER IV
GENOME ANALYSIS OF THREE ISOLATES OF YELLOW HEAD VIRUS (YHV)
AND PHYLOGENY OF NIDOVIRALES

Abstract

Yellowhead virus (YHV) is a major pathogenic nidovirus in penaeid shrimps. I sequenced the genome of 3 isolates from *Penaeus monodon* obtained from Thailand in 1992, 1995, and 1999. The genome of the 3 isolates is 26,673, 26,662 and 26,652 nt in length, respectively. They share identical 5' UTR, ribosomal frameshifting sequence, and a partial fragment of the 3' UTR. The 5 available genome sequences of Okaviruses share 79.3-99.0% nucleotide and 81.8-98.9% amino acid identities within ORF1a, 81.9-99.2% of nucleotide and 88.3-99.5% amino acid identities in ORF1b, 78.6-99.3% of nucleotide and 82.9-99.3% amino acid identities in ORF2, and 72.7-99.5% nucleotide and 75.9-99.3% amino acid identities in ORF3. The only indel event in the coding region for the 4 available isolates of YHV locates in the 5' end of ORF1a, containing a segment of 12 nt (CUAGCCUCUCAG) with 4 corresponding amino acids. Other indels locate in the non-coding region. I predicted 4 hydrophobic transmembrane domains of ORF1a in okaviruses, and that 3' UTR would form a putative pseudoknot. A potential octonucleotide motif UGAAUAGC in the pseudoknot of 3' UTR of *Okavirus* may be a counterpart of the octonucleotide (GGAAGAGC) found in the 3' UTR of *Coronavirus*. The phylogeny of Nidovirales reconstructed by composition vector analysis based on 48 nidovirus proteome sequences, demonstrated a consistency with the contemporary phylogeny.

Introduction

Nidoviruses, among the largest RNA viral groups, excite an increasing amount of research interest, not only because they are associated with severe diseases, but also because they exhibit extraordinary genetic complexity (Siddell & Snijder 2008). Twenty years after publication of the first complete nidovirus genome sequence, the public databases include about 408 full-length and thousands of partial nidovirus sequences listed as of April 2008. The most extensive sequencing efforts started very recently, after the severe acute respiratory syndrome (SARS) outbreak in 2003. This trend increased with the higher efficiency of sequencing techniques and available nidovirus sequences as references.

As a unique family in Nidovirales, Roniviridae has the following characteristics: (a) members parasitizing invertebrates, especially penaeid shrimps; (b) morphologically rod-shaped rather than spheroidal or discal; (c) a short 5' untranslated region (UTR) composing only 68-71 nt, without a typical 5' leader structure as seen in most other nidoviruses (Dhar et al. 2004); (d) 4 hydrophobic transmembrane (TM) domains other than 3 TMs in pp1a (Cowley et al. 2000, Cowley & Walker 2008); (e) different genetic organization of structural proteins, e.g., N protein being the first structural protein rather than the last one as in Coronaviridae and Arteriviridae; and (f) a truncated ORF4 (Sittidilokratna et al. 2008, Wijegoonawardane et al. 2008). Among Roniviridae, the yellowhead virus (YHV) complex in the genus *Okavirus*, contains isolates that have caused serious economic loss to the shrimp farming industry and they exhibit genetic diversity with diverse pathogenic effects (Limsuwan 1991, Lightner & Redman 1998, Lightner et al. 1998, Dhar et al. 2004, Walker 2006). Recent data show that there are at

least 6 genotypes of YHV-complex distributed in farmed shrimps from the Asian regions (Cowley & Walker 2008, Wijegoonawardane et al. 2008). Another rod-shaped virus associated with the mortalities of the freshwater crab, *Eriocheir sinensis*, may also belong to *Okavirus* based on virion morphology and nucleic acid size (Zhang & Bonami 2007). The complete sequence of the gill-associated virus (GAV), which is the type species of *Okavirus* and a low virulent isolate, was the first of the YHV-complex to be determined (Cowley & Walker 2002). Now the whole genome of a YHV isolate collected in 1998 from Chachoengsao, Thailand, a more virulent and devastating strain, has been sequenced (Sittidilokratna et al. 2008).

Whole genomes are believed to contain complete evolutionary information, and the phylogenetic analyses based on those genomes are expected to equate to the evolution of the organisms. But the most profound difficulty in building phylogenies using whole genomes is to effectively and efficiently depict the evolutionary information hidden in the whole genome. Among recently established phylogenetic approaches for whole genome analyses are gene order breakpoint distance analysis (Blanchette et al. 1999), neighbor pair analysis (Herniou et al. 2001), and Z-curve approach (Zheng et al. 2005). Also, composition vector approach has been shown to have some advantages in reconstruction of phylogeny in bacteria, DNA and some RNA viruses (Gao et al. 2003, Qi et al. 2004a, b, Gao et al. 2007, Gao & Qi 2007).

In this chapter, I report the genome sequences of 3 YHV isolates from *Penaeus monodon*, predict the hydrophobic transmembrane domains in pp1a and a secondary structure of 3' UTR, and construct a phylogenetic tree by analyzing the amino acid composition vector tree of 48 sequences of nidoviruses.

Materials and Methods

Source of Yellow Head Virus

Three isolates of YHV were sequenced: 1) the YHV92 isolate (GenBank acc. no. xxxxx), was originally collected from *Penaeus monodon* from Thailand in 1992 and this same virus transferred into penaeid shrimp was used in the research of several authors (e.g., Lu et al. 1994, 1995, Nadala et al. 1997, Tang & Lightner 1999), which I transferred 1 generation into specific pathogen free *Litopenaeus vannamei*; 2) YHV95 (GenBank acc. no. yyyyy) and 3) YHV99 (GenBank acc. no. zzzzz) were collected from commodity *P. monodon* imported from Thailand in 1995 and 1999, respectively, in Tucson, Arizona. The YHV95 from *P. monodon* was transferred into *Litopenaeus stylirostris* for one generation and stored at -80 °C and then this gill homogenate from *L. stylirostris* was injected into local white shrimp *L. setiferus* that were tested white spot syndrome virus (WSSV) and YHV-free. The muscle homogenate of *P. monodon* for YHV99 was injected into WSSV- and YHV-free *L. setiferus* for one generation. When some shrimp became moribund after 3 d post-inoculation (PI), the hemolymph was drawn by EDTA-coated 1 ml syringes and pooled as a reference stock of the virus. The pooled hemolymph and tissue were aliquoted and stored at -80 °C until required.

Total RNA Extraction

Total RNA from hemolymph was extracted following the protocol of the High Pure Viral Nucleic Acid Kit (Roche). The RNA was then eluted into 100 µl of autoclaved RNase-free water and stored at -80 °C.

Table 5

Primers designed for RT-PCR and sequencing based on YHV and GAV sequences using Vector NTI Advance™ 10.

Primers	sequence (5'--3')	segment length	location
Y1a1F	ACGTTACGTTCCACGFACTATTC	788	1-788
Y1a1R	GTTGCAGTGATGAGCAGCGAGAC		
Y1a2F	CTTTCTGCCGTCTCGCTGCTCA	810	756-1565
Y1a2R	GTGAGCGATGTTCGATGTCCGA		
Y1a3F	TAGATGGCACGATCAGGATCTTCC	831	1475-2305
Y1a3R	GGAGGTGGGACGTTGTAAGCATT		
Y1a4F	CCAGTGACTCCATCATCGACATCG	816	2203-3018
Y1a4R	GATAGTGGTGGTGAAGCCGATGC		
Y1a5F	TGTATGGACTCCGAGTCATCGACC	826	2950-3775
Y1a5R	TGCAGGAGGTCTAAGATGGAGTCG		
Y1a6F	AGATGCCAAGTACTTCCGCTTCC	841	3679-4519
Y1a6R	GAGGGGAACAATCGTTGACAAA		
Y1a7F	CAATGCATTGTCAATGTCTGTGGC	841	4425-5265
Y1a7R	CGAACTGGTGACCGTTTGAGTCAT		
Y1a8F	TGTCACAATCATCCACAACATCCC	838	5171-6008
Y1a8R	GGCACTGGTGACGAATCTGT TTC		
Y1a9F	GGTCCTCAAACCGCACTTAGCA	820	5918-6737
Y1a9R	GGGAGTTGGTTCGATGTAAATGGG		
Y1a10F	TACACTTGAACAATTCGGATCGC	832	6677-7508
Y1a10R	GCGGACACCATAGATTCCATGAG		
Y1a11F	ACACCACGTCCAACGAAAGATGTC	822	7444-8265
Y1a11R	CGGTGAGAAGGAAGATGTAGCCG		
Y1a12F	CTCAATGATGAAGCGTCCACGC	817	8165-8981
Y1a12R	GGCGGACATTGAACCAACCCCT		
Y1a13F	CAAATTCGGTAAACTCCAACGCAC	825	8891-9715
Y1a13R	GCAAGAGGGCTGACAGAGATGAAA		
Y1a14F	TTCATCTGCTTCGATCACGGTTC	825	9612-10436
Y1a14R	CATGTTGGAGCGTTGCTTGAAGA		
Y1a15F	GTGGATCTTTGGCATCTTCCTCA	837	10369-11205
Y1a15R	CGTACTTGAGCACATTGTCAGCGT		
Y1a16F	CTCATCAAACCTGACATCTGACTGC	927	11142-12068
Y1a16R	GGCGCATGGAGTATCGATGAGA		
Y1a17F	TGTCTCTATCCTCATGCTTCGC	859	11927-12785
Y1a17R	TGTCCATCTTGAGGATGTTGCATG		
Y1b1F	TACTCTCTCATCGATACTCCATGC	865	12042-12906
Y1b1R	TCGAAGTCATAGACGCCTTCTGGA		
Y1b2F	GCACAGTCATTTCGATTACAAGCA	968	12818-13785

Table 5 (continued).

Primers	sequence (5'--3')	segment length	location
Y1b2R	GGAAGTAGAGGTTTCGAGGAGAGGCG		
Y1b3F	CAATGAGTTCAATGACGTCG	913	13687-14599
Y1b3R	GTGGCTGTCTTAAATTGCTG		
Y1b4F	ACAGCATGCTCATCAGGAAACTGC	915	14529-15443
Y1b4R	CGGTGATTGTAGTGATAATCGCCGA		
Y1b5F	CGAAACAATCATCGGCGAATCAC	897	15409-16305
Y1b5R	TCAGATGGCATGTCTTCACGAGC		
Y1b6F	CACACTCAAGCACTGGATCCAACA	816	16234-17049
Y1b6R	CCAGTGAAGATGACATGACGTGGA		
Y1b7F	CATCGATGAATTCTCAATGGCCAC	1054	16966-18019
Y1b7R	GCGGACTTCCAATTTGGTACGG		
Y1b8aF	GCTAAGCAYCTCATCAACTGGC	723	17888-18610
Y1b8aR	AGGGCATGTGAATCCGTGAAATG		
Y1b8bF	ATTCATTCTCCGCTCTACATGGC	820	18352-19171
Y1b8bR	GTGTAGCCCGTGGATTTGTTCC		
Y1b9F	ATCGACTGCAACAGATGCTATCCC	847	18656-19502
Y1b9R	GTCGGCAGTGGTTGTGTTAGGAGT		
Y1b10F	GATTGACAATGCCCTCAGCACTGC	906	19393-20298
Y1b10R	GGAAAGGCGCATAGTCACITCGTTT		
Y1b11aF	ACGAAGTGACTATGCGCCTTCCA	545	20277-20821
Y1b11R	GCAGAATGGGATCGTTGGGATT		
Y1b11bF	CAACCACGACAATCCCTTTCAATC	409	20413-20821
YN1F	ATGAACCGTCGTACACGCAC	815	20500-21314
YN1R	CCTGGTGCAGAAATGTCATGA		
Y2F	TTCTCTGGACGCAGGCGCAA	812	21159-21970
Y2R	AAACCGCATCGTCTGTGCA		
Ygp3F	TGCAACTCTACCAACTGCGAC	768	21805-22572
Ygp3R	GTATGTTCTACCGAGCCAGCC		
Ygp4F	CACATTCTGATAACTGTTGGGC	763	22334-23096
Ygp4R	AATGGGTGAGTGTCTTGACG		
Ygp5F	TCTATCTACACACGCCACAAGT	772	23001-23772
Ygp5R	GCCAAGAGAGTATGGTCCATT		
Ygp6F	CACGGTATTAATACTGACCTTGGC	763	23665-24427
Ygp6R	CTTGTTGAAGGTGCCAGGAG		
Ygp7F	CCATTATTTCTCCAGCTTCAGC	762	24353-25114
Ygp7R	CGTAGAGGAGATGCTTGGGAT		
Ygp8F	AGTTTTAACATCGCTCATCCCC	902	25018-25919
Ygp8R	AGAAAGACAGGTGTGCCGATG		
Y3F	TTCCATCAAAGGTATTGACTCTCA	1081	25596-26676
Y3R	TTTCATATCACCGGAAACC		

RT-PCR Amplification and Nucleotide Sequencing

The YHV partial sequences and the whole genome of Chachoengsao 1998 strain of Thailand (YHV98) (GenBank acc. no. EU487200) (Sittidilokratna et al. 2008) were used to design 39 sets of primers (Table 5) to amplify overlapping regions covering the genomic RNA using Vector NTI 10 software (Invitrogen). RT-PCR was processed following the protocol of SuperScript[™] III One-Step RT-PCR System with Platinum[®] Taq High Fidelity (Invitrogen). The RT-PCR reactions (25 µl) contained the kit reagents plus 0.1-0.2 µg total RNA and 0.4 µM primers. The above reactions were incubated at 50 °C for 30 min to synthesize the cDNA. Inactivation of the reverse transcriptase at 94 °C for 2 min was followed by 40 cycles of denaturation at 94 °C for 15 sec, annealing at 56 °C for 30 sec, and extension at 68 °C for 60 sec. A final extension step at 68 °C for 5 min completed the reaction, after which the product was held at 4 °C. One µl of PCR product was used to check the presence and purity of the objective segment, with the rest of the product being cleaned by PCR product purification kit (Qiagen) if the segment showed a sharp and clean band on 1.2% agarose electrophoresis; otherwise, new primers were designed to cover the related regions. The concentration and purity of the purified DNA segment was measured by NanoDrop ND-1000 and adjusted to a reasonable range for sequencing. The DNA products were sequenced directly using each of the PCR primers on an ABI 3130 sequencer (Applied Biosystems), with each product sequenced a minimum of 4 times using the forward and reverse primers.

Sequence Assembly and Analysis

Individual sequence fragments were assembled using Vector NTI Advance[™] 10 (Invitrogen). ORF Finder and BLAST 2.0 (Altschul et al. 1997) accessed

at <http://www.ncbi.nlm.nih.gov> were used for identifying open reading frames (ORF) and for database sequence similarity searches. Amino acid sequences were translated and analyzed using EMBOSS Transeq and pI/MW Tool software available at <http://www.expasy.ch/tools/>. Hydrophobic transmembrane domains of ORF1a and ORF3 were predicted by TMHMM and Phobius servers at <http://www.cbs.dtu.dk/services/TMHMM/> (Krogh et al. 2001, Käll et al. 2004). ClustalX 2.0 was used for pair-wise and multiple sequence alignments (Thompson et al. 1997). Ribosomal frameshift (RFS) was scanned by RF Finder server (Moon et al. 2004) at <http://wilab.inha.ac.kr/fsfinder2/>, and the pseudoknots of RFS and the 3' untranslated terminal region (3' UTR) were predicted by Pknotsrg server (Reeder & Giegerich 2004) accessible at <http://bibiserv.techfak.uni-bielefeld.de/pknotsrg/submission.html>. The predicted pseudoknots were redrawn using Photoshop CS2. The ORF3 amino acid sequence was submitted to the NetNGlyc server at <http://www.cbs.dtu.dk/services/NetNGlyc/> for scanning for N-glycosylation sites and at <http://www.cbs.dtu.dk/services/NetOGlyc/> for O-glycosylation sites (Julenius et al. 2005).

Phylogenetic Analysis

Composition vector trees (CVTrees) were generated for the representative proteome sequences in Nidovirales using CVTree program (Qi et al. 2004a, b) available at (<http://cvtree.cbi.pku.edu.cn/>), setting a value of K (= 5 or 6) for both the whole proteome and the ORF1 amino acid sequences. The distance matrix document was then submitted to Phylip package 3.67 for generating the neighbor-joining (NJ) and minimum evolution (ME) trees (Felsenstein 1989).

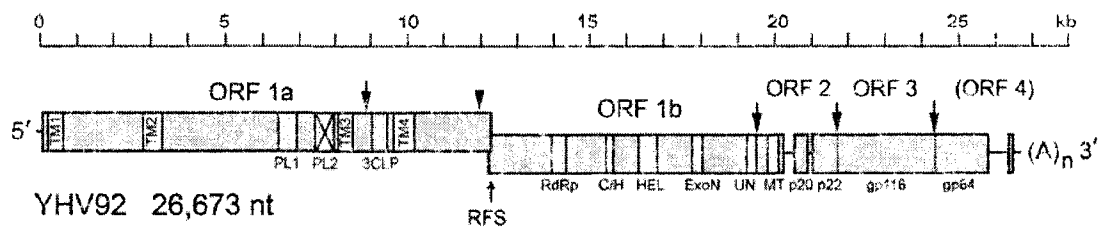


Figure 12. Schematic genomic organization of *Okavirus*. Image from Sittidilokratna et al. 2008). Functional domains in ORF1a: hydrophobic transmembrane regions (TM1-TM4), 3C-like protease (3CLP), papain-like protease (PLP1), and a domain (PLPX) with homology to PLP1. Functional domains in ORF1b: RNA dependent RNA polymerase (RdRp), cysteine- and histidine-rich domain (C/H), helicase (HEL), exoribonuclease (ExoN), uridylate-specific endoribonuclease (UN), and ribose-O-methyl transferase (MT). ORF2 encodes the nucleoprotein (p20, also N protein). ORF3 encodes a polyprotein post-translated to envelope proteins (gp116 and gp64) and N-terminal unknown protein (p22). The ribosomal frameshift site (RFS) allows read-through translation of pp1ab from ORF1a and ORF1b. Known (arrows) and possible (arrowhead) sites of proteolytic cleavage of polyproteins are indicated.

Results

Genome Sequence of the Three YHV Isolates.

The positive sense ssRNA genome of YHV was 26,673, 26,662, and 26,652 nt in length excluding the polyA tail for YHV92, YHV95, and YHV99 (GenBank acc. no. XXXXX, YYYYYY, and ZZZZZ), respectively. The complete genomes of the 3 YHV isolates were composed of 5' UTR (untranslated terminal region), ORF1-4 (open reading frame), intergenic regions (IGRs), and 3' UTR. The genome organization is illustrated in Figure 12 for YHV92 sequence. The 71-nt 5' UTR of the 3 isolates of YHV that I sequenced was identical to that of YHV98.

The nucleotide and amino acid identities among the whole genome of 5 isolates of *Okavirus* are listed in Table 6. They shared 79.3-99.0% nucleotide and 81.8-98.9% amino

corresponding amino acids (aa) (LASQ), whereas the amino acid sequences flanking this indel region were identical (Figure 13A). Other indel events were located in the non-coding regions, with some occurring in IGR1 between ORF1b and ORF2, with 1 nt indel occurring in the conserved transcription regulatory sequence (TRS) site between ORF3 and ORF4 (Figure 13B, the C in UCCAACCU), and with other indel events located in the 3' UTR (not shown).

The 4 YHV isolates contained differences in several non-coding and coding regions. The ORF1a overlapped ORF1b by 37 nt, terminating at a site 30 nt downstream of the 'slippery' sequence (AAAUUUU), at which a -1 ribosomal frameshift (RFS) allowed read-through translation of ORF1b to generate the large pp1ab replicase polyprotein (Figure 14A). Among the coding regions of the 4 YHV isolates, ORF1a that contained 12,219-12,231 nt shares 95.3-99.0% identity; ORF1b that contained 7,887 nt shares 98.2-99.2% identity; ORF2 that contained 441 nt shares 98.6-99.5 identity; ORF3 that contained 5,001 nt shared 98.9-99.5% identity; and ORF4 (63 nt) encoding 20 potential amino acids were identical. For the 4 YHV isolates, IGR1 containing 345-451 nt shared 98.8- 99.7% identity, IGR2 had and identical sequences of 54 nt, and IGR3 containing 298-299 nt shared 99.3-99.7 identity. The 3' UTR, which contained 311-316 nt, shared 98.4-99.7% identity, but the 131 nt from the 3' end was 100% identical for all 4 YHV isolates.

Secondary Structures for RFS and 3' UTR.

A secondary structural model predicted for the RFS of *Okavirus* is shown in Figure 14A. The 4 YHV isolates had an identical RFS sequence, but it differed from that of

The complete 129-nt 3' UTR of GAV and the 131-nt 3' UTR terminus of the 4 isolates of YHV were predicted to generate a pseudoknot (Figure 14B). The 33 nt downstream from the stop codon UAA of ORF4 (for GAV) formed a hairpin containing 2 short stems, a bulge, and a terminal loop, of which the 2 short stems contained 5 and 3 bp, respectively. Downstream from the hairpin there were 3 unpaired nucleotides connecting a large pseudoknot structure. The pseudoknot was formed by 2 stem structures (S1 and S2), an extended loop (L1) with a long stem (S3) and a variable loop (L3), and a short loop (L2) of 4 nt. The 7-bp S1 had 5 CBC nucleotides, S2 was formed by 3 bp, and S3 consisted of 18 bp and 12 unpaired nucleotides. L3, the most variable structure for okaviruses 3' UTR, consisted of 10 nt for YHV and 8 nt for GAV. L3 in YHV had 2-nt insertion (arrowheads) compared with GAV. Other variable nucleotides between GAV and YHV were indicated by arrows (Figure 14B).

Deduced Amino Acid Sequences of Three pp1a and pp1ab Polyproteins.

The ORF1a encoded a polypeptide (pp1a) of 4,072 for YHV95 and YHV99, and 4,076 aa for YHV92. If a RFS occurs in all isolates at the conserved slippage site, translation through YHV ORF1b would result in an extended polyprotein (pp1ab) of 6,700 aa for YHV95 and YHV99, and 6,704 aa for YHV92.

The overall amino acid sequence identity among the 4 isolates of YHV coding regions is shown in Table 6. The pp1a was more variable than pp1b, which involved most of the indel event for Roniviridae, e.g., YHV92 has 4 more amino acid insertions than the other 3 YHV isolates, whereas the later 3 YHV isolates were 12 amino acids longer than the GAV pp1a.

Table 6

Sequence identity matrix for *Okavirus*. For each gene, the left lower half is the nucleotide identity and the right upper half is the amino acid identity.

Gene and virus isolate		YHV92	YHV95	YHV98	YHV99	GAV
ORF1a	YHV92	1	0.973	0.979	0.979	0.818
	YHV95	0.953	1	0.978	0.974	0.819
	YHV98	0.969	0.959	1	0.989	0.819
	YHV99	0.969	0.957	0.990	1	0.819
	GAV	0.794	0.793	0.794	0.793	1
ORF1b	YHV92	1	0.995	0.992	0.995	0.885
	YHV95	0.984	1	0.993	0.995	0.885
	YHV98	0.982	0.99	1	0.994	0.883
	YHV99	0.982	0.988	0.992	1	0.884
	GAV	0.82	0.822	0.821	0.819	1
ORF2	YHV92	1	0.979	0.986	0.986	0.829
	YHV95	0.988	1	0.979	0.993	0.829
	YHV98	0.993	0.986	1	0.986	0.836
	YHV99	0.993	0.99	0.995	1	0.829
	GAV	0.786	0.789	0.786	0.786	1
ORF3	YHV92	1	0.985	0.982	0.983	0.764
	YHV95	0.994	1	0.989	0.992	0.764
	YHV98	0.987	0.989	1	0.993	0.761
	YHV99	0.992	0.995	0.991	1	0.759
	GAV	0.731	0.729	0.728	0.727	1

Scanning the pp1a sequences of YHV and GAV using TMHMM and Phobius servers, I identified 4 conserved hydrophobic domains that may functionally serve as the transmembrane domains (TM1-TM4) (Figures 1, 4) anchoring the nidovirus replication complex to intracellular membranes (Prentice et al. 2004). TM1, containing 197-199 aa (V(A)¹¹⁶-L³¹⁵ for the 4 isolates of YHV and I¹¹⁷-L³¹³ for GAV), had 4 membrane-spanning domains; TM2, containing 221 aa for the 4 YHV isolates (L⁹⁴⁰-V¹¹⁶⁰ for


```

YHV92 TM1 VILWLGALFNAGQVLCGIVLGLFALTYIMVAKITRLKRLQAVGATRS-ENLSCSHFFETHGSKSGVRSRSMININLVNVPVSELIPIVITMCCIPTTASEIIT
YHV95 TM1 AITWFGALFNAGQVLCGIVLGLFALTYIMVAKITRLKRLQAVGATRS-ENLSCSHFFETHGSKSGVRSRSMININLVNVPVSELIPIVITMCCIPTTASEIIT
YHV98 TM1 AITWFGALFNAGQVLCGIVLGLFALTYIMVAKITRLKRLQAVGATRS-ENLSCSHFFETHGSKSGVRSRSMININLVNVPVSELIPIVITMCCIPTTASEIIT
YHV99 TM1 AITWFGALFNAGQVLCGIVLGLFALTYIMVAKITRLKRLQAVGATRS-ENLSCSHFFETHGSKSGVRSRSMININLVNVPVSELIPIVITMCCIPTTASEIIT
GAV TM1 LFWFGALFNAGQVLCGIVLGLFALTYIMVAKITRLKRLQAVGATRS-ENLSCSHFFETHGSKSGVRSRSMININLVNVPVSELIPIVITMCCIPTTASEIIT
*****
YHV92 TM1 APRVLTDTGLSAVSLIITATWLRHQPOTSEVFTNMSTSPGTATGLLIITLLECGITIVSGIPAAFTPSIAKVGSGMVAPILLPIVMWLSRLYLITLILL
YHV95 TM1 APRVLTDTGLSAVSLIITATWLRHQPOTSEVFTNMSTSPGTATGLLIITLLECGITIVSGIPAAFTPSIAKVGSGMVAPILLPIVMWLSRLYLITLILL
YHV98 TM1 APRVLTDTGLSAVSLIITATWLRHQPOTSEVFTNMSTSPGTATGLLIITLLECGITIVSGIPAAFTPSIAKVGSGMVAPILLPIVMWLSRLYLITLILL
YHV99 TM1 APRVLTDTGLSAVSLIITATWLRHQPOTSEVFTNMSTSPGTATGLLIITLLECGITIVSGIPAAFTPSIAKVGSGMVAPILLPIVMWLSRLYLITLILL
GAV TM1 APRVLTDTGLSAVSLIITATWLRHQPOTSEVFTNMSTSPGTATGLLIITLLECGITIVSGIPAAFTPSIAKVGSGMVAPILLPIVMWLSRLYLITLILL
*****

```

A

```

YHV92 TM2 LNLNLSLCLGIIHQYIYDVMYGLRVIDHFEIFMMSIAFTTTIISLHNKIIISIPSTLAGILVGDNPVWFQFLIAHKCNVSCSLQILGILNAINPYSAYGTICLLFYLSPSTC
YHV95 TM2 LNLNLSLCLGIIHQYIYDVMYGLRVIDHFEIFMMSIAFTTTIISLHNKIIISIPSTLAGILVGDNPVWFQFLIAHKCNVSCSLQILGILNAINPYSAYGTICLLFYLSPSTC
YHV98 TM2 LNLNLSLCLGIIHQYIYDVMYGLRVIDHFEIFMMSIAFTTTIISLHNKIIISIPSTLAGILVGDNPVWFQFLIAHKCNVSCSLQILGILNAINPYSAYGTICLLFYLSPSTC
YHV99 TM2 LNLNLSLCLGIIHQYIYDVMYGLRVIDHFEIFMMSIAFTTTIISLHNKIIISIPSTLAGILVGDNPVWFQFLIAHKCNVSCSLQILGILNAINPYSAYGTICLLFYLSPSTC
GAV TM2 LNLNLSLCLGIIHQYIYDVMYGLRVIDHFEIFMMSIAFTTTIISLHNKIIISIPSTLAGILVGDNPVWFQFLIAHKCNVSCSLQILGILNAINPYSAYGTICLLFYLSPSTC
*****
YHV92 TM2 TSLVRFELTLLLVIGAQAEQTEKSDT-HLFKQFTRLIVYALCAHIIVTVKMLEPREHEHETIAVSTKQYSNFVSTQSRITTCSTYOPTTTAVVIAVLELFTLIMV-----
YHV95 TM2 TSLVRFELTLLLVIGAQAEQTEKSDT-HLFKQFTRLIVYALCAHIIVTVKMLEPREHEHETIQVSTIQSSNFTSRRRTTCAYTOPTTAAVVIVVALTFSLII-----
YHV98 TM2 TSLVRFELTLLLVIGAQAEQTEKSDT-HLFKQFTRLIVYALCAHIIVTVKMLEPREHEHETIQVSTIQSSNFTSRRRTTCAYTOPTTAAVVIVVALTFSLII-----
YHV99 TM2 TSLVRFELTLLLVIGAQAEQTEKSDT-HLFKQFTRLIVYALCAHIIVTVKMLEPREHEHETIQVSTIQSSNFTSRRRTTCAYTOPTTAAVVIVVALTFSLII-----
GAV TM2 TSLVRFELTLLLVIGAQAEHETHESDTKHIFHFTRLIVYALCAHIIVTVKMLEPREHEHETVSCSTQTSNFRSTRRTTCAYTOPTTAAVVIVVALTFSLIVSTANAHQIF
*****

```

B

```

YHV92 TM3 LDHSSVSLIIIIIVSYLLRFRFEPVTVCFIYILINVPALIIYQSRDLAYISSVISVLFGLTTEILKRCMVIPVLSFLPTMSYCKKGSMDGRFRDHDFMVFATSMFAFSLINIGVIFLLTGIIVIFIGLY
YHV95 TM3 LDHSSVSLIIIIIVSYLLRFRFEPVTVCFIYILINVPALIIYQSRDLAYISSVISVLFGLTTEILKRCMVIPVLSFLPTMSYCKKGSMDGRFRDHDFMVFATSMFAFSLINIGVIFLLTGIIVIFIGLY
YHV98 TM3 LDHSSVSLIIIIIVSYLLRFRFEPVTVCFIYILINVPALIIYQSRDLAYISSVISVLFGLTTEILKRCMVIPVLSFLPTMSYCKKGSMDGRFRDHDFMVFATSMFAFSLINIGVIFLLTGIIVIFIGLY
YHV99 TM3 LDHSSVSLIIIIIVSYLLRFRFEPVTVCFIYILINVPALIIYQSRDLAYISSVISVLFGLTTEILKRCMVIPVLSFLPTMSYCKKGSMDGRFRDHDFMVFATSMFAFSLINIGVIFLLTGIIVIFIGLY
GAV TM3 LDHSSVSLIIIIIVSYLLRFRFEPVTVCFIYILINVPALIIYQSRDLAYISSVISVLFGLTTEILKRCMVIPVLSFLPTMSYCKKGSMDGRFRDHDFMVFATSMFAFSLINIGVIFLLTGIIVIFIGLY
*****

```

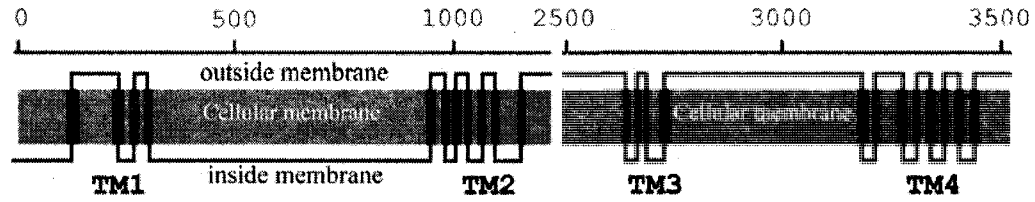
C

```

YHV92 TM4 LIIVYELLQIAFICFDHGFFFRVLRDPHTEHLSIIITVFIISVSPLASTNDILFKYLLSYTLEYRFAYLVNVTLIQSYVLYLSSREAIIFYTSRRVKNL
YHV95 TM4 LIIVYELLQIAFICFDHGFFFRVLRDPHTEHLSIIITVFIISVSPLASTNDILFKYLLSYTLEYRFAYLVNVTLIQSYVLYLSSREAIIFYTSRRVKNL
YHV98 TM4 LIIVYELLQIAFICFDHGFFFRVLRDPHTEHLSIIITVFIISVSPLASTNDILFKYLLSYTLEYRFAYLVNVTLIQSYVLYLSSREAIIFYTSRRVKNL
YHV99 TM4 LIIVYELLQIAFICFDHGFFFRVLRDPHTEHLSIIITVFIISVSPLASTNDILFKYLLSYTLEYRFAYLVNVTLIQSYVLYLSSREAIIFYTSRRVKNL
GAV TM4 CIIIVYELLQIAFICFDHGFFFRVLRDPHTEHLSIIITVFIISVSPLASTNDILFKYLLSYTLEYRFAYLVNVTLIQSYVLYLSSREAIIFYTSRRVKNL
*****
YHV92 TM4 CTVFTVIVMLLIDTFVVEIGGYNVLPVLIICIPFYLRTVMGAAQIQVYFEADLHKPAANFMTLIYFLIINAIISIIYCWGLFSPFNHANTILF
YHV95 TM4 CTVFTVIVMLLIDTFVVEIGGYNVLPVLIICIPFYLRTVMGAAQIQVYFEADLHKPAANFMTLIYFLIINAIISIIYCWGLFSPFNHANTILF
YHV98 TM4 CTVFTVIVMLLIDTFVVEIGGYNVLPVLIICIPFYLRTVMGAAQIQVYFEADLHKPAANFMTLIYFLIINAIISIIYCWGLFSPFNHANTILF
YHV99 TM4 CTVFTVIVMLLIDTFVVEIGGYNVLPVLIICIPFYLRTVMGAAQIQVYFEADLHKPAANFMTLIYFLIINAIISIIYCWGLFSPFNHANTILF
GAV TM4 CTALVIVMMLCVETFFVEIGGYNVLPVLIICIPFYLRTVMGAAQIQVYFEADLHKPAANFMTLIYFLIINAIISIIYCWGLFSPFNHANTILF
*****
YHV92 TM4 ATTIVHPIAFYVLSQEVQKVFPEANFRVPRLIYVAISYISHVLCHYSAALNKVCEWILQIINANRVLVIGSGSFGIFLTICFLFYFF
YHV95 TM4 ATTIVHPIAFYVLSQEVQKVFPEANFRVPRLIYVAISYISHVLCHYSAALNKVCEWILQIINANRVLVIGSGSFGIFLTICFLFYFF
YHV98 TM4 ATTIVHPIAFYVLSQEVQKVFPEANFRVPRLIYVAISYISHVLCHYSAALNKVCEWILQIINANRVLVIGSGSFGIFLTICFLFYFF
YHV99 TM4 ATTIVHPIAFYVLSQEVQKVFPEANFRVPRLIYVAISYISHVLCHYSAALNKVCEWILQIINANRVLVIGSGSFGIFLTICFLFYFF
GAV TM4 LTTIVHPIAFYVLSQEVQKVFPEANFRVPRLIYVAISYISHVLCHYSAALNKVCEWILQIINANRVLVIGSGSFGIFLTICFLFYFF
*****

```

D



E

Figure 15. Alignments and topology of the putative *Okavirus* hydrophobic transmembrane (TM) domains in pp1a. (A) TM1, (B) TM2, (C) TM3, (D) TM4, and (E) schematic topology of TMs in pp1a. Absolutely conserved (*) and similar (: or .) amino acids are indicated according to the similarity groups defined in ClustalX. Scaled line shows the approximate residue position of each domain.

YHV92 and L⁹³⁶-I¹¹⁵⁶ for the other 3 isolates) and 231 aa for GAV (I⁹²⁸-F¹¹⁵⁸), had 7 membrane-spanning domains; TM3, having 132 aa (L²⁶⁰⁹-Y²⁷⁴⁰ for YHV92, L²⁶⁰⁵-Y²⁷³⁶ for the other 3 YHV isolates, and L²⁵⁸⁴-Y²⁷²⁵ for GAV), had 3 membrane-spanning domains; and TM4, containing 279 aa (L³¹⁷¹-F³⁴⁴⁹ for YHV92, L³¹⁶⁷-F³⁴⁴⁵ for the other 3 YHV isolates, and C³¹⁵⁷-C³⁴³⁵ for GAV), had 8 membrane-spanning domains. The TM3 and TM4 domains flanked the 3C-like protease (3CLP) domain.

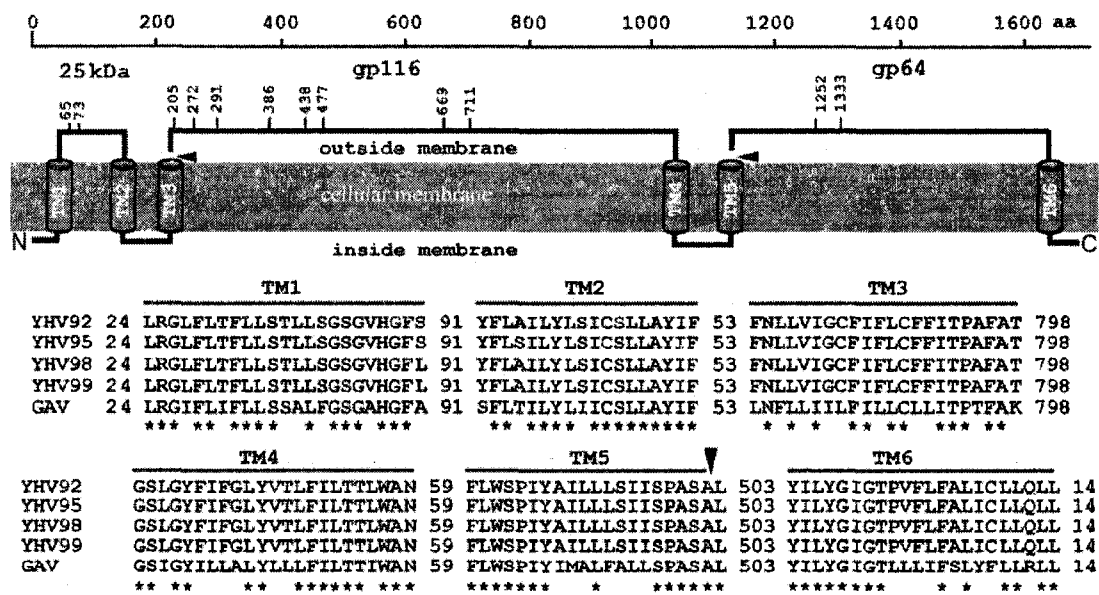


Figure 16. Predicted topology of *Okavirus* ORF3 and alignment of the transmembrane (TM) domains of okaviruses. TMHMM software was used to predict topology (Krogh et al. 2001). Cylinders represent TM1-6, while solid lines indicate the predicted inside and outside domains, with arrowheads showing the proteolytic cleavage sites. Scaled line shows the approximate residue position of each domain. Numbers on the solid line indicate the glycosylation sites predicted by the NetNGlyc server. Numbers among the aligned domains TM1-6 show the residues outside or inside the cellular membrane.

Scanning ORF3 of YHV92 using the TMHMM program, I predicted 6 hydrophobic membrane-spanning domains for YHV (Figure 16) (Jitrapakdee et al. 2003),

of which 3 occurred in the N-terminus (residues L²⁵-S/I⁴⁷, Y¹³⁸-F¹⁵⁵, F²⁰⁸-T²²⁹), 2 in the 3/5 region of ORF3 (residues G¹⁰²⁷-N¹⁰⁴⁹, F¹¹⁰⁶-L¹¹²⁸), and 1 in the C-terminus (residues Y¹⁶³⁰-L¹⁶⁵²). The identities of TM1-TM6 between YHV and GAV ranged from 50-83% (Figure 16).

Twelve potential N-linked glycosylation sites were predicted along the whole length of ORF3 for YHV92 and YHV95 using the NetNGlyc program (Figure 16), with 2 residues (65 and 73) on the 25 kDa domain, with 8 residues (205, 272, 291, 386, 438, 477, 669, and 711) on the gp116 domain, and with 2 residues (11252 and 1333) on the gp64 domain. However, YHV98 and YHV99 did not have the N-linked glycosylation site at residue 65. Using the NetOGlyc3.1 server (Julenius et al. 2005), I predicted O-linked glycosylation sites of Thr residues (296, 297, 298, 301, 302, 309, 569, 807, and 1396) and Ser residues (299 and 304) for YHV95, YHV98, and YHV99, but YHV92 did not have O-linked glycosylated Ser at residue 299.

Phylogenetic Tree Based on Composition Vectors

Coronavirus clustered into 3 distinct groups, of which group 1 has 2 subgroups and group 2 had 4 subgroups; *Arterivirus* formed 4 distinct subgroups: SHFV, PRRSV, EAV, and LDEV. Genera *Torovirus* and *Bafinivirus* exhibited a close relationship (Figure 17). Comparing the CVTrees based on the whole proteomes and ORF1 of the 48 sequences, I detected almost identical tree topology (tree not shown for ORF1). There was no distinct topological difference by analyzing the CVTrees using a different *K* value (5 or 6) for the proteome and the ORF1 amino sequences. Among the 4 isolates of YHV, YHV95 clustered with the other 4 YHV isolates.

Discussion

I report here the genomic sequences of 3 isolates of YHV collected from Thai *Penaeus monodon* in 1992 and frozen *P. monodon* imported into the U.S. in 1995 and 1999. The genomes shared the same organization exhibited by other *Okavirus*. Three YHV isolates had identical 5' UTR and ribosomal frameshift (RFS) sequence as YHV98 and shared 82.4% sequence identity with the 68-nt 5' UTR of GAV (Cowley et al. 2000, Sittidilokratna et al. 2008). The genome sequence of the 5 *Okavirus* isolates had 75.3-99.2% identity. An approximate 57% of the total indel (250 nt) event was found in the IGR1 between ORF1b and ORF2 and in the IGR3 between ORF3 and ORF4; 1 important indel event of okaviruses occurred in the transcription regulatory sequence (TRS) as C in DCCAACCU (*D* refers to G/A/U in standard ambiguous codes) of the IGR3 (Figure 13B). Whether or not different IGRs of *Okavirus* involve different strategies for *Okavirus* replication, transcription, translation, and virulence is still not known; however, the 6 genotypes of YHV-complex found in the Asian regions show a very diverse length of IGR1 (Wijegoonawardane et al. 2008), implying that IGR1 may undergo extensive evolutionary selection pressure and may be a marker for monitoring *Okavirus* epidemiology and evolution.

The nidovirus replicase is expressed as 2 large polyprotein precursors, and further autoproteolytically cleaved into 13-16 functional subunits for *Coronavirus*, including key enzymes and TM subunits (Tijms et al. 2007). Among the 3 reported TMs, TM2 and TM3 are known to affect the structure or function of 3CLP (Tibbles et al. 1996, Piñon et al. 1997), and TM1 is required for PLP2 mediated processing in *Coronavirus* (van der Meer et al. 1998) and the membrane association of the replication complex in *Arterivirus*

(van der Meer et al. 1998). Notably, a unique TM1 as a specific hydrophobic domain detected only in Roniviridae parasitizing invertebrate hosts, is not seen in Coronaviridae and Arteriviridae which cause vertebrate diseases. In *Okavirus*, 4 TM domains have been predicted by Ziebuhr et al. (2003) and Sittidilokratna et al. (2008), and TM2-4 may have potential functions similar to those of TM1-3 of other nidoviruses (arteri-, bafini-, corona-, and toroviruses) because of the relative position in ppla; whereas, TM1 is specifically predicted in *Okavirus*, having 4 membrane-spanning domains with the first domain being further apart from the other 3 domains. The TM1 of *Okavirus* may be specifically related to membrane fusion function in the invertebrate intercellular membrane during the highly coordinated replication, transcription, and translation processing.

Available experimental evidence indicates that partial 3' UTR of *Arterivirus* (Beerens & Snijder 2006, 2007) and *Coronavirus* (Williams et al. 1999, Hsue et al. 2000, Goebel et al. 2007) can form a conserved pseudoknot that plays a critical role in regulating viral RNA synthesis. This structure was found in all coronavirus subgroups and was conserved in terms of location and higher-order structure, but it was not apparent at the sequence level (van den Born & Snijder 2008). Mutagenesis experiments demonstrated that this RNA pseudoknot was involved in BCoV replication (Williams et al. 1999). In the *Coronavirus* 3' UTR, a 68 nt bulged hairpin located at the 5' end upstream of the pseudoknot, appears to be essential for replication and has been suggested to function during plus-strand RNA synthesis in BCoV (Hsue et al. 2000). The counterpart of this 5' UTR upstream hairpin structure for GAV and partial hairpin structure of YHV 3' UTR, a 33-nt structure, was also detected to be immediately

downstream of the stop codon of ORF4 (Figure 14B). As indicated, the 3' UTR pseudoknot in *Coronavirus* has a large loop and a small loop (Goebel et al. 2007), the L2 in *Okavirus* has only 5 nt (UUCCC), but the L1 in *Okavirus* has an extremely extended large stem form (S3) and terminal loop (L3) structure. A total of 13 variable sites were found on 3' UTR in *Okavirus*. L3 contained 6 variable nucleotides, of which YHV had a 2 nt insertion (Figure 14B, arrowheads) compared with 3 other genotypes including GAV (Wijegoonawardane et al. 2008); S1, a stem structure that had 7 bp but contained 5 CBCs for all genotypes of *Okavirus* (Wijegoonawardane et al. 2008), was another highly variable region, but it may have a stable secondary structure. Of the other 2 mutations, 1 occurred in the hairpin structure upstream of the pseudoknot and the other was on S3 as a U:A pair in YHV or a U:U mismatch in the other genotypes of *Okavirus*. S2 is a conserved structure, although it has only 3 bp. Compared with other nidoviruses (except human coronavirus E229), *Okavirus* has more nucleotides and 2 special stem and loop structures (S3 and S4, L3 and L4) involving RFS formation. Moreover, the slippery sequence (Figure 14A, underlined) and the position of ORF1a stop codon UAA (Figure 14A, shaded) also differ from most of the other nidoviruses.

Notably, different secondary structures of 3' UTR were predicted using mFold and Pknotsrg software. These displayed as a stable S3 and variable L3 (= helices 3-4 as discussed by Wijegoonawardane et al. 2008) and a variable 5' end upstream hairpin and pseudoknot structure, implying the predicted pseudoknot may be exchangeable in certain circumstances. A conserved octonucleotide motif UGAAUAGC located in the middle 5' end of S3 in all okaviruses (Figure 14B, shaded in circles) may be the counterpart motif of GGAAGAGC determined in all coronaviruses. Remarkably, further downstream of

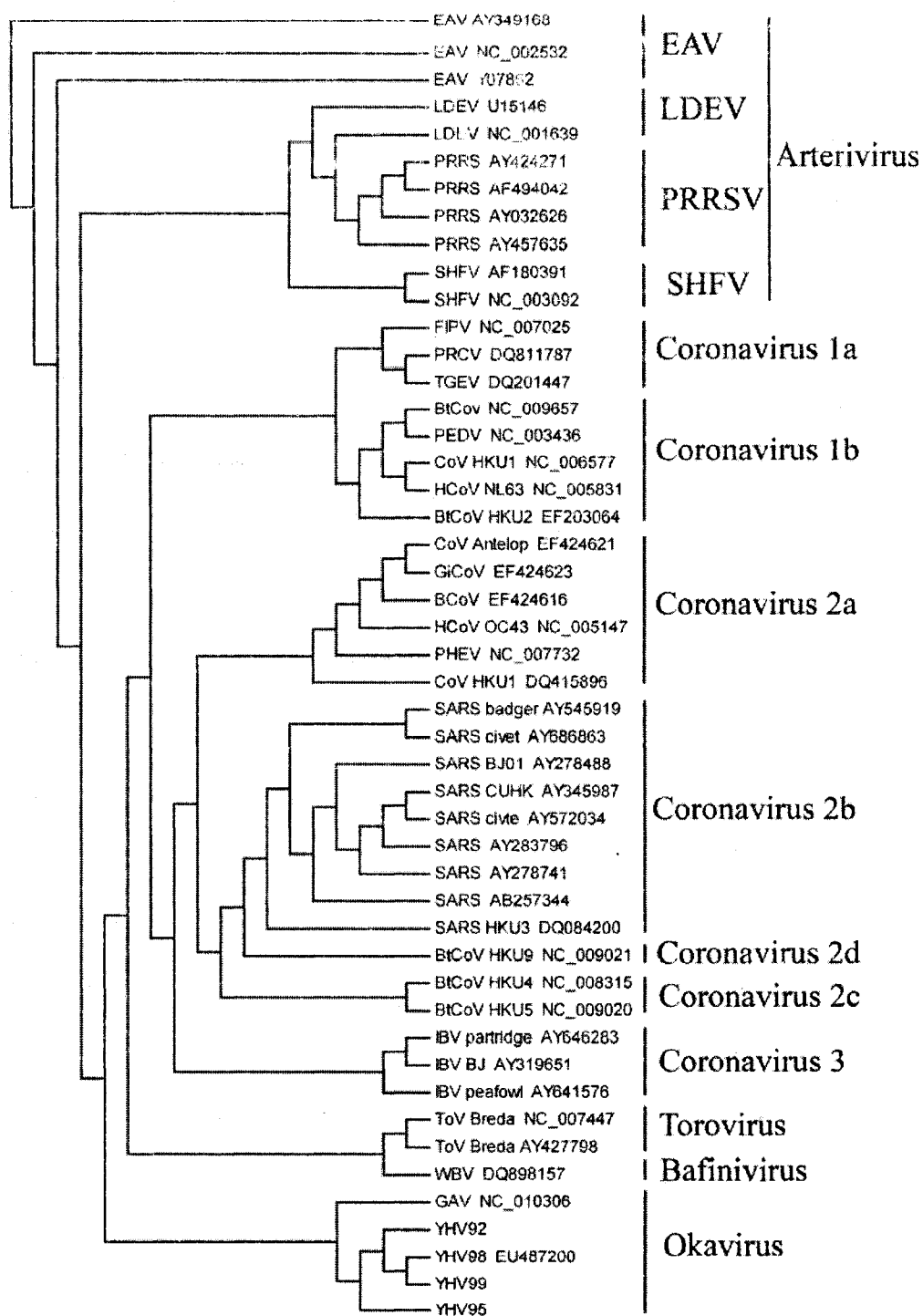


Figure 17. Unrooted NJ tree by analysis of 48 amino acid sequences of Nidovirales using CVTree program. GenBank accession numbers were listed after virus type.

3' UTR in some coronaviruses, a large hairpin structure could be identified where the deletion of part of this hairpin affected the viral replication, and more importantly, the deletion extensively influenced the viral pathogenicity (Liu et al. 2001, Goebel et al. 2004, Goebel et al. 2007).

The contemporary comment on the nidovirus phylogenetic tree asserts that oka-, toro-, corona-, and even the recently sequenced bafinivirus should group together to form a supercluster of large nidoviruses; arteriviruses would then be the first to split from the nidovirus trunk (Gorbalenya et al. 2006). The exact relationship among nidoviruses is yet to be rigorously resolved (Gorbalenya et al. 2006). If RdRp is used as a gene marker, the overall relative position of roniviruses and arteriviruses remain poorly supported (Gorbalenya et al. 2006). Moreover, I find it noteworthy that roniviruses are located between coronaviruses and toroviruses in the phylogenetic trees based on the amino acid sequences of helicase 1. Part of the original and remaining confusion concerning nidovirus phylogeny could be partially attributed to the technical aspects, e.g., alignment quality, genes analyzed, and software used, all of which may cause uncertainty in the alignment and could lead to the use of different alignment methods resulting in different conclusions and other problems (Wong et al. 2008). Moreover, with the large number of whole genome sequences being deposited in public databases, the traditional phylogenetic analysis methods based on 1 or few genes having short sequences which consist less than 10% of genome information will suffer more challenges and can hardly reflect a realistic phylogeny and evolution.

The CVTree program provides a recent method inferring phylogeny using complete proteome sequences. This program facilitates a user to avoid the difficult and

seemingly impossible task of making alignments from distantly related sequences, and it analyzes the entire genome or proteome rather than sections that may have evolved separately. The phylogenetic analysis of large dsDNA viruses and 432 prokaryotic genomes using the composition vector approach concurs well with the systematist method (Gao et al. 2007). This approach has also been used to determine the phylogeny of 11 representative viruses of 3 families in Nidovirales. From this analysis, *Torovirus* should be further separated from *Coronavirus* (Draker et al. 2006). A distance matrix was generated from analysis of the proteomes of 48 representatives in Nidovirales, and it calculates the frequency of short amino acid sequences of a fixed length (K string of amino acid, with K being the only parameter that can be adjusted in each analysis). Our phylogenetic analyses of *Coronavirus* support the conclusion that coronaviruses are probably better classified into group 1 (subgroups 1a and 1b), group 2 (subgroups 2a, 2b, 2c, and 2d), and group 3 rather than into 7 groups (Woo et al. 2007). Our results show that coronaviruses 2b, 2c, and 2d are monophyletic; BCoV, HCoV OC43, and PHEV cluster together with CoV HKU1 to form group 2a. The FIPV, PRCV, and TGEV cluster to form group 1a, and BtV HKU2, HCoV NL63, PEDV, and BtCoV G1 cluster to form group 1b. Three groups of *Coronavirus* have the most recent common ancestor. *Torovirus* and *Bafinivirus* are closely related to form a distinct cluster as discussed by Gorbalenya (2008). Moreover, when the ORF1 sequences that consist of approximately 2/3 of the proteome were used to analyze the phylogeny, the topology was very similar to that of the whole proteome, which further shows the advantage of this method.

CHAPTER V
EVOLUTION OF YELLOW HEAD VIRUS THROUGH RECOMBINATION

Abstract

Recombination in RNA viruses is considered to play a major role as a driving force in virus diversity and evolution. Analyzing 5 genome sequences of okaviruses, important pathogens in penaeid shrimps, I detected 7 recombination events using an RDP3 program among the 4 available yellow head virus (YHV) genomes with high statistical support. Two recombination events were detected in YHV92, with 1 from nucleotide 3444 to 3574 and the other from 12074 to 13489; 2 recombination events were determined in YHV95, with 1 from nucleotide 3793 to 4230 and the other from 16573 to 18422; 2 events were detected in YHV98, with 1 from nucleotide 6694 to 9324 and the other from 21507 to 25644; and 2 events were determined in YHV99, with the first being the same as that in YHV98 and the other from 11932 to 14863. No recombination event was detected in gill-associated virus. Analyzing 3 aligned data sets from a 1473-nt of the 5' end and a 2620-nt of the 3' end of ORF1a and a 3939-nt of the 3' end of ORF3 sequences, which have mean substitution rates of 5.51×10^{-3} , 5.66×10^{-3} , and 2.64×10^{-3} , respectively, I dated back the divergence times for the most recent common ancestor of the YHV lineage in 1976 (95% highest posterior density, 95% HPD, 1951-1992), 1983 (95% HPD, 1961-1992), and 1971 (95% HPD, 1921-1992), respectively. These values are consistent with the shrimp culture practice in Asia.

Introduction

Yellow head disease (YHD), caused by yellow head virus (YHV), was first recognized in 1990 from shrimp farms in Thailand (Limsuwan 1991) and then later in other Asian countries such as China (including Taiwan), India, Sri Lanka, Vietnam, Malaysia, and the Philippines. The YHV was also detected from imported commodity shrimp in US, and it caused serious bioassay shrimp mortality (Durand et al. 2000). The economic loss from YHV in Asian countries was about \$500 million US from its outbreak to 2006 (Lightner, personal communication). After the pandemic outbreaks of the white spot syndrome virus (WSSV) in Asia and America in the middle 1990s, YHD seemed to have been concealed by infections with WSSV. However, recent studies showed that YHV was present in Mexican shrimp farms along Pacific coastal areas in salt- and freshwater environments (de la Rosa-Vélez et al. 2006, Sánchez-Barajas et al. 2008). On the other hand, at least 6 genotypes of YHV-like viruses (including the pathogenic YHV and the related gill-associated virus, GAV) have been widely detected in postlarvae, juvenile, and even healthy penaeid shrimps (Cowley & Walker 2008).

The genome of YHV comprises a non-segmented single-stranded (ss) positive-sense RNA of approximately 26.6 kb (Sittidilokratna et al. 2008). In a previous study, I reported the genome of 3 isolates of YHV collected in *Penaeus monodon* in 1992, 1995, and 1999, the genome of the 3 isolates is 26673, 26662, and 26652 nt in length, respectively. They share an identical 5' untranslated region (UTR), ribosomal frameshifting sequence, and a partial of the 3' UTR. The 5 available genome sequences of okaviruses share 79.3-99.0% of the nucleotide and 81.8-98.9% of the amino acid identities within ORF1a, 81.9-99.2% and 88.3-99.5%, respectively, in ORF1b, 78.6-

99.3% and 82.9-99.3%, respectively, in ORF2, and 72.7-99.5% and 75.9-99.3%, respectively, in ORF3. The only indel event in the coding region for the 4 available isolates of YHV is located in the 5' end of ORF1a, containing a segment of 12 nt with 4 corresponding amino acids. Other indels are located in the non-coding region (Ma et al. 2009).

As a unique family in Nidovirales, Roniviridae has the following characteristics: (a) members parasitizing invertebrates, especially penaeid shrimps; (b) rod-shaped rather than spheroidal or discal; (c) a short 5' UTR composing only 68-71 nt, without a typical 5' leader structure as seen in other nidoviruses (Dhar et al. 2004); (d) 4 hydrophobic transmembrane (TM) domains rather than 3 in pp1a as reported in Coronaviridae and Arteriviridae (Cowley et al. 2000b, Cowley & Walker 2008); (e) genetic organization of structural proteins, having a nucleocapsid (N) protein the first structural protein rather than the last one as in Coronaviridae and Arteriviridae; and (f) ORF4 truncated (Sittidilokratna et al. 2008, Wijegoonawardane et al. 2008).

Recombination in RNA viruses is considered to play a major role as a driving force in virus variability and thus in virus evolution. The emergence of new pathogenic RNA viruses is frequently due to RNA recombination (Lai 1992, Worobey & Holmes 1999), which can lead to dramatic changes in viral genomes by creating novel combinations of genes, motifs, or regulatory RNA sequences. RNA recombination can change the infectious properties of RNA viruses and render vaccines and other antiviral methods ineffective (Serviene et al. 2005). Although the importance of recombination was underappreciated in early studies of viral genome evolution, it is now recognized as a widespread phenomenon among positive-stranded RNA viruses in humans, animals

(Wilson et al. 1988, Nagy & Simon 1997, Holmes et al. 1999, Worobey & Holmes 1999, Moya et al. 2004, Oberste et al. 2004, Oliver et al. 2004, Heath et al. 2006, Pyre et al. 2006, Valli et al. 2007, Vijaykrishna et al. 2007, Lukashev et al. 2008, Qin et al. 2008), and plants (Aaziz & Tepfer 1999, Delatte et al. 2005, Martin et al. 2005b, Lefeuvre et al. 2007, Owor et al. 2007, Weng et al. 2007). Shrimp farming practices showed that viral accommodation is a common phenomenon for host-viral interaction in shrimps; accommodation involves not only RNA viruses but can also involve DNA viruses (Flegel 2007). The driving forces for viral accommodation in shrimp may involve multiple factors from hosts, environment, and viruses, but viral genomic recombination may also play one of the important roles in accommodation. Current models of RNA recombination are based on a template-switching mechanism driven by viral replicase (Lai 1992, Nagy & Simon 1997) or RNA breakage and ligation (Chetverin et al. 1997).

Herein, I detected that YHV isolates appear to have been recombining actively and naturally amongst themselves. Using the BEAST program, I can date the divergence time for the most recent common ancestor (TMRCA) of YHV lineage back in 1970-1980s using 3 data sets located in ORF1 and ORF3. The prediction result is consistent with the rapid development of the shrimp aquaculture industry in Asia.

Materials and Methods

Sequence Data of Yellow Head Virus

Four isolates of YHV were used in this study. The YHV92 (GenBank acc. no. xxxxx), was originally collected in 1992 from *Penaeus monodon* in Thailand and was the same isolate studied by several authors (e.g., Lu et al. 1994, 1995, Nadala et al. 1997, Tang & Lightner 1999) after being injected 1 time into specific pathogen free

Litopenaeus vannamei. YHV95 (GenBank acc. no. yyyyy) and YHV99 (GenBank acc. no. zzzzz) were collected from imported commodity shrimp (*P. monodon*) in 1995 and 1999 in Tucson, Arizona, USA. YHV95 was injected into *Litopenaeus stylirostris* for 1 time and then stored at -80°C, this homogenate of *L. stylirostris* was then injected into white spot syndrome virus (WSSV) and YHV-free local white shrimp *Litopenaeus setiferus*; the YHV99 homogenate from *P. monodon* was injected into WSSV- and YHV-free *L. setiferus* for 1 time and then the viral RNA was extracted and sequenced. The viral genome for YHV98 was obtained from GenBank (acc. no. EU487200). PCR amplification and sequencing of YHV92, YHV95, and YHV99 were reported previously (Ma et al. unpublished).

Codon Substitution Statistics

The synonymous and non-synonymous analysis program (SNAP) available at <http://www.hiv.lanl.gov/content/index> was used to analyze the substitution.

Analysis of Natural Recombinants

ClustalX 2.0 was used for pair-wise and multiple sequence alignments (Thompson et al. 1997). The aligned data sets containing the whole genomes of *Okavirus* were further analyzed using the Recombination Detection Program (Martin & Rybicki 2000), Maximum Chi Square (Maynard Smith 1992), Bootscan (Martin et al. 2005a), Geneconv (Padidam et al. 1999), Chimaera (Martin et al. 2005a), and Siscan (Gibbs et al. 2000) recombination detection methods as implemented in RDP3 (Martin et al. 2005a) available from <http://darwin.uvigo.es/rdp/rdp.html>. The analysis was performed with default settings for the different detection methods and a Bonferroni corrected *P*-value cut-off of 0.05. The breakpoint positions and recombinant sequence(s) inferred for every

detected potential recombination event were manually checked and adjusted when necessary using the extensive phylogenetic and recombination signal analysis features available in RDP3. Once a set for a unique potential recombination event was identified, I compiled a breakpoint map by plotting the positions of all clearly identifiable breakpoints. A breakpoint density plot was then constructed from this map and the statistical significance of potential breakpoint.

The aligned data sets containing ORF1a, ORF1b, ORF2, and ORF3 were also submitted to GARD server (Kosakovsky Pond et al. 2006) available at <http://www.datamonkey.org/GARD/> for further multiple breakpoint detection. Both positive and negative selection models were detected by the HYPHY package in the GARD server (Kosakovsky Pond & Frost 2005).

Estimation of Divergence Dates

The divergence dates for *Okavirus* lineage were estimated based on 3 alignments of partial sequences that contained a 1473-nt of the 5' end of ORF1a, a 2620-nt of the 3' end of ORF1a, and a 3939-nt of the 3' end of ORF3. Before submission for divergence dates, the aligned sequences were scanned using the RDP3 program as mentioned above to trim out the recombination regions. The uncorrelated relaxed clock model in BEAST version 1.4.7 (<http://beast.bio.ed.ac.uk/>) was used to analyze the divergence dates (Drummond & Rambaut 2007). Under this model, the rates were allowed to vary at each branch independently. Sampling dates for each isolate were used as calibration points, and constant population coalescent priors were assumed for all data sets. Depending on the data set, I ran Markov chain Monte Carlo (MCMC) sample chains for 10, 7, and 20 million generations for the data sets from the 5' and 3' end of ORF1a and from the 3' end

of ORF3, respectively. Those data sets were sampled every 200, 100, and 200 generations using the HKY nucleotide substitution model, allowing γ rate heterogeneity. The convergence of MCMC chains was confirmed for each data set by using the program Tracer version 1.4 available at <http://tree.bio.ed.ac.uk/software/tracer/>. The times of divergence were estimated utilizing prior values obtained from earlier runs, with a discarded burn-in of 10% of total generated trees. The generated trees were drawn using FigTree v1.1.2 (<http://tree.bio.ed.ac.uk/software/figtree/>). The alignments used for divergence dates were also analyzed by the MEGA program (Tamura et al. 2007) with a bootstrap value of 1000.

Table 7

Statistic data of nonsynonymous to synonymous substitutions for yellow head virus coding regions*.

Gene	amino acids	d_N	d_S	d_S/d_N	pS/pN
ORF1a	4076	0.0094	0.1258	12.5615	11.5395
ORF1b	2628	0.0041	0.0468	12.2790	11.9462
ORF2	144	0.0066	0.0193	3.6691	3.6225
ORF3	1666	0.0060	0.0145	2.6634	2.6434

* d_N and d_S : average of Jukes-Cantor correction for non-synonymous and synonymous substitution rate, respectively; d_S/d_N : average ratio of synonymous to nonsynonymous substitution; pS/pN: average ratio of proportion of synonymous to non-synonymous substitution.

Results

Substitution of Coding Regions

Analyzing the cumulative substitution of ORF1a, ORF1b, ORF2, and ORF3 genes, I detected that the 2 non-structural genes, ORF1a and ORF1b, had a larger value of d_S/d_N than the 2 structural genes, ORF2 and ORF3 (Table 7). Compared with non-

structural genes ORF1a and ORF1b, the structural genes ORF3 and ORF2 showed a higher cumulative non-synonymous substitution rate (Figure 18).

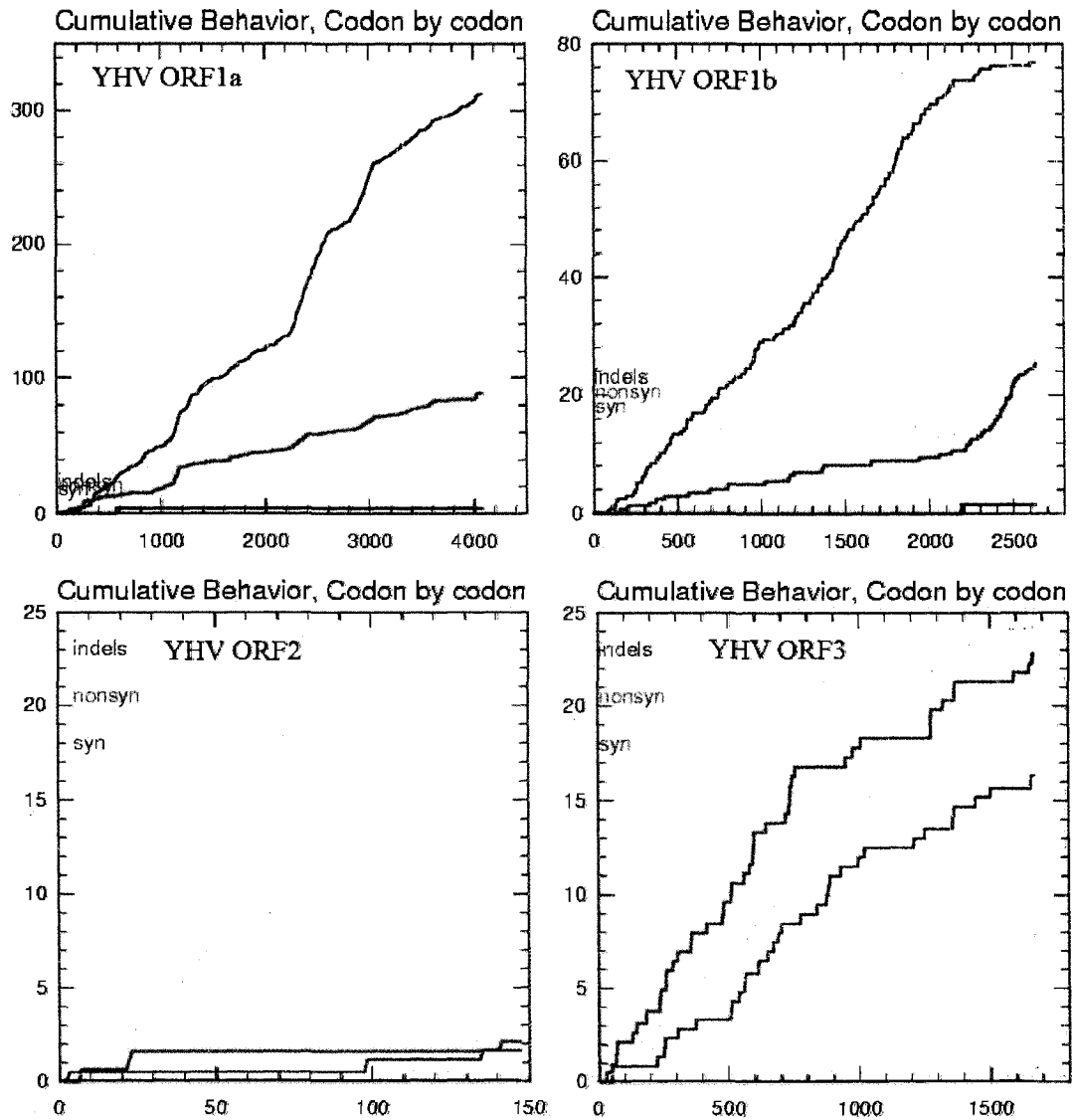


Figure 18. Cumulative substitution rates of 4 coding genes. Cumulative synonymous, non-synonymous, and indel substitution rates are showed in red, green, and black, respectively.

Table 8

Statistic data detected by BEAST and Tracer program for *Okavirus*.

Summary statistic	mean	standard error of mean	95% HPD		effective sample size (ESS)
			lower	upper	
posterior	-3276.0	0.28	-3287.6	-3265.3	463.0
	-5650.1	0.34	-5661.0	-5640.5	262.1
	-8731.8	0.23	-8764.4	-8741.2	734.8
likelihood	-3257.6	0.11	-3263.6	-3252.1	924.9
	-5632.2	0.06	-5637.5	-5627.0	1768.3
	-8725.7	0.03	-8731.0	-8721.1	8389.1
mean substitution rate	5.51E-03	1.79E-04	5.91E-06	1.23E-02	419.3
	5.66E-03	2.88E-04	2.03E-05	1.28E-02	157.4
	2.64E-03	8.83E-05	7.42E-06	6.05E-03	420.5
TMRCA for <i>Okavirus</i> (years)	79.5	12.8	7.5	180.3	1087.4
	55.7	10.9	7.5	132.6	624.7
	221.1	19.4	18.2	626.7	2384.3
TMRCA for YHV (years)	23.4	3.1	7.2	47.8	1148.7
	16.2	1.6	7.0	38.2	770.7
	27.7	2.0	7.0	77.6	2560.3
relative substitution rate on codon 1	0.750	1.70E-03	0.575	0.927	2779.9
	0.558	1.20E-03	0.451	0.666	2103.9
	0.485	3.00E-04	0.419	0.553	13000.0
relative substitution rate on codon 2	0.418	1.40E-03	0.287	0.561	2512.7
	0.277	6.67E-04	0.202	0.352	3323.9
	0.286	1.72E-04	0.239	0.338	21850.0
relative substitution rate on codon 3	1.832	2.91E-03	1.598	2.058	1630.8
	2.165	1.61E-03	2.032	2.307	1862.9
	2.23	3.05E-04	2.146	2.315	19890.0

TMRCA, time of the most recent common ancestor; HPD, highest posterior density. First row, the 5' end of 1473 nt of ORF1a gene; second row, 2620 nt close to 3' end of ORF1a gene; and third row, 3939 nt of 3' end of ORF3.

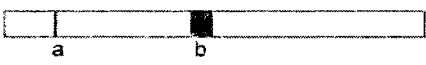
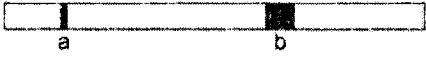

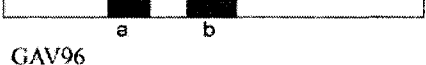
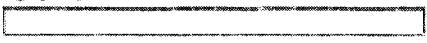
	Event	Region	Parental sequences		Detected by	P-value
			Minor	Major		
 YHV92	a	3444-3574	Unknown	YHV95, 98, 99	<i>RGBMCS3S</i>	5.88E-17
	b	12074-13489	YHV99	YHV95, 98	<i>rGM3S</i>	8.84E-03
 YHV95	a	3793-4230	YHV92	YHV99	<i>rgbmc</i>	7.92E-03
	b	16573-18422	YHV92	YHV99, 98	<i>mc</i>	5.19E-03
 YHV98	a	6694-9324	YHV92	YHV95	<i>RGBMCS3S</i>	1.44E-46
	b	21607-25644	Unknown	YHV99	<i>RBmC3S</i>	9.11E-09
 YHV99	a	6694-9324	YHV92	YHV95	<i>RGBMCS3S</i>	1.44E-46
	b	11932-14863	Unknown	YHV98	<i>RGBMCS3S</i>	1.11E-15
 GAV96						

Figure 19. Recombinant regions detected within yellow head virus (YHV) sequences based on the RDP3 program. The genome in the heading corresponds with the schematic representation of sequences given below it. Region coordinates are nucleotide positions of detected recombination breakpoints in the multiple sequence alignment used to detect recombination. Wherever possible, parental sequences are identified. ‘Major’ and ‘minor’ parents are sequences that were used, along with the indicated recombinant sequence, to identify recombination. For each identified event, the minor parent contributes the sequence within the indicated region, and the major parent contributes the rest of the sequence. Note that the identified ‘parental sequences’ are not the actual parents but are simply those sequences most similar to the actual parents in the analyzed data set. Recombinant regions and parental viruses were identified using the RDP (R), GENECONV (G), BOOTSCAN (B), Maxchi (M), Chimaera (C), SiSscan (S), and 3Seq (3S) methods. The reported *P*-value is for the method shown in bold and italic type and represents the best *P*-value calculated for the region in question. Upper-case letters imply a method detected recombination with a multiple comparison corrected *P*-value <0.01, and lower-case letters imply the method detected recombination with a multiple comparison corrected *P*-value < 0.05 but larger than or equal to 0.01.

Recombination Events during Evolution of the Okavirus

I investigated the positive selection pressure along the full-length genome sequence of 1 GAV and 4 YHV isolates in an attempt to determine the evolutionary stability. By using multiple recombination detection methods implemented in RDP3, I detected 2 recombination events in YHV92, with 1 from nucleotide 3444 to 3574 and the other from 12074 to 13489; 2 recombination events were determined in YHV95, with 1 from nucleotide 3793 to 4230 and the other from 16573 to 18422; 2 events were detected in YHV98, with 1 from nucleotide 6694 to 9324 and the other from 21507 to 25644; and 2 events were determined in YHV99, with the first being the same as that in YHV98 and the other from 11932 to 14863. No recombination event was detected in gill-associated virus (Figure 19, Supplement 1 & 2).

Using GARD server, I detected 12 breakpoints in ORF1a, 6 breakpoints in ORF1b, and 5 breakpoints in ORF3 in the alignments with statistical support (Figure 20). However, I did not detect any breakpoints in ORF2 of *Okavirus*.

Estimation of Divergence Dates

To determine the divergence dates of *Okavirus*, I searched for recombination-free sequences because recombination can cause chaos or errors in reconstruction of phylogenetic relationships. I detected 3 recombination-free data sets, of which 1 data set of 1473-nt was located in the 5' end of ORF1a, a second data set of 2620-nt located close to the 3' end of ORF1a, and a third data set of 3939-nt was near the 3' end of ORF3. The TMRCA for YHV and *Okavirus* were analyzed using the above 3 recombination-free data sets under the uncorrelated relaxed clock model with statistic support (Table 8).

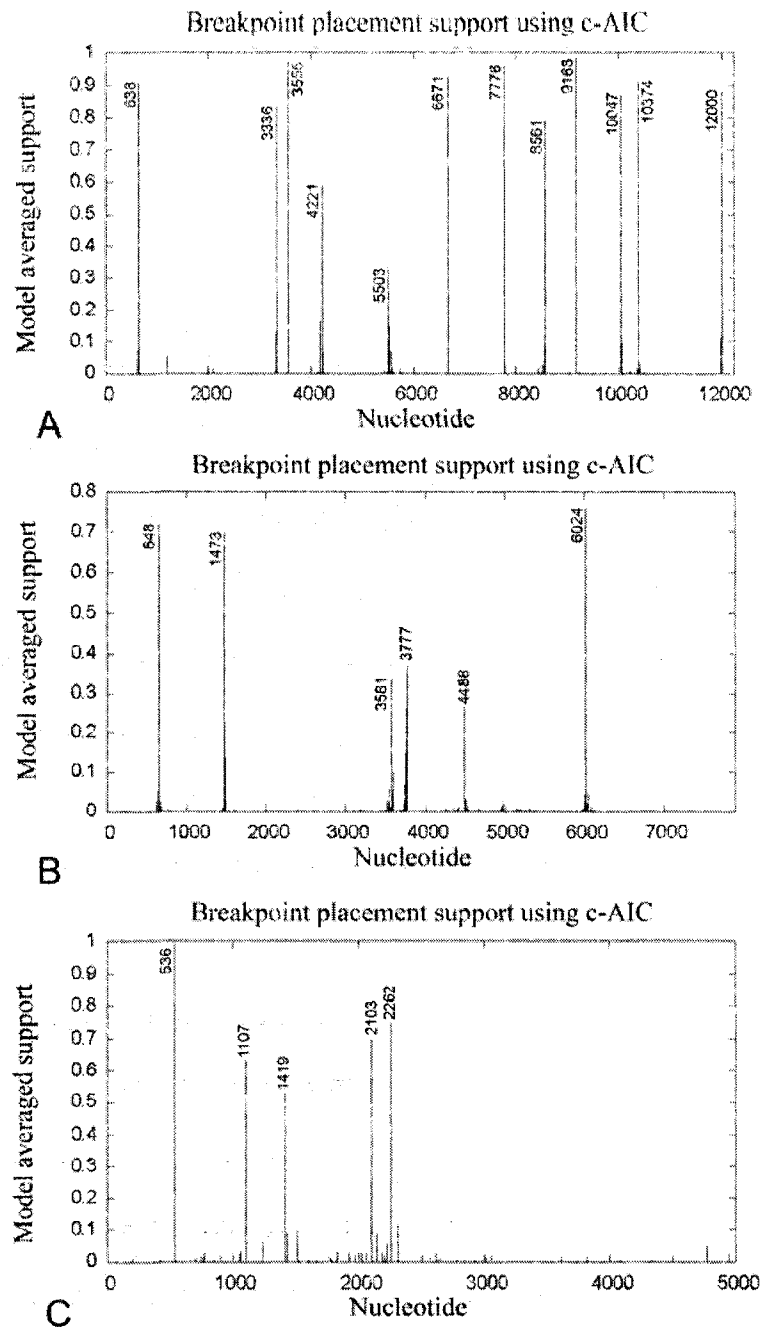


Figure 20. Detection of recombination on ORF1a (A), ORF1b (B), and ORF3 (C) of *Okavirus*. Mean values calculated using Genetic Algorithms for Recombination Detection (GARD) website. The Akaike information criterion (c-AIC) for the best-fitting model was 29160.1, 33752.1, and 14776.9 for ORF1a, ORF1b, and ORF3, respectively. The specific breakpoints are labeled.

However, the large highest posterior density values (HPDs) associated with most of these dates necessitate caution in interpreting these results. The TMRCA was estimated to 1976 (95% HPD, 1951-1992) for YHV and 1919 (95%HPD, 1819-1991) for *Okavirus*, respectively, using the 5' end of partial ORF1a (Figure 21A). Using partial 3' end ORF1a sequence, the TMRCA was dated back to 1983 (95% HPD, 1961-1992) for YHV and 1943 for *Okavirus* with a range of 125 years (95% HPD, 1776-1992) (Figure 21B). The TMRCA was dated back to 1971 (95% HPD, 1921-1992) for YHV and 1778 for *Okavirus* with 95% HPD range of 600 years using partial ORF3 sequence (Figure 21C). Even though using different gene sequences, the TMRCA for YHV may date back to the 1970s, a date corresponding with the development of shrimp farming in Asia (Table 8).

Analysis also showed that the average mutation rate was 5.51×10^{-3} per site per year for the 5' end, 5.66×10^{-3} for the 3' end of ORF1a, and 2.64×10^{-3} for the partial ORF3. The relative substitution rate for these 3 data sets is different among the 3 codon positions in which the third codon is 3-7 folds higher than the first and the second codons (Table 8).

Discussion

Recombination is a hallmark of RNA virus genetics. I detected 7 natural recombination events distributed in all protein coding regions except in ORF2. The length of recombination segments ranges from as short as 0.1 kb to as long as 4.0 kb. Among these recombination events, both YHV98 and YHV99 have a 2630-nt segment derived from YHV92 with a P -value of 1.44×10^{-46} . However, I did not detect any recombination events between YHV and GAV which may be either because the sequenced GAV isolated from Australia was too distant from Thailand where all the

sequenced YHV isolates originated or because only 1 GAV genome sequence was available in GenBank for comparison.

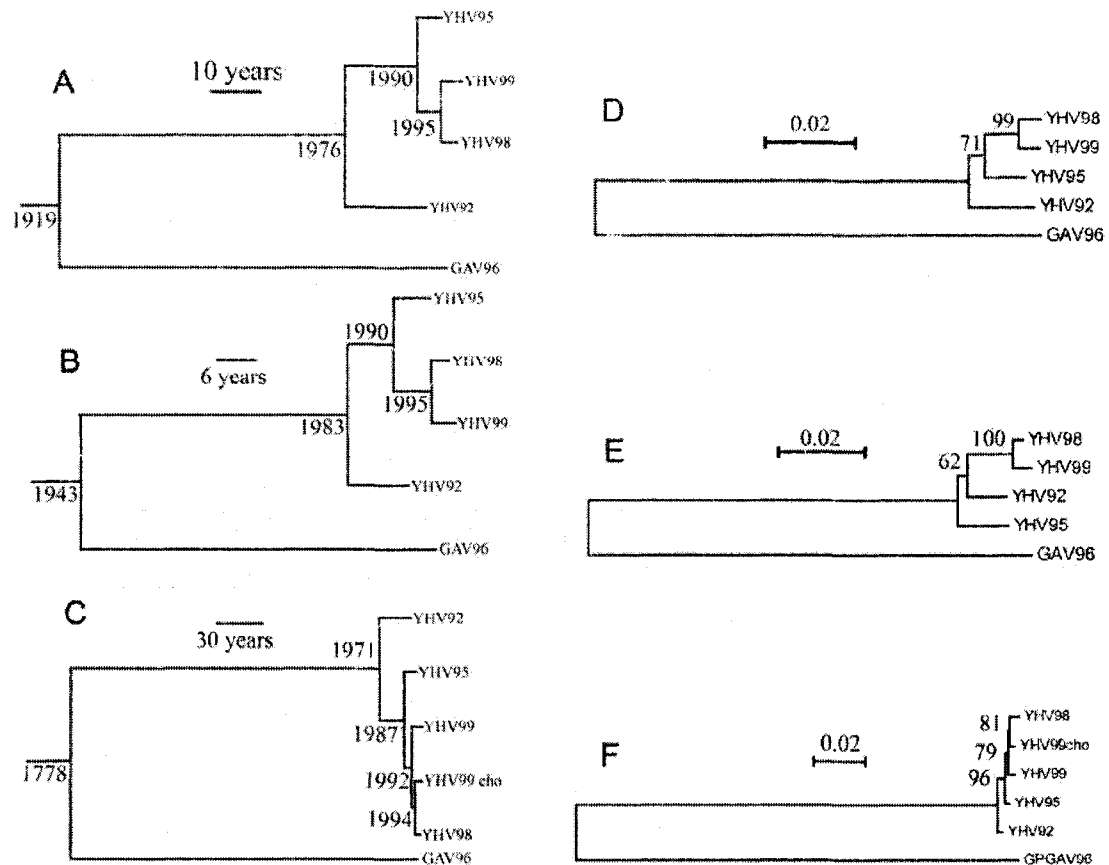


Figure 21. Phylogenetic analyses and divergence dates of *Okavirus* lineages based on alignments of 3 data sets. Divergence dates with number at branch nodes indicate the times of divergence calculated using the uncorrelated relaxed-clock model in BEAST v1.4.7 based on 5' end of ORF1a (A), 3' end of ORF1a (B), and 3' end of ORF3 (C); Neighbor-joining trees based on partial 5' end (D) and 3' end (E) of ORF1a gene and partial 3' end of ORF3 (F), with numbers at tree nodes indicating percentages of bootstrap support.

Among the YHV data sets, I also detected multiple phylogenetic conflicts.

Phylogenetic analysis of YHV based on 2 data sets from ORF1a and 1 data set from ORF3 confirms that YHV98 and YHV99 clusters together, demonstrating a close

relationship between the 2 YHV isolates, which both originated from Thailand in *P. monodon*. However, YHV95 was a distinct isolate from the other 3 YHV isolates, which had more mutation or recombination. Interestingly, I sequenced these isolates from different hosts even though the original isolates were from *P. monodon*, YHV92 was transferred 1 generation to *L. vannamei*, YHV95 was transferred to *L. stylirostris* and then from *L. stylirostris* to *L. setiferus*, and YHV99 was transferred 1 generation to *L. setiferus*. Even though available data showed that host genes can affect the recombination of a plant RNA tombusvirus (Serviene et al. 2005), I do not know whether different shrimp hosts or genes could affect YHV recombination. Whether the high variability of YHV95 was due to more host passage or whether the high variability of YHV95 and recombination can affect the viral virulence still needs to be unraveled. Unfortunately, the *P. monodon* infected by YHV95 and YHV99 were also infected concurrently with the pathogenic dsDNA virus, WSSV, making it difficult to evaluate the virulence of these YHV isolates.

Currently, the validity of applying a molecular clock to RNA virus evolution is still unclear (Holmes 2003). Saturation of synonymous mutations leading to potential underestimation of substitution rates, recombination, RNA secondary structure, and selection pressures can undoubtedly all contribute to misleading estimates of evolutionary rate (Hughes et al. 2005). Nidoviruses were analyzed to have a high mutation rate and some groups of them have been emerging recently. Based on ORF3 gene sequences, the common ancestor of European-type porcine reproductive and respiratory syndrome virus (PRRSV) was 10 years before the emergence of disease in the 1990s, and it had a substitution rate of 5.8×10^{-3} (Forsberg et al. 2001). Based on the phylogeny determined

from helicase and nucleocapsid protein genes, Vijaykrishna et al. (2007) hypothesized that the mean substitution rates of different coronavirus groups varied from 5.35×10^{-3} to 8.4×10^{-2} , and they also deduced that the SARS-CoV, which may switch from civet to human, had a TMRCA in 1986; however, based on the spike gene sequences, Pyrc et al. (2006) determined that HCoV-NL63 and HCoV-229E had a TMRCA in 1053, a controversial difference with those having a TMRCA in 1927 (Pyrc et al. 2006, Vijaykrishna et al. 2007). This uncertain result may reflect the natural recombination phenomenon or the different genes used to determine the controversial TMRCA. Hence, to generate a more reasonable divergence time for YHV, I selected 3 regions that had no recombination within genes using RDP3 program before I determined the divergence time. Using the 5' end of ORF1a, I dated back the TMRCA of YHV to 1976; using the 3' end of ORF1a, I dated the TMRCA back to 1983; and using partial ORF3 gene, I dated the TMRCA back to 1971. A TMRCA of YHV from 1971 to 1983 is basically consistent with the modern shrimp farming practices that began in the 1950s and the semi-intensive shrimp culture that started in the 1970s. Shrimp farming developed very quickly since then, but began as a “capture and culture” procedure in which viruses from the natural environment may have had considerable opportunity to adapt or jump to new hosts, especially when fed on diets of wild organisms and cultured under the eutrophic and intensive pond environments associated with canals containing wild animals. The YHD outbreaks in Asia in the 1990s indicated that YHV should have been enzootic in local reservoir hosts for at least 7-19 years before suddenly emerging as a virulent virus in *P. monodon* in the 1990s. Our results also show that the TMRCA of YHV and GAV are incongruent according to the 3 data sets from ORF1a and ORF3 genes. The TMRCA

implied from the 2 data sets of ORF1a is similar, but the phylogenetic trees are incongruent for MrBayes and bootstrap approaches; when the partial gene of ORF3 was considered, the TMRCA dated back to 1778 with an associated large range of 95% HPD. The highly variable TMRCA for *Okavirus* may be explained by the low number of sequences used in this study and the different substitution rate of the genes. To evaluate the okavirus evolution, I recommend sequencing additional isolates of the okaviruses, including YHV, GAV, and lymphoid organ virus (LOV) circulating in the farmed shrimps and reservoir hosts from different geographic regions.

The characterization of YHV recombination presented in this study provides insights into the process of adaptation of YHV among penaeid shrimps, or process important for understanding the evolutionary events that led to the origin of YHV outbreaks.

Okaviruses have a high natural prevalence in disparate populations of *P. monodon*, and commonly exist as life long chronic infections that may be transmitted vertically to offspring (Cowley et al. 2000a, 2002, Cowley & Walker 2008, Spann et al. 1997). Because both abundantly cultured *P. monodon* and *L. vannamei* are susceptible to YHV infection and mortality in the 2 species often reaches near 100% in a few days, it is possible that YHV may have been transmitted from some chronically infected reservoir hosts. Based on these hypotheses, I suggest that investigations aimed at unraveling the origins of YHV should have 2 foci: 1) to identify candidate species which may have harbored YHV or the YHV-complex before the viruses acquired penaeid shrimps as hosts as well as the factors that may have facilitated a potential host-species shift and 2) to investigate potential reservoirs in which the virus may have existed during the period

between a potential species shift and the onset of the current epidemic as well as environmental factors that may have facilitated transmission from these reservoirs.

Supplements

Recombination Detection Program v. 3.27: C:\Documents and Settings\hema\Desktop\Drissertation\MS_Virus Res.ms\Supplement 2_RDP3 result for Okavirus genom... [5] X

Open Save X-Over Trees Matrices Options Exit

GENECONV

EVENT NUMBER 1
 Starting Position: 68949
 Ending Position: 8000 (8059)
 Daughter: YH66
 Major Parent: YH65 (88.4%)
 Minor Parent: YH62 (88.1%)
 KA P-Value: 4.168 E-44
 Global KA P-Value: 4.168 E-43
 Permutation P-Value: No permutations done
 POSSIBLE MISIDENTIFICATION OF DAUGHTER
 YH66 MAY BE ACTUAL DAUGHTER

Methods	Events	Au. P-Val
RDP	2	1.307 X 10 ⁻¹²
GENECONV	2	7.736 X 10 ⁻¹⁸
Boot Scan	2	1.362 X 10 ⁻³⁸
Max Chi	2	1.670 X 10 ⁻²⁵
Chimera	2	1.635 X 10 ⁻²³
SScan	2	1.723 X 10 ⁻³⁰
PhyInfo	-	-
LARD	-	-
3Seq	2	3.471 X 10 ⁻¹⁴

Confirmation Table

Unique sequences: 1

YH65 YH62 YH68 YH69

Sequences

YH65
YH62
YH68
YH69

23049,35-467

Highest P 0.05

Check Using GENECONV

Options STOP

Log(P-A-V)

Position in alignment

YH65 - YH62

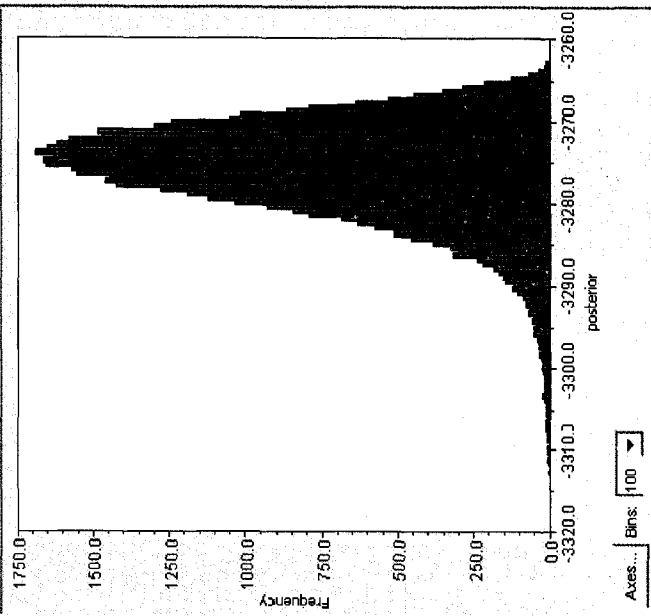
Matrices

Supplement 1. RDP3 genome analysis of Okavirus (RDP3 project file)

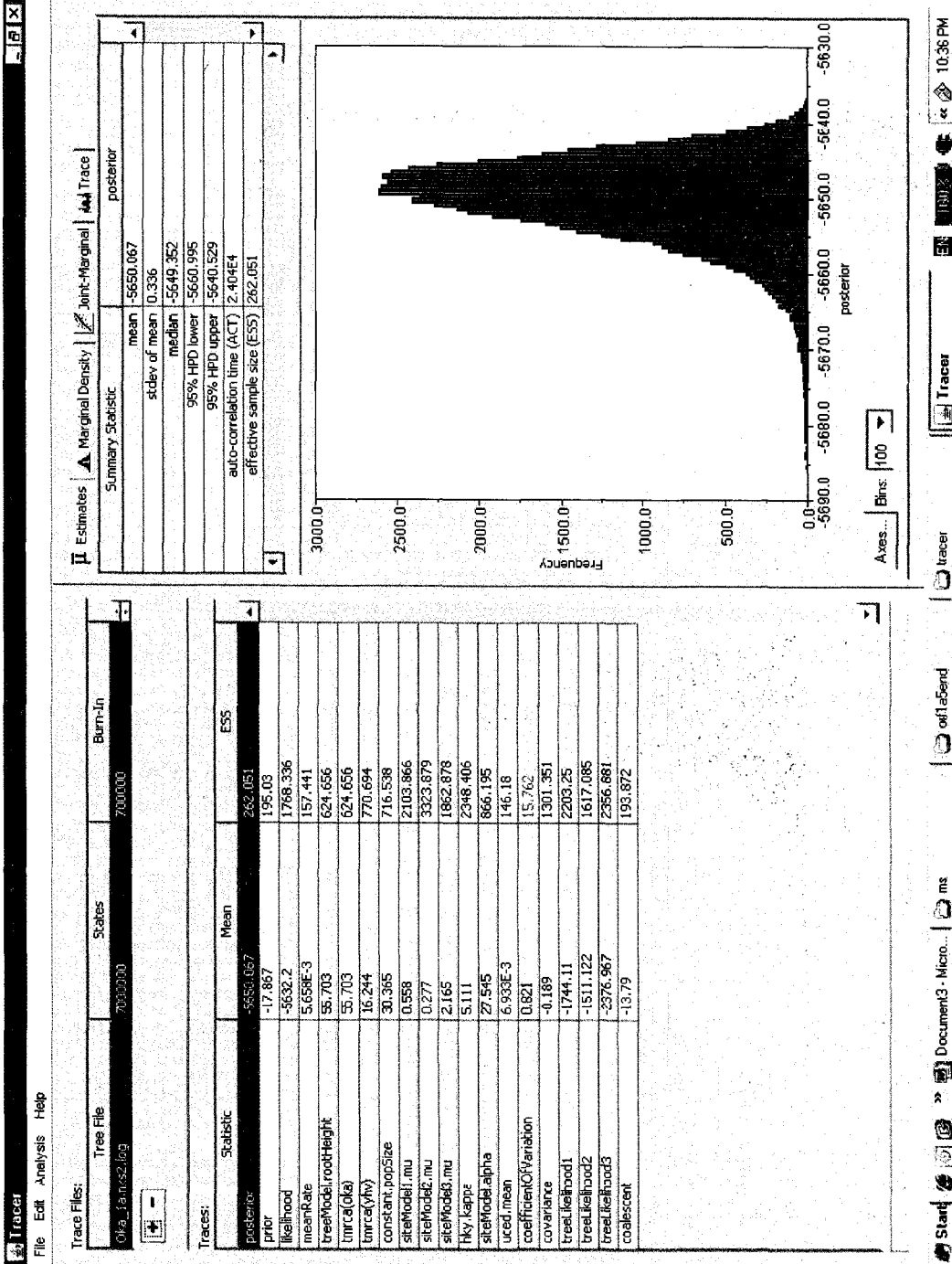
Trace Files:	Tree File	States	Burn-In
	01715.nu.slog	100000000	10000000

Statistic	Mean	E55
posterior	-3275.996	463.049
prior	-18.377	392.404
likelihood	-3257.619	924.947
meanRate	5.51E-3	419.284
treeModel.rootHeight	79.46	1087.399
tmrca(Ok)	79.46	1087.399
tmrca(yhv)	23.362	1148.667
constant.popSize	46.01	1228.781
siteModel1.mu	0.75	2779.916
siteModel2.mu	0.418	2912.71
siteModel3.mu	1.832	1630.772
hxy.kappa	4.538	1780.742
siteModel.alpha	14.477	465.851
uned.mean	7.059E-3	427.274
coefficientOfVariation	0.821	11.259
covariance	-0.201	5889.927
treeLikelihood1	-1041.726	931.161
treeLikelihood2	-910.356	4424.584
treeLikelihood3	-1305.537	3020.871
coalescent	-14.301	392.284

Summary Statistic	posterior
mean	-3275.996
stdev of mean	0.281
median	-3275.242
95% HPD lower	-3287.626
95% HPD upper	-3265.332
auto-correlation time (ACT)	1.944E4
effective sample size (ESS)	463.049



Supplement 2A. Tracer statistics of data set from 5' end of ORF1a for Okavirius

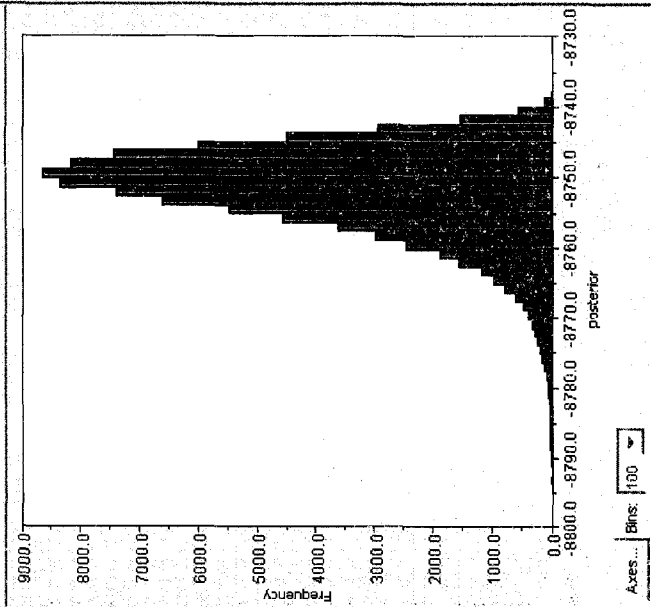


Supplement 2B. Tracer statistics of data set from 3' end of ORF1a for Okavirius

Trace Files:	Tree File	States	Burn-In
Okavirus-gp2.log	20000000		3000000

Statistic	Mean	ESS
posterior	-8751.823	734.833
prior	-26.117	592.494
likelihoood	-8725.705	8389.073
meanRate	2.638E-3	420.514
treeModel.rootHeight	221.077	2384.32
tmrca(yiv)	27.732	2560.266
tmrca(ole)	221.077	2384.32
constant.popSize	78.191	3117.604
siteModel.mu	0.465	1.3E4
siteModel2.mu	0.286	2.185E4
siteModel3.mu	2.23	1.989E4
hky.kappa	3.068	2.051E4
siteModel.alpha	58.23	1.528E4
uced.mean	2.232E-3	449.1
coefficientOfVariation	0.829	22.517
covariance	-0.188	2422.36
treeLikelihoood1	-2799.919	1.066E4
treeLikelihoood2	-2458.819	1.644E4
treeLikelihoood3	-3466.967	9545.356
coalescent	-21.665	591.962

Estimates	Marginal Density	Joint-Marginal	Trace
Summary Statistic	mean	-8751.823	posterior
	stdev of mean	0.232	
	median	-8750.775	
	95% HPD lower	-8764.404	
	95% HPD upper	-8741.18	
	auto-correlation time (ACT)	2.45E4	
	effective sample size (ESS)	734.833	



REFERENCES

- Aaziz R, Tepfer M (1999) Recombination in RNA viruses and in virus-resistant transgenic plants. *J Gen Virol* 80:1339-1346
- Alavandi SV, Babu TD, Abhilash KS, Kalaimani N, Chakravarthy N, Santiago TC (2007) Loose shell syndrome causes low-level mortality in India's black tiger shrimp. *Global Aquacult Advocate* 10:80-81
- Altschul SF, Madden TL, Schäffer AA, Zhang J, Zhang Z, Miller W, Lipman DJ (1997) Gapped BLAST and PSI-BLAST: a new generation of protein database search programs. *Nucleic Acids Res* 25:3389-3402
- Anantasomboon G, Poonkhum R, Sittidilokratna N, Flegel TW, Withyachumnarnkul B (2008) Low viral loads and lymphoid organ spheroids are associated with yellow head virus (YHV) tolerance in whiteleg shrimp *Penaeus vannamei*. *Dev Comp Immunol* 32:613-626
- Anantasomboon G, Sriurairatana S, Flegel TW, Withyachumnarnkul B (2006) Unique lesions and viral-like particles found in growth retarded black tiger shrimp *Penaeus monodon* from East Africa. *Aquaculture* 253:197-203
- Anderson G (1985) Species profiles: life histories and environmental requirements of coastal fishes and invertebrates (Gulf of Mexico) – grass shrimp. U. S. Fish Wildlife Service: Biological Report 82 (11.35). U.S. Army Corps of Engineers, p 1-19
- Andrade TPD, Srisuvan T, Tang KFJ, Lightner DV (2007) Real-time reverse transcription polymerase chain reaction assay using TaqMan probe for detection and quantification of infectious myonecrosis virus (IMNV). *Aquaculture* 264:9-15

- Assavalapsakul W, Smith DR, Panyim S (2006) Identification and characterization of a *Penaeus monodon* lymphoid cell-expressed receptor for the yellow head virus. *J Virol* 80:262-269
- Bangrak P, Graidist P, Chotigeat W, Phongdara A (2004) Molecular cloning and expression of a mammalian homologue of a translationally controlled tumor protein (TCTP) gene from *Penaeus monodon* shrimp. *J Biotechnol* 108:219-226
- Bastide L, Lebleu B, Robbins I (2006) Modulation of nucleic acid information processing by PNAs: potential use in anti-viral therapeutics. In: Janson CG, During MJ (eds) *Peptide Nucleic Acids, Morpholinos and Related Antisense Biomolecules*. Kluwer Academic/Plenum Publishers, New York, p 18-29
- Beerens N, Snijder EJ (2006) RNA signals in the 3' terminus of the genome of equine arteritis virus are required for viral RNA synthesis. *J Gen Virol* 87:1977-1983
- Beerens N, Snijder EJ (2007) An RNA pseudoknot in the 3' end of the arterivirus genome has a critical role in regulating viral RNA synthesis. *J Virol* 81:9426-9436
- Belák S (2007) Molecular diagnosis of viral diseases, present trends and future aspects. A view from the OIE Collaborating Centre for the application of polymerase chain reaction methods for diagnosis of viral diseases in veterinary medicine. *Vaccine* 25:5444-5452
- Blanchette M, Kunisawa T, Sankoff D (1999) Gene order break point evidence in animal mitochondrial phylogeny. *J Mol Evol* 49:193-203
- Bonami JR, Lightner DV, Redman RM, Poulos BT (1992) Partial characterization of a togavirus (LOVV) associated with histopathological changes of the lymphoid organ of penaeid shrimps. *Dis Aquat Org* 14:145-152

- Boonyaratpalin S, Supamataya KK, Kasornchnadra J, Direkbusarakom S, Aekpanithanpong U, Chantanachookin C (1993) Non-occluded baculo-like virus, the causative agent of yellow-head disease in the black tiger shrimp (*Penaeus monodon*). *Fish Pathol* 28:103-109
- Brierley I (1995) Ribosomal frameshifting on viral RNAs. *J Gen Virol* 76:1885-1892
- Brierley I, Boursnell ME, Binns MM, Bilimoria B, Blok VC, Brown TD, Inglis SC (1987) An efficient ribosomal frame-shifting signal in the polymerase-encoding region of the coronavirus IBV. *EMBO J* 6:3779-3785
- Brierley I, Digard P, Inglis SC (1989) Characterisation of an efficient coronavirus ribosomal frameshifting signal: requirement for an RNA pseudoknot. *Cell* 57:537-547
- Brierley I, Rolley NJ, Jenner AJ, Inglis SC (1991) Mutational analysis of the RNA pseudoknot component of a coronavirus ribosomal frameshifting signal. *J Mol Biol* 220:889-902
- Brock JA, Gose R, Lightner DV, Hasson KW (1995) An overview on Taura syndrome, an important disease of farmed *Penaeus vannamei*. In: Browdy CI, Hopkins JS (eds) *Swimming Through Troubled Waters, Proceedings of the Special Session on Shrimp Farming, Aquaculture 95*. World Aquaculture Society, Baton Rouge, LA, p 84-94
- Brock JA, Lightner DV (1990) Diseases of crustacea: Diseases caused by microorganisms. In: Kinne O (ed) *Disease of Marine Animals*. Biologische Anstalt Helgoland, Hamburg, Germany, p 245-349
- Brock JA, Nakagawa LK, Van-Campen H, Hayashi T, Teruya S (1986) A record of

- Baculovirus penaei* from *Penaeus marginatus* Randall in Hawaii. J Fish Dis 9:353-355
- Burrer R, Neuman BW, Ting JPC, Stein DA, Moulton HM, Iversen PL, Kuhn P, Buchmeier MJ (2007) Antiviral effects of antisense morpholino oligomers in murine coronavirus infection models. J Virol 81:5637-5648
- Chamorro M, Parkin N, Varmus HE (1992) An RNA pseudoknot and an optimal heptameric shift site are required for highly efficient ribosomal frameshifting on a retroviral messenger RNA. Proc Natl Acad Sci USA 89:713-717
- Chantanachookin C, Boonyaratpalin S, Kasornchandra J, Direkbusarakom S, Ekpanithanpong U, Supamataya K, Sriurairatana S, Flegel TW (1993) Histology and ultrastructure reveal a new granulosis-like virus in *Penaeus monodon* affected by yellow-head disease. Dis Aquat Org 17:145-157
- Chapman RW, Browdy CL, Savin S, Prior S, Wenner E (2004) Sampling and evaluation of white spot syndrome virus in commercially important Atlantic penaeid shrimp stocks. Dis Aquat Org 59:179-185
- Chayaburakul K, Nash G, Pratanpipat P, Sriurairatana S, Withyachumnarnkul B (2004) Multiple pathogens found in growth-retarded black tiger shrimp *Penaeus monodon* cultivated in Thailand. Dis Aquat Org 60:89-96
- Chen W, He B, Li C, Zhang X, Wu W, Yin X, Fan B, Fan X, Wang J (2007) Real-time RT-PCR for H5N1 avian influenza A virus detection. J Med Microbiol 56:603-607
- Cheng WT, Liu CH, Tsai CH, Chen JC (2005) Molecular cloning and characterisation of a pattern recognition molecule, lipopolysaccharide- and beta-1, 3-glucan binding protein (LGBP) from the whiter shrimp *Litopenaeus vannamei*. Fish Shellfish

Immunol 18:297-310

Chetverin AB, Chetverina HV, Demidenko AA, Ugarov VI (1997) Nonhomologous

RNA recombination in a cell-free system: evidence for a transesterification mechanism guided by secondary structure. *Cell* 88:503-513

Christmas JY, Langley W (1973) Estuarine invertebrates, Mississippi. In: Christmas JY

(ed) Cooperative Gulf of Mexico Estuarine Inventory and Study, Mississippi. Gulf Coast Research Laboratory, Ocean Springs, p 287-291

Cominetti MR, Marques MRF, Lorenzini DM, Lofgren SE, Daffre S, Barracco MA

(2002) Characterization and partial purification of a lectin from the hemolymph of the white shrimp *Litopenaeus schmitti*. *Dev Comp Immunol* 26:715-721

Couch JA (1974) Free and occluded virus similar to Baculovirus in hepatopancreas of

pink shrimp. *Nature* 247:229-231

Cowley JA and Walker PJ (2002) The complete genome sequence of gill-associated virus

of *Penaeus monodon* prawns indicates a gene organisation unique among nidoviruses. *Arch Virol* 147:1977-1987

Cowley JA, Cadogan LC, Wongteerasupaya C, Hodgson RAJ, Boonsaeng V, Walker PJ

(2004) Multiplex RT-nested PCR differentiation of gill-associated virus (Australia) from yellow head virus (Thailand) of *Penaeus monodon*. *J Virol Methods* 117:49-59

Cowley JA, Dimmock CM, Spann KM, Walker PJ (2000) Detection of Australian gill-

associated virus (GAV) and lymphoid organ virus (LOV) of *Penaeus monodon* by RT-nested PCR. *Dis Aquat Org* 39:159-167

Cowley JA, Dimmock CM, Spann KM, Walker PJ (2000) Gill-associated virus of

- Penaeus monodon* prawns: an invertebrate virus with ORF1a and ORF1b genes related to arteri- and coronaviruses. *J Gen Virol* 81:1473-1484
- Cowley JA, Hall MR, Cadogan LC, Spann KM, Walker PJ (2002) Vertical transmission of gill-associated virus (GAV) in the black tiger prawn *Penaeus monodon*. *Dis Aquat Org* 50:95-104
- Cowley JA, Walker PJ (2002) The complete genome sequence of gill-associated virus of *Penaeus monodon* prawns indicates a gene organisation unique among nidoviruses. *Arch Virol* 147:1977-1987
- Cowley JA, Walker PJ (2008) Molecular biology and pathogenesis of roniviruses. In: Perlman S, Gallapher T, Snijder EJ (eds) *Nidoviruses*. AMS Press, Washington, p 361-377
- Curtis KM, Yount B, Sims AC, Baric RS (2004) Reverse genetic analysis of the transcription regulatory sequence of the *Coronavirus* transmissible gastroenteritis virus. *J Virol* 78:6061-6066
- de Gerbehaye A-I, Bodéus M, Robert A, Horsmans Y, Goubau P (2002) Stable hepatitis C virus RNA detection by RT-PCR during four days storage. *BMC Infect Dis* 2: 22-27
- de la Rosa-Vélez J, Cedano-Thomas Y, Cid-Becerra J, Méndez-Payán JC, Vega-Pérez C, Zambrano-García J, Bonami J-R (2006) Presumptive detection of yellow head virus by reverse transcriptase-polymerase chain reaction and dot-blot hybridization in *Litopenaeus vannamei* and *L. stylirostris* cultured on the Northwest coast of Mexico. *J Fish Dis* 29:717-726
- de la Vega E, Degnan BM, Hall MR, Cowley JA, Wilson KJ (2004) Quantitative real-

time RT-PCR demonstrates that handling stress can lead to rapid increases of gill-associated virus (GAV) infection levels in *Penaeus monodon*. *Dis Aquat Org* 59:195-203

Delatte H, Martin DP, Naze F, Goldbach R, Reynaud B, Peterschmitt M, Lett J-M (2005)

South West Indian Ocean islands tomato begomovirus populations represent a new major monopartite begomovirus group. *J Gen Virol* 86:1533-1542

Deming D, Baric RS (2008) Genetics and reverse genetics of nidoviruses. In: Perlman S,

Gallagher T, Snijder EJ (eds) *Nidoviruses*. ASM Press, Washington, D. C., p 47-64

Dhar AK, Cowley JA, Hasson KW, Walker PJ (2004) Genomic organization, biology, and diagnosis of Taura Syndrome Virus and Yellowhead Virus of penaeid shrimp.

Adv Virus Res 63:354-421

Dhar AK, Roux MM, Klimpel KR (2001) Detection and quantification of infectious

hypodermal and hematopoietic necrosis virus and white spot virus in shrimp using real-time quantitative PCR and SYBR Green chemistry. *J Clin Microbiol* 39:2835-

2845

Dhar AK, Roux MM, Klimpel KR (2002) Quantitative assay for measuring the Taura

syndrome virus and yellow head virus load in shrimp by real-time RT-PCR using SYBR Green chemistry. *J Virol Methods* 104:69-82

Do JW, Cha SJ, Lee NS, Kim YC, Kim JW, Kim JD, Park JW (2006) Taura syndrome

virus from *Penaeus vannamei* shrimp cultured in Korea. *Dis Aquat Org* 70:171-174

Draker R, Roper RL, Petric M, Tellier R (2006) The complete sequence of the bovine

torovirus genome. *Virus Res* 115:56-68

Durand SV and Lightner DV (2002) Quantitative real time PCR for the measurement of

- white spot syndrome virus in shrimp. *J Fish Dis* 25:381-389
- Durand SV, Tang KFJ, Lightner DV (2000) Frozen commodity shrimp: potential avenue for introduction of white spot syndrome virus and yellow head virus. *J Aquat Anim Health* 12:128-135
- Drummond AJ, Rambaut A (2007) BEAST: Bayesian evolutionary analysis by sampling trees. *BMC Evol Biol* 7:214
- Espy MJ, Uhl JR, Sloan LM, Buckwalter SP, Jones MF, Vetter EA, Yao JDC, Wengenack NL, Rosenblatt JE, Cockerill III FR, Smith TF (2006) Real-time PCR in clinical microbiology: applications for routine laboratory testing. *Clin Microbiol Rev* 19: 165-256
- Felsenstein J (1989) PHYLIP - Phylogeny Inference Package (Version 3.2). *Cladistics* 5:164-166
- Flegel TD, Fegan DF, Sriurairatana S (1995a) Environmental control of infectious shrimp disease in Thailand. In: Shriff M, Subasinghe RP, Arthur JR (eds) *Diseases in Asian Aquaculture II*. Asian Fisheries Society, Manila, the Philippines, p 65-79
- Flegel TW (1997) Special topic review: Major viral diseases of the black tiger prawn (*Penaeus monodon*) in Thailand. *World J Microbiol Biotechnol* 13:433-442
- Flegel TW (2006) Detection of major penaeid shrimp viruses in Asia, a historical perspective with emphasis on Thailand. *Aquaculture* 258:1-33
- Flegel TW (2007) Update on viral accommodation, a model for host-viral interaction in shrimp and other arthropods. *Dev Comp Immunol* 31:217-231
- Flegel TW and Alday-Sanz V (1998) The crisis in Asian shrimp aquaculture: current status and future needs. *J Appl Ichthyol* 14:269-273

- Flegel TW, Boonyaratpalin S, Withyachumnarnkul B (1997) Progress in research on yellow-head virus and white-spot virus in Thailand. In: Flegel TW, MacRae IH (eds) Diseases in Asian Aquaculture III. Fish Health Section. Asian Fisheries Society, Manila, the Philippines, p 285-296
- Flegel TW, Sriurairatana S, Wongterrasupaya C, Boonsaeng V, Panyim S, Withyachumnarnkul B (1995b) Progress in characterization and control of yellow-head virus of *Penaeus monodon*. In: Browdy CL, Hopkins JS (eds) Swimming through Troubled Water: Proceedings of the Special Session on Shrimp Farming, Aquaculture '95. World Aquaculture Society, Baton Rouge, LA, p 76-83
- Forsberg R, Oleksiewicz MB, Krabbe Petersen A-M, Hein J, Bøtner A, Storgaard T (2001) A molecular clock dates the common ancestor of European-type porcine reproductive and respiratory syndrome virus at more than 10 years before the emergence of disease. *Virology* 289:174-179
- Fraser CA, Owens L (1996) Spawner-isolated mortality virus from Australian *Penaeus monodon*. *Dis Aquat Org* 27:141-148
- Gao L, Qi J (2007) Whole genome molecular phylogeny of large dsDNA viruses using composition vector method. *BMC Evol Biol* 7:41
- Gao L, Qi J, Sun J, Hao B (2007) Prokaryote phylogeny meets taxonomy: an exhaustive comparison of composition vector trees with systematic bacteriology. *Sci China C Life Sci* 50:587-599
- Gao L, Qi J, Wei H, Sun Y, Hao B (2003) Molecular phylogeny of coronaviruses including human SARS-CoV. *Chin Sci Bull* 48:1170-1174
- Gibbs MJ, Armstrong JS, Gibbs AJ (2000) Sister-scanning: a Monte Carlo procedure for

- assessing signals in recombinant sequences. *Bioinformatics* 16:573-582
- Giedroc DP, Theimer CA, Nixon PL (2000) Structure, stability and function of RNA pseudoknots involved in stimulating ribosomal frameshifting. *J Mol Biol* 298:167-185
- Godeny EK, Chen L, Kumar SN, Methven SL, Koonin EV, Brinton MA (1993) Complete genomic sequence and phylogenetic analysis of the lactate dehydrogenase-elevating virus (LDV). *Virology* 194:585-596
- Goebel SJ, Hsue B, Dombrowski TF, Masters PS (2004) Characterization of the RNA components of a putative molecular switch in the 3' untranslated region of the murine coronavirus genome. *J Virol* 78:669-682
- Goebel SJ, Miller TB, Bennett CJ, Bernard KA, Masters PS (2007) A hypervariable region within the 3' cis-acting element of the murine coronavirus genome is nonessential for RNA synthesis but affects pathogenesis. *J Virol* 81:1274-1287
- Gopalakrishnan A, Parida A (2005) Incidence of loose shell syndrome disease of the shrimp *Penaeus monodon* and its impact in the grow-out culture. *Curr Sci* 88:1148-1154
- Gorbalenya AE (2008) Genomics and evolution of the *Nidovirales*. In: Perlman S, Gallagher T, Snijder EJ (eds) *Nidoviruses*. ASM Press, Washington, p 15-28
- Gorbalenya AE, Enjuanes L, Ziebuhr J, Snijder EJ (2006) *Nidovirales*: evolving the largest RNA virus genome. *Virus Res* 117:17-37
- Granados-Dieseldorff, P (2006) Habitat use by nekton in a salt marsh estuary along a stream-order gradient in northeastern Barataria Bay, Louisiana. M.S. thesis. Baton Rouge, Louisiana, Louisiana State University

- Grant PR, Kitchen A, Barbara JA, Hewitt P, Sims CM, Garson JA, Tedder RS (2000)
Effect of handling and storage of blood on the stability of hepatitis C virus RNA:
implications for NA T testing in transfusion practice. *Vox Sang* 78:137-142
- Hasson KW, Lightner DV, Poulos BT, Redman RM, White BL, Brock JA, Bonami JR
(1995) Taura syndrome in *Penaeus vannamei*: demonstration of a viral etiology.
Dis Aquat Org 23:115-126
- Heard RW (1982) Guide to Common Tidal Marsh Invertebrates of the Northeastern Gulf
of Mexico. Mississippi-Alabama Sea Grant Consortium, Booneville, Mississippi
- Heath L, van der Walt E, Varsani A, Martin DP (2006) Recombination patterns in
aphthoviruses mirror those found in anther picornaviruses. *J. Virol.* 80:11827-
11832
- Herniou EA, Luque T, Chen X, Vlak JM, Winstanley D, Cory JS, O'Reilly DR (2001)
Use of whole genome sequence data to infer baculovirus phylogeny. *J Virol*
75:8117-8126
- Holmes EC (2003) Molecular clocks and the puzzle of RNA virus origins. *J. Virol.*
77:3893-3897
- Holmes EC, Worobey M, Rambaut A (1999) Phylogenetic evidence for recombination in
dengue virus. *Mol Biol Evol* 16:405-409
- Hsue B, Hartshorne T, Masters PS (2000) Characterization of an essential RNA
secondary structure in the 3' untranslated region of the murine coronavirus genome.
J Virol 74:6911-6921
- Hughes GJ, Orciari LA, Rupprecht CE (2005) Evolutionary timescale of rabies virus
adaptation to North American bats inferred from the substitution rate of the

- nucleoprotein gene. *J Gen Virol* 86:1467-1474
- Hukuhara T, Bonami JR (1991) Reoviridae. In: Adams JR, Bonami (eds) *Atlas of Invertebrate Viruses*. CRC Press, Boca Raton, FL, p 393-434
- Jacks T, Power MD, Masiarz FR, Luciw PA, Barr PJ, Varmus HE (1988) Characterization of ribosomal frameshifting in HIV-1 gag-pol expression. *Nature* 331:280-283
- Jitrapakdee S, Unajak S, Sittidilokratna N, Hodgson RAJ, Cowley JA, Walker PJ, Panyim S, Boonsaeng V (2003) Identification and analysis of gp116 and gp64 structural glycoproteins of yellow head nidovirus of *Penaeus monodon* shrimp. *J Gen Virol* 84:863-873
- Julenius K, Molgaard A, Gupta R, Brunak S (2005) Prediction, conservation analysis, and structural characterization of mammalian mucin-type O-glycosylation sites. *Glycobiology* 15:153-164
- Käll L, Krogh A, Sonnhammer ELL (2004) A combined transmembrane topology and signal peptide prediction method. *J Mol Biol* 338:1027-1036
- Kennedy VS, Oesterling M, van Engel WA (2007) History of blue crab fisheries on the U.S. Atlantic and Gulf Coasts. In: Kennedy VS, Cronin LE (eds) *The Blue Crab: Callinectes sapidus*. Maryland Sea Grant College, College Park, Maryland, p 655-709
- Kiatpathomchai W, Jitrapakdee S, Panyim S, Boonsaeng V (2004) RT-PCR detection of yellow head virus (YHV) infection in *Penaeus monodon* using dried hemolymph spots. *J Virol Methods* 119:1-5
- Kneib RT (1987) Seasonal abundance, distribution and growth of postlarval and juvenile

- grass shrimp (*Palaemonetes pugio*) in Georgia, USA. salt marsh. *Mar Biol* 96:215-223
- Kneib RT, Wagner SL (1994) Nekton use of vegetated marsh habitats at different stages of tidal inundation. *Mar Ecol Prog Ser* 106:227-238
- Kosakovsky Pond SL and Frost SDW (2005) Not so different after all: A comparison of methods for detecting amino acid sites under selection. *Mol Biol Evol* 22:1208-1222
- Kosakovsky Pond SL, Posada D, Gravenor MB, Woelk CH, Frost SDW (2006) Automated phylogenetic detection of recombination using a genetic algorithm. *Mol Biol Evol* 23:1891-1901
- Krajden M, Minor JM, Rifkin O, Comanor L (1999a) Effect of multiple freeze-thaw cycles on hepatitis B virus DNA and hepatitis C virus RNA quantification as measured with branched-DNA technology. *J Clin Microbiol* 37:1683-1686
- Krajden M, Minor JM, Zhao J, Rifkin O, Comanor L (1999b) Assessment of hepatitis C virus RNA stability in serum by the quantiplex branched DNA assay. *J Clin Virol* 14:137-143
- Krogh A, Larsson B, von Heijne G, Sonnhammer EL (2001) Predicting transmembrane protein topology with a hidden Markov model: application to complete genomes. *J Mol Biol* 305:567-580
- Lai MMC (1992) RNA recombination in animal and plant viruses. *Microbiol Rev* 56:61-79
- Laughlin, R. A. (1979) Trophic ecology and population distribution of blue crab, *Callinectes sapidus* Rathbun, in the Apalachicola estuary (North Florida, U.S.A.).

Tallahassee, Florida, USA. Florida State University

- Leber KM (1985) The influence of predatory decapods, refuge, and microhabitat selection on seagrass communities. *Ecology* 66:1951-1964
- Lefeuvre P, Martin DP, Hoareau M, Naze F, Delatte H, Thierry M, Varsani A, Becker N, Reynaud B, Lett J-M (2007) Begonovirus 'melting pot' in the south-west Indian Ocean islands: molecular diversity and evolution through recombination. *J Gen Virol* 88:3458-3468
- Lester RJG, Doubrovsky A, Paynter JL, Sambhi SK, Atherton JG (1987) Light and electron microscope evidence of baculovirus infection in the prawn *Penaeus plebejus*. *Dis Aquat Org* 3:217-219
- Lewis TL, Matsui SM (1997) Studies of the astrovirus signal that induces (-1) ribosomal frameshifting. *Adv Exp Med Biol* 412:323-330
- Lightner DV (1996a) A Handbook of Shrimp Pathology and Diagnostic Procedures for Diseases of Cultured Penaeid Shrimp. World Aquaculture Society, Baton Rouge, LA, USA
- Lightner DV (1996b) Epizootiology, distribution, and the impact on international trade of two penaeid shrimp viruses in the Americas. *Rev Sci Off Int Epiz* 5:597-601
- Lightner DV (1999) The penaeid shrimp viruses TSV, IHHNV, WSSV, and YHV: current status in the Americas, Available diagnostic methods, and management strategies. *J Appl Aquacult* 9:27-51
- Lightner DV (2003) The penaeid shrimp viral pandemics due to IHHNV, WSSV, TSV and YHV: current status in the Americas. World Aquaculture Society Meeting, Book of Abstracts, vol. 1. World Aquaculture Society, Baton Rouge, LA, p 418

- Lightner DV, Hasson KW, White BL, Redman RM (1998) Experimental infection of western hemisphere penaeid shrimp with Asian white spot syndrome virus and Asian yellow head virus. *J Aquat Anim Health* 10:271-281
- Lightner DV, Pantoja CR, Poulos BT, Tang KFJ, Redman RM, Pasos-de-Andrade T, Bonami JR (2004) Infectious myonecrosis, new disease in Pacific white shrimp. *Global Aquacult Advocate* 7:85
- Lightner DV, Redman RM (1985) A parvo-like virus disease of penaeid shrimp. *J Invertebr Pathol* 45:47-53
- Lightner DV, Redman RM (1993) A putative iridovirus from the penaeid shrimp *Protrachypene precipua* Burkenroad (Crustacea: Decapoda). *J Invertebr Pathol* 62:107-109
- Lightner DV, Redman RM (1998) Shrimp diseases and current diagnostic methods. *Aquaculture* 164:201-220
- Lightner DV, Redman RM, Bell TA (1983) Infectious hypodermal and hematopoietic necrosis a newly recognized virus disease of penaeid shrimp. *J Invertebr Pathol* 42:62-70
- Lightner DV, Redman RM, Poulos BT, Nunan LM, Mari JL, Hasson KW (1997) Risk of spread of penaeid shrimp viruses in the Americas by the international movement of live and frozen shrimp. *Revue Scientifique et Technique Office International des Epizooties* 16:146-160
- Limsuwan C (1991) *Handbook for Cultivation of Black Tiger Prawns*. Tansetakit, Bangkok, Thailand
- Liu B, Yu Z, Song X, Guan Y (2007) Studies on the transmission of WSSV (white spot

- syndrome virus) in juvenile *Marsupenaeus japonicus* via marine microalgae. *J Invertebr Pathol* 95:87-92
- Liu Q, Johnson RF, Leibowitz JL (2001) Secondary structural elements within the 3' untranslated region of mouse hepatitis virus strain JHM genomic RNA. *J Virol* 75:12105-12113
- Livingston RJ (1984) *The Ecology of the Apalachicola Bay System: an Estuarine Profile*. Fish and Wildlife Service, U. S. Department of the Interior, Washington, D. C.
- Livingston RJ (2002) *Trophic Organization in Coastal Systems*. CRC Press, Washington D. C.
- Longyant S, Sattaman S, Chaivisuthangkura P, Rukpratanporn S, Sithigorngul W, Sithigorngul P (2006) Experimental infection of some penaeid shrimps and crabs by yellow head virus (YHV). *Aquaculture* 257:83-91
- Longyant S, Sithigorngul P, Chaivisuthangkura P, Rukpratanporn S, Sithigorngul W, Menasveta P (2005) Differences in susceptibility of palaemonid shrimp species to yellow head virus (YHV) infection. *Dis Aquat Org* 64:5-12
- Lopinski JD, Dinman JD, Bruenn JA (2000) Kinetics of ribosomal pausing during programmed -1 translational frameshifting. *Mol Cell Biol* 20:1095-1103
- Lu Y, Tapay LM, Brock JA, Loh PC (1994) Infection of the yellow head baculo-like virus (YBV) in two species of penaeid shrimp, *Penaeus stylirostris* (Simpson) and *Penaeus vannamei* (Boone). *J Fish Dis* 17:649-656
- Lu Y, Tapay LM, Gose RB, Brock JA, Loh PC (1997) Infectivity of yellow head virus (YHV) and the Chinese baculo-like virus (CBV) in two species of penaeid shrimp *Penaeus stylirostris* (Stimpson) and *Penaeus vannamei* (Boone). In: Flegel TW,

- MacRae IH (eds) Diseases in Asian Aquaculture III. Asian Fisheries Society, Manila, the Philippines. p 297-304
- Lu Y, Tapay LM, Loh PC, Brock JA, Gose RB (1995) Distribution of yellow-head virus in selected tissues and organs of penaeid shrimp *Penaeus vannamei*. Dis Aquat Org 23:67-70
- Lukashev AN, Ivanova OE, Eremeeva TP, Iggo RD (2008) Evidence of frequent recombination among human adenoviruses. J Gen Virol 89:380-388
- Luo T, Yang HJ, Li F, Zhang XB, Xu X (2006) Purification, characterization and cDNA cloning of a novel lipopolysaccharide-binding lectin from the shrimp *Penaeus monodon*. Dev Comp Immunol 30:607-617
- Ma H, Overstreet RM, Jovonovich JA (2008) Stable yellow head virus (YHV) RNA detection by qRT-PCR during six-day storage. Aquaculture 278:10 – 13
- Mackay IM, Arden KE, Nitsche A (2002) Real-time PCR in virology. Nucleic Acids Res 30: 1292-1305
- Marczinke B, Bloys AJ, Brown TD, Willcocks MM, Carter MJ, Brierley I (1994) The human astrovirus RNA-dependent RNA polymerase coding region is expressed by ribosomal frameshifting. J Virol 68:5588-5595
- Martin D and Rybicki E (2000) RDP: detection of recombination amongst aligned sequences. Bioinformatics 16:562-563
- Martin DP, van der Walt E, Posada D, Rybicki EP (2005a) The evolutionary value of recombination is constrained by genome modularity. PLoS Genetics 1:e51
- Martin DP, Williamson C, Posada D (2005b) RDP2: recombination detection and analysis from sequence alignments. Bioinformatics 21:260-262

- Masters PS and Rottier PJM (2005) Coronavirus reverse genetics by targeted RNA recombination. *Curr Top Microbiol Immunol* 287:133-159
- Mayavu P, Purushothaman A, Kathiresan K (2003) Histology of loose-shell affected *Penaeus monodon*. *Curr Sci* 85:1629-1634
- Maynard Smith J (1992) Analyzing the mosaic structure of genes. *J Mol Evol* 34:126-129
- Mayo MA (2002) A summary of taxonomic changes approved by ICTV. *Arch Virol* 147:1655-1656
- Mekata T, Kono T, Savan R, Sakai M, Kasornchandra J, Yoshida T, Itami T (2006) Detection of yellow head virus in shrimp by loop-mediated isothermal amplification (LAMP). *J Virol Methods* 135:151-156
- Molthathong S, Senapin S, Klinbunga S, Puanglarp N, Rojtinnakorn J, Flegel TW (2008) Down-regulation of defender against apoptotic death (DAD1) after yellow head virus (YHV) challenge in black tiger shrimp *Penaeus monodon*. *Fish Shellfish Immunol* 24:173-179
- Moon S, Byun Y, Kim H-J, Jeong S, Han K (2004) Predicting genes expressed via -1 and +1 frameshifts. *Nucleic Acids Res* 32:4884-4892
- Morales JBT, Dardeau MR (1987) Food habits of early juvenile red drum (*Sciaenops ocellatus*) in coastal Alabama. In: Lowery TA (ed) Symposium on the Natural Resources of the Mobile Bay Estuary. Alabama Sea Grant Extension Service, Auburn University, Alabama, p 38-43
- Morgan MD (1980) Grazing and predation of the grass shrimp *Palaemonetes pugio*. *Limnol Oceanogr* 25:896-902
- Mouillessieux KP, Klimpel KR, Dhar AK (2003) Improvement in the specificity and

sensitivity of detection for the Taura syndrome virus and yellow head virus of penaeid shrimp by increasing the amplicon size in SYBR Green real-time RT-PCR.

J Virol Methods 111:121-127

Moya A, Holmes EC, González-Candelas F (2004) The population genetics and evolutionary epidemiology of RNA viruses. Nat Rev Microbiol 2:279-288

Munro J, Owens L (2007) Yellow head-like viruses affecting the penaeid aquaculture industry: a review. Aquacult Res 39:893-908

Nadala ECB, Jr., Tapay LM, Cao S, Loh PC (1997) Detection of yellowhead virus and Chinese baculovirus in penaeid shrimp by the western blot technique. J Virol Methods 69:39-44

Nadala ECB, Jr, Lu Y, Loh P, Brock JA (1992) Infection of *Penaeus stylirostris* (Boone) with a rhabdovirus from *Penaeus* spp. Fish Pathol 27:143-147

Nagy PD and Simon AE (1997) New insights into the mechanisms of RNA recombination. Virology 235:1-9

Natividad K, Magbanua FO, Migo VP, Alfafara CG, Albaladejo JD, Nadala ECB, Jr, Loh PC, Tapay LM (1999) Evidence of yellow head virus in cultured black tiger shrimp (*Penaeus monodon* Fabricius) from selected shrimp farms in the Philippines. Fourth Symposium on Diseases in Asian Aquaculture, p 60

Neuman BW, Stein DA, Kroeker AD, Churchill MJ, Kim AM, Kuhn P, Dawson P, Moulton HM, Bestwick RK, Iversen PL, Buchmeier MJ (2005) Inhibition, escape, and attenuated growth of severe acute respiratory syndrome coronavirus treated with antisense morpholino oligomers. J Virol 79:9665-9676

Neuman BW, Stein DA, Kroeker AD, Moulton HM, Bestwick RK, Iversen PL,

- Buchmeier MJ (2006) Inhibition and escape of SARS-CoV treated with antisense morpholino oligomers. *Adv Exp Med Biol* 581:567-571
- Nielsen L, Sangoum W, Cheevadhanarak S, Flegel TW (2005) Taura syndrome virus (TSV) in Thailand and its relationship to TSV in China and the Americas. *Dis Aquat Org* 63:101-106
- Nunan LM, Poulos BT, Lightner DV (1998) The detection of white spot syndrome virus (WSSV) and yellow head virus (YHV) in imported commodity shrimp. *Aquaculture* 160:19-30
- Oberste MS, Peñaranda S, Pallansch MA (2004) RNA recombination plays a major role in genomic change during circulation of coxsackie B viruses. *J Virol* 78:2948-2955
- Odum WE, McIvor CC, Smith TG (1982) *The Florida Mangrove Zone: a Community Profile*. U.S. Fish and Wildlife Service, Office of Biological Services, Washington D. C.
- Oliver SL, Brown DWG, Green J, Bridger JC (2004) A chimeric bovine enteric calicivirus: evidence for genomic recombination in genogroup III of the *Norovirus* genus of the *Caliciviridae*. *Virology* 326:231-239
- Olmi EJI, Lipcius RN (1991) Predation on postlarvae of the blue crab *Callinectes sapidus* Rathbun by sand shrimp *Crangon septemspinosa* Say and grass shrimp *Palaemonetes pugio* Holthuis. *J Exp Biol Ecol* 151:169-183
- Overstreet RM, Heard RW (1978) Food of the red drum, *Sciaenops ocellata*, from Mississippi Sound. *Gulf Res Rep* 6:131-135
- Overstreet RM, Heard RW (1982) Food contents of six commercial fishes from Mississippi Sound. *Gulf Res Rep* 7:137-149

- Owens L (1993) Description of the first haemocytic rod-shaped virus from a penaeid prawn. *Dis Aquat Org* 16:217-221
- Owens L, De-Beer S, Smith J (1991) Lymphoid parvovirus-like particles in Australian penaeid prawns. *Dis Aquat Org* 11:129-134
- Owor BE, Martin DP, Shepherd DN, Edema R, Monjane AL, Rybicki EP, Thomson JA, Varsani A (2007) Genetic analysis of maize streak virus isolates from Uganda reveals widespread distribution of a recombinant variant. *J Gen Virol* 88:3154-3165
- Padidam M, Sawyer S, Fauquet CM (1999) Possible emergence of new geminiviruses by frequent recombination. *Virology* 265:218-225
- Pennak, RW (1978) *Fresh-water Invertebrates of the United States*, 2nd ed., John Wiley and Sons, New York, NY
- Pérez Farfante I, Kensley B (1997) *Penaeoid and Sergestoid Shrimps and Prawns of the World (Keys and Diagnoses for the Families and Genera)*. Muséum National d'Histoire Naturelle, Paris.
- Phan YTN (2001) Prevalence and co-prevalence of white spot syndrome virus (WSSV) and yellow head complex viruses (YHV-complex) in cultured giant tiger prawn (*Penaeus monodon*) in Vietnam. M.S. thesis. Brisbane, Australia, University of Queensland
- Piñon JD, Mayreddy RR, Turner JD, Khan FS, Bonilla PJ, Weiss SR (1997) Efficient autoproteolytic processing of the MHV-A59 3C-like proteinase from the flanking hydrophobic domains requires membranes. *Virology* 230:309-322
- Poulos BT and Lightner DV (2006) Detection of infectious myonecrosis virus (IMNV) of penaeid shrimp by reverse-transcriptase polymerase chain reaction (RT-PCR). *Dis*

Aquat Org 73:69-72

- Poulos BT, Tang KFJ, Pantoja CR, Bonami JR, Lightner DV (2006) Purification and characterization of infectious myonecrosis virus of penaeid shrimp. J Gen Virol 87:987-996
- Prakasha BK, Ramakrishna RP, Karunasagar I, Karunasagar I (2007) Detection of Laem-Singh virus (LSNV) in cultured *Penaeus monodon* from India. Dis Aquat Org 77:83-86
- Prentice E, McAuliffe J, Lu X, Subbarao K, Denison MR (2004) Identification and characterization of severe acute respiratory syndrome coronavirus replicase proteins. J Virol 78:9977-9986
- Prüfer D, Tacke E, Schmitz J, Kull B, Kaufmann A, Rohde W (1992) Ribosomal frameshifting in plants: a novel signal directs the -1 frameshift in the synthesis of the putative viral replicase of potato leafroll luteovirus. EMBO J 11:1111-1117
- Pyrc K, Dijkman R, Deng L, Jebbink MF, Ross HA, Berkhout B, van der Hoek L (2006) Mosaic structure of human *Coronavirus* NL63, one thousand years of evolution. J Mol Biol 364:964-973
- Qi J, Luo H, Hao B (2004a) CVTree: a phylogenetic tree reconstruction tool based on whole genomes. Nucleic Acids Res 32:W45-7
- Qi J, Wang B, Hao B-I (2004b) Whole proteome prokaryote phylogeny without sequence alignment: a K-string composition approach. J Mol Evol 58:1-11
- Qin Z, Sun L, Ma B, Cui Z, Zhu Y, Kitamura Y, Liu W (2008) F gene recombination between genotype II and VII Newcastle disease virus. Virus Res 131:299-303
- Quinones-Rivera ZJ, Fleeger JW (2005) The grazing effects of grass shrimp,

Palaemonetes pugio, on epiphytic microalgae associated with *Spartina alterniflora*.

Estuaries 28:274-285

Rajendran KV, Cowley JA, McCulloch RJ, Waiker PJ (2006) A TaqMan real-time RT-PCR for quantifying Mourilyan virus infection levels in penaeid shrimp tissues. J Viral Methods 137:265-271

Reeder J, Giegerich R (2004) Design, implementation and evaluation of a practical pseudoknot folding algorithm based on thermodynamics. BMC Bioinformatics 5:104

Robalino J, Bartlett T, Shepard E, Prior S, Jaramillo G, Scura E, Chapman RW, Gross P, Browdy CL, Warr GW (2005) Double-stranded RNA induces sequence-specific antiviral silencing in addition to nonspecific immunity in marine shrimp: convergence of RNA interference and innate immunity in the invertebrate antiviral response? J Virol 79:13561-13571

Robalino J, Browdy CL, Prior S, Metz A, Parnell P, Gross P, Warr G (2004) Induction of antiviral immunity by double-stranded RNA in a marine invertebrate. J Virol 78:10442-10448

Romo-Figueroa MG, Vargas-Requena C, Sotelo-Mundoa RR, Vargas-Albores F, Higuera-Ciapara I, Soderhall K, Yepiz-Plascencia G (2004) Molecular cloning of a beta-glucan pattern-recognition lipoprotein from the white shrimp *Penaeus (Litopenaeus) vannamei*: correlations between the deduced amino acid sequence and the native protein structure. Dev Comp Immunol 28:713-728

Roux MM, Pain A, Klimpel KR, Dhar AK (2002) The lipopolysaccharide and beta-1,3-glucan binding protein gene is upregulated in white spot virus-infected shrimp

- (*Penaeus stylirostris*). J Virol 76:7140-7149
- Rozas LP, Minello TJ (2001) Marsh terracing as a wetland restoration tool for creating fishery habitat. Wetlands 21:327-341
- Sakaew W (2006) Bamboo-shaped disease in *Litopenaeus vannamei*. M.S. thesis. Mahidol University
- Sánchez-Barajas M, Liñán-Cabello MA, Mena-Herrera A (2008) Detection of yellow-head disease in intensive freshwater production systems of *Litopenaeus vannamei*. Aquac Int 16:
- Schütze H, Ulferts R, Schelle B, Bayer S, Granzow H, Hoffmann B, Mettenleiter TC, Ziebuhr J (2006) Characterization of white bream virus reveals a novel genetic cluster of nidoviruses. J Virol 80:11598-11609
- Senapin S, Phewsaiya K, Briggs M, Flegel TW (2007) Outbreaks of infectious myonecrosis virus (IMNV) in Indonesia confirmed by genome sequencing and use of an alternative RT-PCR detection method. Aquaculture 266:32-38
- Serviene E, Shapka N, Cheng C-P, Panavas T, Phuangrat B, Baker J, Nagy PD (2005) Genome-wide screen identifies host genes affecting viral RNA recombination. Proc. Natl. Acad. Sci. USA 102:10545-10550
- Shapiro-Ilan DI, Fuxa JR, Lacey LA, Onstad DW, Kaya HK (2005) Definitions of pathogenicity and virulence in invertebrate pathology. J Invertebr Pathol 88:1-7
- Siddell S, Snijder EJ (2008) An introduction to nidoviruses. In: Perlman S, Gallagher T, Snijder EJ (eds) Nidoviruses. ASM Press, Washington, DC, p 1-13
- Sittidilokratna N, Dangtip S, Cowley JA, Walker PJ (2008) RNA transcription analysis and completion of the genome sequence of yellow head nidovirus. Virus Res (in

press)

- Sittidilokratna N, Hodgson RAJ, Cowley JA, Jitrapakdee S, Boonsaeng V, Panyim S, Walker PJ (2002) Complete ORF1b-gene sequence indicates yellow head virus is an invertebrate nidovirus. *Dis Aquat Org* 50:87-93
- Smith PT (2000) Diseases of the eye of farmed shrimp *Penaeus monodon*. *Dis Aquat Org* 43:159-173
- Snijder EJ and Meulenberg JJ (1998) The molecular biology of arteriviruses. *J Gen Virol* 79:961-979
- Snijder EJ, den Boon JA, Bredenbeek PJ, Horzinek MC, Rijnbrand R, Spaan WJ (1990) The carboxyl-terminal part of the putative Berne virus polymerase is expressed by ribosomal frameshifting and contains sequence motifs which indicate that toro- and coronaviruses are evolutionarily related. *Nucleic Acids Res* 18:4535-4542
- Spann KM, Cowley JA, Walker PJ, Lester RJG (1997) A yellow-head-like virus from *Penaeus monodon* cultured in Australia. *Dis. Aquat.Org.* 31:169-179
- Spann KM, Vickers JE, Lester RJG (1995) Lymphoid organ virus of *Penaeus monodon* from Australia. *Dis Aquat Org* 23:127-134
- Sritunyalucksana K, Apisawetakan S, Boon-nat A, Withyachumnarnkul B, Flegel TW (2006) A new RNA virus found in black tiger shrimp *Penaeus monodon* from Thailand. *Virus Res* 118:31-38
- Sritunyalucksana N, Lee SY, Soderhall K (2002) A beta-1, 3-glucan binding protein from the black tiger shrimp, *Penaeus monodon*. *J Biochem Mol Biol* 26:237-245
- Stallknecht DE, Kearney MT, Shane SM, Zwank PJ (1990) Effects of pH, temperature, and salinity on persistence of Avian Influenza viruses in water. *Avian Dis* 34:412-

418

- Summerton JE (1999) Morpholino antisense oligomers: the case for an RNase H-independent structural type. *Biochim Biophys Acta* 1489:141-158
- Summerton JE (2005) Endo-Porter: a novel reagent for safe, effective delivery of substances into cells. *Ann N Y Acad Sci* 1058:62-75
- Summerton JE (2007) Morpholino, siRNA, and S-DNA compared: impact of structure and mechanism of action on off-target effects and sequence specificity. *Curr Top Med Chem* 7:651-660
- Takahashi Y, Itami T, Maeda M, Suzuki N, Kasornchandra J, Supamattaya K, Khongpradit R, Boonyaratpalin S, Kondo M, Kawai K, Kusuda R, Hirono I, Aoki T (1996) Polymerase chain reaction (PCR) amplification of bacilliform virus (RV-PJ) DNA in *Penaeus japonicus* Bate and systemic ectodermal and mesodermal baculovirus (SEMBV) DNA in *Penaeus monodon* Fabricius. *J Fish Dis* 19:399-403
- Tamura K, Dudley J, Nei M, Kumar S (2007) MEGA4: Molecular evolutionary genetics analysis (MEGA) software version 4.0. *Mol Biol Evol* 24:1596-1599
- Tang KFJ and Lightner DV (1999) A yellow head virus gene probe: nucleotide sequence and application for in situ hybridization. *Dis Aquat Org* 35:165-173
- Tang KFJ and Lightner DV (2001) Detection and quantification of infectious hypodermal and hematopoietic necrosis virus in penaeid shrimp by real-time PCR. *Dis Aquat Org* 44:79-85
- Tang KFJ, Pantoja CR, Poulos BT, Redman RM, Lightner DV (2005) In situ hybridization demonstrates that *Litopenaeus vannamei*, *L. stylirostris* and *Penaeus monodon* are susceptible to experimental infection with infectious myonecrosis

- virus (IMNV). *Dis Aquat Org* 63:261-265
- Tang KFJ, Pantoja CR, Redman RM, Lightner DV (2007) Development of in situ hybridization and RT-PCR assay for the detection of a nodavirus (PvNV) that causes muscle necrosis in *Penaeus vannamei*. *Dis Aquat Org* 75:183-190
- Tang KFJ, Spann KM, Owens L, Lightner DV (2002) In situ detection of Australian gill-associated virus with a yellow head virus gene probe. *Aquaculture* 205:1-5
- Tang KFJ, Wang J, Lightner DV (2004) Quantitation of Taura syndrome virus by real-time RT-PCR with a TaqMan assay. *J Virol Methods* 115:109-114
- ten Dam E, Brierley I, Inglis S, Pleij C (1994) Identification and analysis of the pseudoknot-containing gag-pro ribosomal frameshift signal of simian retrovirus-1. *Nucleic Acids Res* 22:2304-2310
- ten Dam EB, Pleij CW, Bosch L (1990) RNA pseudoknots: translational frameshifting and readthrough on viral RNAs. *Virus Genes* 4:121-136
- Thomas SR and Elkinton JS (2004) Pathogenicity and virulence. *J Invertebr Pathol* 85:146-151
- Thompson JD, Gibson TJ, Plewniak F, Jeanmougin F, Higgins DG (1997) The ClustalX windows interface: flexible strategies for multiple sequence alignment aided by quality analysis tools. *Nucleic Acids Res* 25:4876-4882
- Tibbles KW, Brierley I, Cavanagh D, Brown TD (1996) Characterization in vitro of an autocatalytic processing activity associated with the predicted 3C-like proteinase domain of the coronavirus avian infectious bronchitis virus. *J Virol* 70:1923-1930
- Tijms MA, Nedialkova DD, Zevenhoven-Dobbe JC, Gorbalenya AE, Snijder EJ (2007) Arterivirus subgenomic mRNA synthesis and virion biogenesis depend on the

- multifunctional nsp1 autoprotease. *J Virol* 81:10496-10505
- Tirasophon W, Roshorm Y, Panyim S (2005) Silencing of yellow head virus replication in penaeid shrimp cells by dsRNA. *Biochem Biophys Res Commun* 334:102-107
- Tirasophon W, Yodmuang S, Chinnirunvong W, Plongthongkum N, Panyim S (2007) Therapeutic inhibition of yellow head virus multiplication in infected shrimps by YHV-protease dsRNA. *Antiviral Res* 74:150-155
- Tsing A, Bonami JR (1997) A new virus disease of the tiger shrimp *Penaeus japonicus* (Bate). *J Fish Dis* 10:139-141
- Tzeng TH, Tu CL, Bruenn JA (1992) Ribosomal frameshifting requires a pseudoknot in the *Saccharomyces cerevisiae* double-stranded RNA virus. *J Virol* 66:999-1006
- Valli A, López-Moya JJ, García JA (2007) Recombination and gene duplication in the evolutionary diversification of P1 proteins in the family Potyviridae. *J Gen Virol* 88:1016-1028
- van den Born E, Snijder EJ (2008) RNA signals regulating nidovirus RNA synthesis. In: Perlman S, Gallapher T, Snijder EJ (eds) *Nidoviruses*. ASM Press, Washington, p 115-131
- van den Born E, Stein DA, Iversen PL, Snijder EJ (2005) Antiviral activity of morpholino oligomers designed to block various aspects of Equine arteritis virus amplification in cell culture. *J Gen Virol* 86:3081-3090
- van den Born, E, (2006) RNA structures regulating nidovirus RNA synthesis. PhD dissertation. Leiden, Netherlands, Leiden University
- van der Meer Y, van Tol H, Krijnse Locker J, Snijder EJ (1998) ORF1a-encoded replicase subunits are involved in the membrane association of the Arterivirus

- replication complex. *J Virol* 72:6689-6698
- van Marle G, Dobbe JC, Gulyaev AP, Luytjes W, Spaan WJ, Snijder EJ (1999) Arterivirus discontinuous mRNA transcription is guided by base pairing between sense and antisense transcription-regulating sequences. *Proc Natl Acad Sci USA* 96:12056-12061
- van Vliet ALW, Smits SL, Rottier PJM, de Groot RJ (2002) Discontinuous and non-discontinuous subgenomic RNA transcription in a nidovirus. *EMBO J* 21:6571-6580
- Vanpatten KA, Nunan LM, Lightner DV (2004) Seabirds as potential vectors of penaeid shrimp viruses and the development of a surrogate laboratory model utilizing domestic chickens. *Aquaculture* 241:31-46
- Vijaykrishna D, Smith GJD, Zhang JX, Peiris JSM, Chen H, Guan Y (2007) Evolutionary Insights into the Ecology of Coronaviruses. *J Virol* 81:4012-4020
- Walker PJ (2006) Yellowhead disease. In: OIE Aquatic Animal Health Standards Commission (ed) OIE Manual of Diagnostic Tests for Aquatic Animals. Office International des Épizooties, Paris, p 392-404
- Walker PJ, Bonami JR, Boonsaeng V, Chang PSCJA, Enjuanes L, Flegel TW, Lightner DV, Loh PC, Snijder EJ, Tang K (2005) Family *Roniviridae*. In: Fauquet CM, Mayo MA, Maniloff J, Desselberger U, Ball LA (eds) *Virus Taxonomy: Eighth Report of the International Committee on Taxonomy of Viruses*. Elsevier Academic Press, San Diego, CA, p 263-265
- Walker PJ, Cowley JA, Spann KM, Hodgson RAJ, Hall MR, Withyachumnarnkul B (2001) Yellow head complex viruses: transmission cycles and topographical

- distribution in the Asia-Pacific region. In: Brewdy CL, Jory DE (eds) *The New Wave: Proceedings of the Special Session on Sustainable Shrimp Culture, Aquaculture 2001*. The World Aquaculture Society, Baton Rouge, LA,
- Wang CS, Tang KJ, Kuo GH, Chen SN (1996) Yellow head disease-like virus infection in the Kuruma shrimp *Penaeus japonicus* cultured in Taiwan. *Fish Pathol* 31:177-182
- Watzinger F, Ebner K, Lion T (2006) Detection and monitoring of virus infections by real-time PCR. *Mol. Aspects Med* 27:254-298
- Weng Z, Barthelson R, Gowda S, Hilf ME, Dawson WO, Galbraith DW, Xiong Z (2007) Persistent infection and promiscuous recombination of multiple genotypes of an RNA virus within a single host generate extensive diversity. *PLoS ONE* 2:e917
- Wijegoonawardane PMK, Cowley JA, Phan T, Hodgson RAJ, Nielsen L, Kiatpathomchai W, Walker PJ (2008) Genetic diversity in the yellow head nidovirus complex. *Virology*
- Wijegoonawardane, PKM (2007) Molecular epidemiology of yellow head-complex viruses of cultured prawns in the Asian region. University of Queensland
- Williams GD, Chang R-Y, Brian DA (1999) A phylogenetically conserved hairpin-type 3' untranslated region pseudoknot functions in coronavirus RNA replication. *J Virol* 73:8349-8355
- Wilson V, Taylor P, Desselberger U (1988) Crossover regions in foot-and-mouth disease virus (FMDV) recombinants correspond to regions of high local secondary structure. *Arch Virol* 102:131-139
- Wong KM, Suchard MA, Huelsenbeck JP (2008) Alignment uncertainty and genomic

analysis. *Science* 319:473-476

- Wongteerasupaya C, Sriurairatana S, Vickers JE, Akrajamorn A, Boonsaeng V, Panyim S, Tassanakajon A, Withyachumnarnkul B, Flegel TW (1995a) Yellow-head virus of *Penaeus monodon* is an RNA virus. *Dis Aquat Org* 22:45-50
- Wongteerasupaya C, Tongchuea W, Boonsaeng V, Panyim S, Tassanakajon A, Withyachumnarnkul B, Flegel TW (1997) Detection of yellow-head virus (YHV) of *Penaeus monodon* by RT-PCR amplification. *Dis Aquat Org* 31:181-186
- Wongteerasupaya C, Vickers JE, Sriurairatana S, Nash GL, Akarajamorn A, Boonsaeng V, Panyim S, Tassanakajon A, Withyachumnarnkul B, Flegel TW (1995b) A non-occluded, systemic baculovirus that occurs in cells of ectodermal and mesodermal origin and causes high mortality in the black tiger prawn *Penaeus monodon*. *Dis Aquat Org* 21:69-77
- Woo PCY, Wang M, Lau SKP, Xu H, Poon RWS, Guo R, Wong BHL, Gao K, Tsoi H, Huang Y, Li KSM, Lam CSF, Chan K, Zheng B, Yuen K (2007) Comparative analysis of twelve genomes of three novel group 2c and group 2d coronaviruses reveals unique group and subgroup features. *J Virol* 81:1574-1585
- Wootton S, Yoo D, Rogan D (2000) Full-length sequence of a Canadian porcine reproductive and respiratory syndrome virus (PRRSV) isolate. *Arch Virol* 145:2297-2323
- Worobey M and Holmes EC (1999) Evolutionary aspects of recombination in RNA viruses. *J Gen Virol* 80:2535-2543
- Wyban J (2007) Thailand's white shrimp revolution. *Global Aquacult Advocate* 10:56-58
- Yang L-S, Yin Z-X, Liao J-X, Huang X-D, Guo C-J, Weng S-P, Chan S-M, Yu X-Q, He

- J-G (2007) A Toll receptor in shrimp. *Mol Immunol* 44:1999-2008
- Yodmuang S, Tirasophon W, Roshorm Y, Chinnirunvong W, Panyim S (2006) YHV-protease dsRNA inhibits YHV replication in *Penaeus monodon* and prevents mortality. *Biochem Biophys Res Commun* 341:351-356
- Yount B, Curtis KM, Fritz EA, Hensley LE, Jahrling PB, Prentice E, Denison MR, Geisbert TW, Baric RS (2003) Reverse genetics with a full-length infectious cDNA of severe acute respiratory syndrome coronavirus. *Proc Natl Acad Sci USA* 100:12995-13000
- Yount B, Roberts RS, Lindesmith L, Baric RS (2006) Rewiring the severe acute respiratory syndrome coronavirus (SARS-CoV) transcription circuit: engineering a recombination-resistant genome. *Proc Natl Acad Sci USA* 103:12546-12551
- Yu CI, Song YL (2000) Outbreaks of Taura Syndrome in Pacific white shrimp *Penaeus vannamei* cultured in Taiwan. *Fish Pathol* 32:21-24
- Zhang S, Bonami J-R (2007) A ronin-like virus associated with mortalities of the freshwater crab, *Eriocheir sinensis* Milne Edwards, cultured in China, exhibiting 'sighs disease' and black gill syndrome. *J Fish Dis* 30:181-186
- Zheng W-X, Chen L-L, Ou H-Y, Gao F, Zhang C-T (2005) Coronavirus phylogeny based on a geometric approach. *Mol Phylogenet Evol* 36:224-232
- Ziebuhr J, Bayer S, Cowley JA, Gorbalenya AE (2003) The 3C-like proteinase of an invertebrate nidovirus links coronavirus and potyvirus homologs. *J Virol* 77:1415-1426
- Ziebuhr J, Snijder EJ, Gorbalenya AE (2000) Virus-encoded proteinases and proteolytic processing in the Nidovirales. *J Gen Virol* 81:853-879

Zúiga S, Sola I, Alonso S, Enjuanes L (2004) Sequence motifs involved in the regulation of discontinuous coronavirus subgenomic RNA synthesis. *J Virol* 78:980-994